Preconditioning Methods in Cartilage Tissue Engineering: Influences of Silk Material Properties and Hypoxia on Chondrogenesis

Supansa Yodmuang

Submitted in partial fulfillment of the
requirements for the degree of
Doctor of Philosophy
in the Graduate School of Arts and Sciences

COLUMBIA UNIVERSITY

2013

ABSTRACT

Preconditioning Methods in Cartilage Tissue Engineering: Influences of Silk Material Properties and Hypoxia on Chondrogenesis

Supansa Yodmuang

Cartilage has limited intrinsic healing potential, due to the low cell density and the lack of blood supply. Current treatments for cartilage repair rarely restore full structure and function to the native state. Tissue engineering holds promise to create cartilage grafts capable to withstand the stresses present in joints. More than 90% of articular cartilage tissue is composed of extracellular matrix and is located in the loading environment under low oxygen tension in knee joints. To form engineered constructs with mechanical properties compatible to native tissue, scaffolds should provide structural support, maintain cell phenotype and subsequently promote tissue development. The focus of this dissertation is on utilizing the physiological conditions found in joints to regulate biological behavior of cells. The first factor that was studied was the extracellular matrix. Two formats of silk fibroin – hydrogel and porous scaffolds – were examined for their potential as a supporting material for creating cartilage tissue constructs. The composite silk made from nano-fibers and hydrogel – a structure resembling the collagen network and proteoglycan in native cartilage - improved equilibrium and dynamic modulus of engineered tissue by 50% and 60%, respectively, in comparison to silk hydrogel without fibers.

The second factor studied was the modulation of oxygen level, which is a major regulator during native cartilage development. Chondrogenic differentiation was induced in human

embryonic stem cells under hypoxic conditions, in conjunction with biochemical cues from bovine chondrocytes. As a result, *SOX9*, a key transcription factor of cartilaginous lineage, was upregulated in the induced cells. Subsequent cultivation under normoxic conditions resulted in robust formation of cartilage tissue.

Taken together, studies conducted in my thesis work address two major challenges in cartilage tissue engineering: i) providing cells with structural and mechanical properties similar to native ECM for generating *in vitro* cartilaginous tissue and ii) preconditioning cells with physiological environment for directing chondrogenic differentiation.

Table of Contents

List of Figures

Acknowledgements

I cannot believe this day has come. I realized that this is really happening, when I sent an email to Jarmaine to reserve the conference room for my thesis defense on May 14, 2013. I started writing the acknowledgement in The New York Public Library near Bryant Park. This library is filled with all kinds of beautiful energy and dynamics; a businessman was carrying the Wall Street Journal in his hands, an artist was drawing tangled lines on his small sketchbook by a wooden pencil, students were working on their term-papers, tourists from around the world were wandering around the building and a homeless person was eating a sandwich on the steps of the building. This is a perfect workplace to make a list of people who have influenced my life and are a part of this journey with me.

Foremost, I would like to express my sincere gratitude to my advisor, Dr. Gordana Vunjak-Novakovic. She gave me an opportunity to study abroad and to join the lab. Opportunity is important, because it is a ticket to bring one to the next level. Gordana is an inspiring person and I have learned so much from her. One day I will work in academia. I will see all kinds of students who have different backgrounds and have various learning needs. To be a great teacher, one has to understand the rhythm of his/her students and know when is a good time to push your students to move forward. Gordana has all qualities to be a great teacher.

I am a biologist by training. I learn things descriptively. When I was accepted to the Engineering School, it was a great challenge for me to think quantitatively; how to make it better, faster, stronger and measurable. I would like to thank Dr. Lance Kam and Dr. Barclay Morrison for showing me how life sciences and engineering merge during the Quantitative Physiology Class. My first impression of tissue engineering was from Dr. Helen H. Lu and Dr. Clark T.

Hung in the Tissue Engineering class. I am very thankful for their generosity and guidance from day one until today when they are serving on my Ph.D. dissertation committee. Another person to whom I want to express my gratitude is Dr. David Kaplan from Tufts University. He always has a big smile on his face. He is also one of the kindest people I know. My tissue engineering project has a dimension because of a wonderful collaboration between our laboratory and his in Tufts. Additionally, I could not have asked for better from Dr. Grace Chao – a postdoc alumna of our lab, who showed me the cell culture technique. I started from scratch. When I joined the lab, she patiently walked me through the process step by step until I gained my full confidence to work independently. Dr. Grace has been my sister in the lab. I am heartily thankful for her support and to have her on my thesis committee.

Laboratory for Stem Cells and Tissue Engineering is a little world in itself, or to be more precise, small society, where I have developed various social statuses based on my network of interactions within it. I am a student, a friend, a co-worker, a sister, and a trainer. Being part of the lab taught me how to give and take, share and own, say yes and say no, express my pride or confess my silliness. These are the people, alphabetically, who brought me into a colorful and memorable adventure: Amandine Godier-Furnémont, Benjamin Lee, George Eng, Jonathan Bernhard, Monica Agarwal, Surapon Charoensook, and Zhang Yue Shelby. Ick Sarindr Bhumniratana helped me with mechanical testing devices. He was always there when I needed advice. Jenny Yuan and Chandhanarat Chandhanayingyong were a great contribution to my animal studies. I appreciated their talented surgical skills. Thanks to Dr. Leo Q. Wan, Dr. Donald Freytes, Dr. Kara Spiller, Dr. Darja Marolt and Dr. Aranzazu Villasate for constructive criticism and prompt responses to my queries.

Living in Columbia University would be much more difficult if I did not receive kind assistances from wonderful people and organizations. I would like to thank Susan Halligan, Anna Sokolov, Qi Zhao and Nebojsa Mirkovic for their logistical support in the lab. Shila Maghji, Michelle Cintron and Jarmaine Lomax from the Biomedical Engineering Department always helped me navigate the administrative system. I want to thank Health Services and International Students and Scholars Office (ISSO) for their support.

As an international student, I wish to thank Thai Students Association (TSA) for being a home-like community. Kritsada Leungchavaphongse, Puttisarn Mongkolwisetwara, and Tassaneewan Laksanasopin are three Thai-BME students who helped me with the coursework in the first few years in school. Also, Chutima Talchai and Thaned Kangsamaksin were my very best friends in New York City at that time.

Dr. Ivana Gadjanski is one of my best friends and I do not know how to express my gratitude for her amazing friendship. Dr. Oleg Kogan is my best fellow. He came to my life at the perfect time with an insightful understanding of my strengths and weaknesses.

It was such a short period of time to know them, but David and Margot, my surf and pottery instructors, respectively, influenced the way I see life. In the Ocean, you must keep swimming to generate sufficient momentum before standing up on the board. On the other hand, an uneven pot is hard to fix. Sometimes, it is not worth it to obsess over repairing a pot that did not go right -- you must let go and start over with new clay.

I was lucky to have wonderful teachers in Thailand starting from my early age to grad school. They helped me move forward from one stage to the next one. If they were relay runners, I was being a baton passed from the first leg to the second leg and so on. I am very grateful to The Royal Thai Government in the year 2006 term for having faith in me, “you can do it,

Supansa". The government provided financial assistance and a round trip ticket Bangkok - New York. I already used the outbound ticket. Sooner or later, I will have to use the return ticket.

I am not the same person that I was in 2006, but the only thing that remains the same are the warm friendships that I have with friends from my junior high school. They are the incredible group of people who shaped my personality, taught me to be street-smart, and provided me with a comfort zone.

The writing of a dissertation is an experience filled with solitude, in contrast to all of the Ph.D. process, but it would not be possible without the true wind beneath my wings. I would like to express my deepest gratitude to my parents. Now, my dad and mom are a retired couple. My dad used to be a college physics professor and my mom used to be a high school art teacher. Both of them influenced me in very separate ways. However, I cannot be a genius scientist or a talented artist. I am somewhere in between. My parents were a part of an amazing generation. They have lived their lives about equally in 2 different eras. They have seen advanced technology, such as a notebook, a smart phone, and the Internet in their middle age. However, this was a big change for them, compared to what they saw in their childhood. Adapting to these changes must have required a lot of energy. Last but not least, thanks for my younger sister, Sirinee for taking care of my parents while I was here. We have always supported and stood up for each other.

CHAPTER 1

1. Introduction

Articular cartilage injuries occur as a result of either traumatic mechanical destruction, often sports-related injury or progressive mechanical degeneration, mostly found in elder patients. Once cartilage cells are damaged or lost, the surrounding matrix gradually degenerates. Even small cartilage defects, without a proper treatment, can progress to osteoarthritis over time (Wang et al 2006). Osteoarthritis (OA) – a common form of arthritis that affects 27 million people in the United States alone (1). By 2030, an estimated 70 million American with age over 65 will have a greater occurrence of age-related OA.

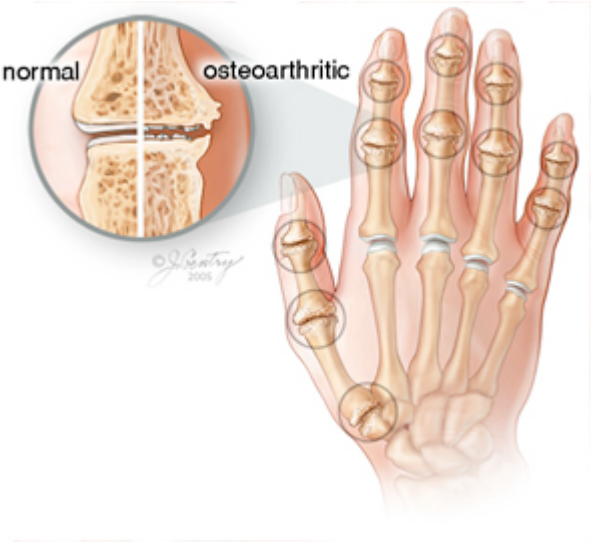

Figure 1. Healthy joints and osteoarthritis joints (2)

Current treatment options involve pain medications and surgical intervention. Non-surgical interventions include lavage, shaving, debridement, abrasion chondroplasty, Pridie drilling, microfracture and spongilization (3). The scientific rationale behind the first four of

these techniques is not clear, whereas the last four methods are designed to stimulate a repair reaction by causing a disturbance of the bone tissue for example, or inducing therapeutic bleeding (3). Surgical approaches include a procedure called osteotomy – a procedure involving cutting bone for realignment or mechanical load re-distribution, and distraction of joints – the use of a surgical frame around the joint. The third class of therapy centers on implantation of cartilage tissue (3). However, these therapeutic strategies rarely restore structure and function of damaged cartilage to the level of native, uninjured tissue.

Tissue engineering is a promising alternative in the treatment of cartilage damage. One ultimate goal in this field of research is to develop a replacement graft, which has a structure and composition that resembles the native cartilage to fully restore the damaged tissue. Articular cartilage is believed to be one of the less complex tissue structures, because it contains only one cell type, chondrocytes, which are responsible for maintenance of tissue function and synthesis of extracellular matrix (ECM). Chondrocytes mostly reside individually within dense surrounding ECM. Cartilage tissue is avascular and aneural and typically relies on nutrients and oxygen that diffuse from synovial fluid. Cartilage tissues do not require extensive blood supply, as found in bone or cardiac tissues. The simplicity of tissue components (one cell type, no blood supply) make cartilages an ideal target tissue to develop for regenerative medicine applications. However, artificial regeneration is considerably constrained by (i) an inert chondrocyte cellular activity resulting in discrepancy of innate repair response, (ii) insufficient mechanical properties of neocartilage and (iii) lack of integration between graft substitutes and native tissues.

2. Motivation

This dissertation is motivated by the need to improve the cartilage tissue engineering methodology, a very challenging and complex task bound to have profound implications on clinical treatments for cartilage injury and osteoarthritis. Damaged cartilage tissue has low self-healing capacity because it does not have a direct blood supply. Thereby, the defect areas are isolated from local mesenchymal progenitor cells, which can stimulate the healing process. Cartilage injury and osteoarthritis are associated with a significant socio-economical burden worldwide. Tissue engineering provides alternative approaches for therapeutics and regeneration in orthopedic research, holding the promise for improving the quality of life of millions of patients by creating graft substitutes via recapitulation of tissue development in vitro.

My research focused on following the biomimetric paradigm by re-creating the cellular environment to be similar to that found in a living organism for *in vitro* tissue development, remodeling and differentiation. Biomimetic approach to tissue engineering in this dissertation involved around developing biomaterials for cartilage tissue engineering and utilizing physiological condition found in knee joints to direct chondrogenic differentiation of human embryonic stem cells. Although search for material and cell source used in cartilage tissue engineering continues to develop, there are controversies in long-term success.

2.1 Hydrogel

Hydrogels offer a unique opportunity to generate a functional cartilage substitute. Agarose hydrogel has long been used in cartilage tissue engineering to encapsulate chondrocytes because it provides hydrated environment and mechanical similarity to native cartilage and preserves chondrogenic phenotype (4). Although the functional outcomes of engineered

cartilage-based agarose showed comparable mechanical properties to native tissue, the mechanism underlying beneficial effects of agarose hydrogels limit the use and optimization of this material. Additional concern of using agarose in cartilage tissue engineering is due to the fact that our body cannot metabolize agarose, which may lead to a complication related to tissue integration (5).

2.2 Cell source

Autologous and adult stem cells, which are isolated from patients or donors, have shown varying degrees of proliferation and chondrogenic differentiation potential. These cells have never fulfilled the requirement for being the building blocks of cartilage graft substitutes as a result of dedifferentiation during expansion, insufficient cell number and production of non-cartilaginous matrix (6). Also cell isolation gets involved in the invasive procedures and induces donor site morbidity. Therefore, to circumvent biological and technical constrains of current cell source, we aim to develop alternative cell source, which possesses high proliferative capabilities and chondrogenic lineage differentiation. Human embryonic stem cells offer possibilities for obtaining an unlimited supply of cells for cartilage tissue engineering. The complications associated with the used of hESCs are the ways of controlling and directing their differentiation potentials to chondrogenic lineage. These challenges motivated me to undertake search for new strategies to direct chondrogenic differentiation of hESCs.

3. Hypothesis

The unifying hypothesis of this work was that the chondrogenic differentiation and functional assembly of cartilage tissue can be improved by engineering cartilage under conditions resembling those in developing native tissue. To test this hypothesis, studies were done to (*i*) optimize the structural and mechanical properties of the scaffolding material, using fiber-reinforced silk hydrogel scaffolds, and (*ii*) define the oxygen profiles during cultivation to first induce cell differentiation and then enhance functional cell assembly.

3.1 Silk hydrogel for cartilage tissue engineering

Hydrogel is widely used as a biomimetic of ECM. Silk hydrogel has great a potential to be a supportive material in cartilage tissue engineering. Still, mechanical strength of silk hydrogel does not sufficient to meet mechanical demands of joint loading and not match to that of agarose the standard material in cartilage tissue engineering.

Providing cells with the mechanically optimized silk hydrogels, which has similar mechanical and diffusional properties to those in agarose, would promote tissue development with mechanical properties approaching the native tissue.

3.2 Chondrogenesis: recreating physiological conditions of articular joints: hypoxia and chondrocyte-secreted factors

Human embryonic stem cells (hESCs) have potential to differentiate to all 3 germ layers and can be an alternative cell source for cartilage regeneration. The experiments are designed to

determine effects of mimicking physiological condition on articular joints on chondrogenic differentiation of hESCs.

The hypothesis in this study is *priming hESCs during embryoid bodies formation with physiological condition would induce chondrogenic differentiation.*

4. Specific aims

4.1 Silk hydrogel for cartilage tissue engineering

Aim 1. To optimize silk fibroin properties for functional cartilage tissue engineering

Silk fibroin materials in various structural forms (fiber, porous, thin film) have been successfully used as tissue engineering scaffolds because of their versatility, biodegradation and biocompatibility. To explore the influence of different 3D silk structures on tissue development, hydrogel, a standard supportive material for cartilage tissue engineering, and porous scaffold are compared. Silk hydrogel is further examined for concentration, and mechanical and diffusional properties. To this end, the silk hydrogel concentration is selected to match the diffusivity of agarose that yielded constructs with mechanical properties approaching those of native cartilage. Silk fibers are also included to modify mechanical properties of silk hydrogel.

Aim 2. To correlate the hydrogel material properties to cartilage tissue development

The mechanically optimized silk hydrogels from specific aim 1 are used as supportive material to investigate tissue development. This study attempts to test the hypothesis that silk hydrogel with mechanical properties matched to agarose can yield cartilage constructs approaching native tissue after 6 weeks of culture.

4.2 Chondrogenesis: recreating physiological conditions of articular joints: hypoxia and chondrocyte-secreted factors

<u>Aim 1.</u> To study the effects of hypoxia-normoxia regimes on cartilage tissue properties in a robust cellular model

The regulation of cartilage ECM production under low oxygen tensions is studied to determine if hypoxia is a favorable condition for maintaining cartilage structure and function. The investigation is carried out using bovine chondrocyte-laden agarose hydrogel. Engineered cartilage constructs are cultured in hypoxic condition (5% O_2) with various exposure times and tested for tissue properties compared to those cultured under normal oxygen levels (21% O_2).

<u>Aim 2.</u> To establish protocol for chondrogenic differentiation of hESCs through controlled oxygen tension and molecular conditioning

The limited self-renewal and differentiation of human mesenchymal stem cells (hMSCs) with increasing patient age have motivated utilization of human embryonic stem cells (hESCs) for chondrogenic differentiation. Soluble morphogenetic factors secreted from bovine chondrocytes in conjunction with hypoxia are used to induce embryoid bodies (EBs) for 3 weeks. The resulting induced cells were evaluated for chondrogenic differentiation potentials in pellet culture for 6 weeks.

CHAPTER 2

Cartilage tissue engineering

Tissue engineering is an interdisciplinary field that applies principles of cell biology, engineering and medicine to generate tissue substitutes that restore, maintain or improve tissue function (7). Fundamental components of engineered tissues that enable them to mimic native tissue structures and functions include matrices, stimuli and cells. In cartilage tissue engineering, recapitulation of mechanics needed for sustaining mechanical loading in joints is crucial in the success of engineered constructs.

Cartilage is a connective tissue composed of cells, chondrocytes, dispersed in dense extracellular matrix (ECM). ECM is composed of complex macromolecules organized in 3D network forming a gel-like material and its function is to resist mechanical loading in joints. The hydrophilic environment of ECM enables cartilage tissues to exhibit swelling pressure, which is countered by tensile strength generated from collagen network. Besides mechanical loading, another intense physiological condition found in joints is low oxygen tension, i.e. hypoxia. Therefore, to create cartilage tissue replacement, ECM architecture, chondrocytic cells and physiological environment must have been orchestrated to achieve tissue properties similar to those present in native tissues.

1. Paradigms of cartilage tissue engineering

Besides hydrogels as a material of choice to restore gel-like environment for cartilage tissue development, physiological conditions found in joints such as, hypoxia, mechanical loading and soluble growth factors must have been considered and applied to cell culture in order to mimic the environment in which chondrocytes reside. Established protocols for cell and stem cell culture have provided a wide range of alternative cell sources for cartilage. This chapter will provide an overview of crucial components for cartilage tissue engineering; hydrogel matrices for cell encapsulation, stimulating physical conditions and cells as building blocks of tissue formation.

1.1 Hydrogels for cartilage tissue engineering

Hydrogels are 3D network of hydrophilic polymers that absorb and retain substantial amount of water >30% (8). The state where soluble branched polymers start crosslinking and become less soluble is called “sol-gel transition”. Hydrogels have been used in tissue engineering research due to their unique mechanical and structural support similar to ECM. The use of hydrogel for tissue engineering can be found in various therapeutic applications aiming at delivering cells/tissue and bioactive molecules to defect sites (9). Hydrogels have long been investigated as an encapsulation matrix for islet cells in the production of insulin, and for microencapsulation drug in control-release applications (10). They recently received attention in regenerative tissue applications, i.e. creating engineered neuron, skin, fat, bone and cartilage. An ideal hydrogel for functional cartilage tissue substitute is not only biocompatible to encapsulated cells, e.g. provokes no damage or toxicity to cells, but also accommodates a sufficient nutrient and metabolite transport to and from cells. An adequate mechanical support to withstand load in

implant sites is one of the important aspects to consider before choosing hydrogels for cartilage tissue replacement.

Hydrogels in engineered cartilage research have been prepared from synthetic and naturally derived polymers. Representative synthetic hydrogels are poly(ethylene)oxide (PEO), poly(vinyl alcohol) (PVA), poly(acrylic acid) (PAA) (11). However, degradation by-products of synthetic material elevate local pH and induce inflammation. Natural hydrogels include agarose, alginate, chitosan, fibrin, gelatin and silk. While the synthetic hydrogel allows easy processing and modifications, the naturally derived hydrogel offers better biocompatibility, immunocompatibility, and low toxicity of degradation by-products. The use of hydrogels in cartilage tissue engineering aims at preserving chondrocytic phenotypes, recapitulating viscoelastic properties found in native tissue microenvironment. In this thesis, naturally derived hydrogels, agarose and silk, were exploited for encapsulating cells, and the effects of specific parameters on cartilage tissue development were studied. Cell-laden agarose served as a gold standard of cartilage model to determine effects of hypoxia on matrix production and mechanical properties. The novel silk hydrogel for cartilage tissue engineering will be presented in chapter 4.

1.1A Agarose

Agarose is a hydrophilic linear polymer isolated from marine seaweed, *Gelidium gracilaria*. The polymer structure is composed of a repeating unit of disaccharide, D-galactose and 3,6-anhydro-L-galactose **(Figure 2).** Low melting temperature agarose is used in cell encapsulation because it exhibits hysteresis, which means that its melting point (65 ºC) is not the same as its gel point (26 - 30 ºC) at 1.5 % gel. Hence, temperature difference is advantageous to cell encapsulation by allowing cells to be encapsulated before gel setting.

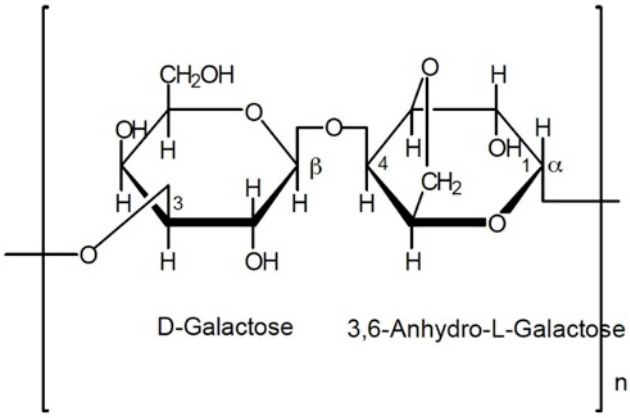

Figure 2. Agarose is a linear polymer of disaccharide subunit of D-galactose and 3,6-anhydro-L-galactose (12)

Agarose is thermally reversible as a result of hydrogel bond formation and the gel stiffness that can be controlled by varying the agarose concentration. The smaller the pores, the higher is the mechanical stiffness of the gel at high concentration of agarose. In the solution (sol) state, as the temperature approaches the melting point, agarose is in a random coil conformation, while in gelation (gel) state, agarose subunit is a double helix with multiple chain aggregation leading to three-dimensional network formation (5). Despite the fact that agarose hydrogel does not contain charge groups for cell adhesion or biomolecule interaction, the hydrophilicity of the gel from hydroxyl groups (-OH) on the polysaccharide chains allows the covalent coupling to charge molecules, e.g., chitosan and peptides (13).

An initial application of agarose in tissue engineering is to prevent immune system from reaching encapsulated cells owing to its inert properties that allow cells to survive and secrete insulin, as demonstrated in pancreatic cell microencapsulation (10). However, the major concern

regarding the use of agarose in tissue replacement applications is that mammals do not have enzyme to metabolize agarose, which can give rise to further complication related to tissue integration.

1.1B Silk

Silk is natural biopolymer extracted from the cocoons of silkworm, *Bombyx mori*. Silk fibers are composed of 2 different self-assembled proteins, sericin and fibroin. Sericin is a glue-like protein that can be removed by degumming process. Native structure of silk fibers contains 2 fibroin strands, which are wrapped around by sericin **(Figure 3)**. Silk fibroin is composed of repetitive amino acids Gly-X (X being Ala, Ser, Thr, Val), which can form antiparallel β-sheet alternating with random coil structure in amorphous region. The unique protein structure organization of silk fibroin leads to the superior mechanical properties compared to other naturally derived polymers.

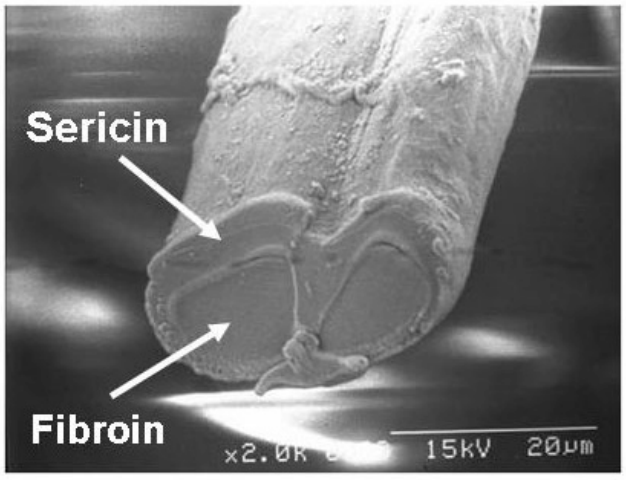

Figure 2. Scanning electron micrograph of silk fibers. Two fibroin core proteins are coated with sericin (14)

Silk fibroin can be used in biomedical applications in various material formats, including film, three-dimensional porous scaffold, electrospun fibers, microspheres and hydrogel (15, 16). In order to create silk hydrogel, the main application for cartilage tissue engineering, silk fibers are extracted from the cocoon and dissolved in aqueous solution before initiating sol-gel transition, the state in which to start encapsulating cells. Silk gelation can be controlled by several parameters, such as the concentration of silk fibroin, temperature, pH and ionic strength (salt). Gelation time of silk solution from 0.6% - 15% (w/v) varies from days to weeks depending on the initiating factors used to induce hydrogen bond formation (cross-link) between silk polypeptide chains. Recently, ultrasonication has been used to accelerate sol-gel transition in a temporally controllable manner from minutes to hours based on silk fibroin concentration and sonication parameters (energy output and time) (17).

Silk fibroin in aqueous solution is in the random coil structure, whereas silk fibroin in sol-gel transition is in the β-sheet structure (18). The sonicated silk fibroins contain multiple regions of active β-sheet blocks along the silk polypeptide chains. These active β-sheet blocks form cross-links to the other blocks on adjacent silk polypeptide chains. The propagation of inter-peptide chain formation eventually transforms sol-gel transition to gel. The mechanical properties of silk hydrogel can be controlled by silk fibroin concentration.

The major advantages of silk compared to other natural biopolymers are its excellent mechanical properties and biodegradability. Furthermore, silk can be chemically modified, mixed and cross-linked with other functional groups or other biopolymers to obtain desired properties suitable for particular tissues (19). Unlike agarose, silk fibroin completely disappeared in 1 year after subcutaneous implantation suggesting that silk can be metabolized in the body

(20). However, further long-term studies of silk immunogenicity are needed to get an insightful understanding about host responses to silk-based engineered tissues.

2. Pre-conditioning cells for tissue engineering

Tissue engineering, a cell-based treatment, offers new therapeutic options for cartilage damages by combining cells, scaffold and stimulating conditions to fabricate functional new grafts to replace damaged sites (7). Cells are crucial components of tissue engineering, because they serve as building blocks to generate tissues and therefore cell-based replacement requires sufficient amount of cells to be seeded into the scaffold. Cells in cartilage tissue engineering come from two major sources, which are fully differentiated chondrocytes from non weight-bearing cartilage tissue of patients/donor and pluripotent stem cells (adult stem cells, embryonic stem cells and induced pluripotent stem cells) (6, 21). The former source needs to be expanded, while in the same time maintaining a chondrocytic phenotype. The latter needs to be differentiated to the stage of mature chondrocytes. Native chondrocytes (autologous or allogeneic) are cultured in monolayer with several passages to get considerable amount of cells. However, these isolated chondrocytes undergo a process of dedifferentiation that is characterized by a transition to a fibroblast-like phenotype. Stem cells, on the other hand, proliferate extensively due to their self-renewal capability. However, the challenge of stem cells involves directing pluripotent cells to chondrocytes.

Pre-conditioning is fine-tuning step that maintains and/or induces chondrocytic phenotype. Pre-conditioning provides an environment for i) re-differentiation of de-differentiated chondrocytes, ii) differentiation of stem cells into cartilaginous lineages. To prepare mature early chondrocytes, physical and chemical conditioning can be introduced during cell culture.

2.1 Hydrogel

Isolated chondrocytes are unable to retain their phenotype during expansion in monolayer culture. Use of hydrogels allowed chondrocytes to re-acquire their rounded shape and to continue producing cartilage matrix components. Generally, differentiated chondrocytes have a spherical morphology associated with type II collagen and proteoglycan synthesis. After serial passages in monolayer, these cartilage-specific components are gradually lost and predominantly replaced by type I collagen alongside the flatten cell morphology. The most well known study of the influence of hydrogel on cell shape was performed by Benya et al (22). The de-differentiated chondrocytes reexpress their differentiated phenotype during suspension culture in 0.5% low T_m agarose. It indicated that conditioning cells in 3D environment using hydrogel encapsulation modulates cell shape and biosynthetic program transition from de-differentiated to differentiated state.

2.2 Low oxygen tension

Articular cartilage resides in hypoxic environment with oxygen concentrations ranging from 10% at the surface to <1% in the deep (23). Oxygen and nutrient exchange within cartilage tissue depend on diffusion from the synovial fluid that flows through the tissue during the joint movement. In order to survive in such a harsh environment, chondrocytes must be able to sense oxygen availability and adjust cellular metabolism to consume less oxygen at lower oxygen concentrations (24, 25). Chondrocytes have very low oxygen consumption compared to other cell types.

During limb development, the differentiation of mesenchymal cells into chondrocytes and early formation of the tissues in the joints occur at low oxygen levels in which hypoxic

inducible factor (HIF) plays an important role in cellular adaptation to hypoxia (26). HIF is a heteromeric transcription factor that mediates the effects of SOX9, a chondrogenic transcription factor responsible for skeleton formation (27). The putative mechanism of type II collagen and aggrecan synthesis involves transcriptional control of ECM synthesis via SOX9 binding to responsive sequences of aggrecan and type II collagen. The orchestrated regulation of cartilage ECM production by the HIF and SOX9 supports the assumption that hypoxia is a favorable condition for maintaining cartilage structure and function.

Today, most cartilage constructs are engineered by cultivation of chondrocytes or their progenitors under ambient oxygen concentrations (21%) that is much higher than the oxygen level in native joints (28). Cultivations of engineered cartilage at reduced levels of oxygen tension have been investigated with varying degrees of success. In general, cultures were subjected to a constant level of hypoxia, for a period of up to 4 weeks (29, 30), without transferring cultures low and high oxygen environments. The effects reported from these studies were controversial. The implementation of hypoxia in cartilage tissue engineering resulted in either adverse effects of low oxygen on cell growth and ECM assembly, or no significant effects (31, 32).

Recently our laboratory demonstrated transiently low oxygen tension has beneficial effect on cartilage tissue development. The hypoxic conditioning regime used in cell culture was an initial exposure constructs to 5% O_2 for 7 days (to activate cell proliferation) followed by 21% O_2/21 days (to enhance matrix synthesis). This reoxygenation maintained cell proliferation, and enhanced proteoglycan and collagen type II along with upregulation of COL2A1 throughout the duration of culture.

2.3 Chemical cues: exogenous growth factors and soluble factors from chondrocytes

2.3A Exogenous growth factors

Growth factors are used in cartilage tissue engineering to modulate cellular differentiation, maintain chondrocyte phenotype, as well as to regulate specific ECM synthesis. There are three main families of growth factors involved in chondrogenic differentiation; the transforming growth factor beta (TGF-β) family, fibroblast growth factors family (FGFs), the insulin-like growth factor (IGF). The effects of many of these growth factors alone and in combination have been studied for cartilage tissue engineering,

Members of the TGF-β family are probably the most widely used growth factors in cartilage tissue engineering. The notable members of the TGF-β family include TGF-β1, TGF-β3 and bone morphogenetic proteins (BMPs). They not only have been shown to regulate cell growth but also to up-regulate proteoglycan and collagen type II synthesis. Several groups demonstrated the use of TGF-β family in chondrogenic differentiation of MSCs and embryonic stem cells (33). BMPs, especially BMP-2 and BMP-7, play an important role in chondrogenesis and osteogenesis during skeleton development and have been demonstrated to stimulate chondrogenesis in adipose stem cells (34).

Basic fibroblast growth factor (bFGF) has been shown to stimulate chondrocyte proliferation. FGF-18 in conjunction with FGF receptor 3 has recently been shown to activate signaling, which promotes chondrogenic differentiation of limb bud mesenchymal cells, and enhance matrix production of articular cartilage *in vivo* (35).

The effects of IGF-1 were demonstrated in monolayer culture chondrocytes by increasing anabolic activity of chondrocytes resulting in profound synthesis GAG and up-regulation of aggrecan and collagen type II gene expression(36). The effects of platelet-derived growth factor (PDGF) on proliferation and ECM synthesis have not been extensively reported, but it has been shown to have an effect on chondrocyte proliferation (37).

Furthermore, synergistic effects of several growth factors applied simultaneously have been detected in several studies. BMP-2 and TGF-β1 work in concert for the chondrogenesis of periosteal cells (38); it was suggested that BMP-2 induces neochondrogenesis, while TGF-β1 modulates the terminal differentiation in BMP-2-induced chondrogenesis. Combined treatments with TGF-β3 and BMP-6 or TGF-β3 and IGF-1 were shown to be the most effective combinations for chondrogenic induction of bone marrow MSCs (39). However, growth factor combinations do not always interact synergistically. For example, the addition of IGF-1 and TGF-β in combination did not improve the histologic features or mechanical performance of tissue engineered cartilage constructs (40).

Perhaps the most exciting new results have come from studying the synergism between growth factor application and mechanical stimulation. Bonassar et al. found that the combination of IGF-1 and dynamic compression led to a 290% increase in proteoglycan synthesis, a degree far greater than that achieved by either stimulus alone (41). Also, Mauck et al. showed that the combination of dynamic deformational loading with either TGF-β1 or IGF-1 increased the stiffness of engineered constructs by 277% or 245%, respectively, with respect to untreated free-swelling constructs (42).

2.3B Soluble factors from chondrocytes

Soluble substances from cells known under the collective term of cytokines play essential role to mediate cell growth and survival. There are 2 approaches to deliver soluble factors to cell culture. 1) co-culturing cells with helper cells secreting molecules and 2) growing cells in conditioned medium.

2.4 Co-culture

Co-culturing was first used in *in vitro* culture of embryos and embryonic fibroblasts (helper cells). Embryos are grown on top of monolayer fibroblasts. Fibroblasts provide chemical and physical supports to embryos by secreting growth factors and nutrients needed for embryo development and serving as a substrate for embryo attachment, respectively. The idea of using paracrine secretion in embryo cultures has been adopted for culture 2 cell types separate by transwell while maintain cell-cell communication through secreted proteins and molecules across nanometer-size pore. In chondrogenic differentiation, co-culture MSCs with articular chondrocytes seeding on transwell showed a decrease in hypertrophic differentiation (43). Hwang et al. demonstrated chondrogenic commitment in ESCs co-cultured with bovine chondrocytes (44).

It is important to not that target cells could also secrete substance to the culture medium and alter phenotype of other cells on the transwell. To eliminate artifacts from 2-way communication, culturing target cells in conditioned medium may be an alternative approaches to deliver soluble factors. Conditioned medium may help to extract the effects of substance on target cells and maintain batch-to-batch consistency.

2.5 Conditioned medium

Conditioned medium is a spent medium harvested from culture cells. It contains metabolites, growth factors (e.g. interleukins, EGF, and PDGF), and extracellular matrix protein (e.g. collagen, fibronectin and various proteoglycan), which are secreted into the medium by the cultured cells. The medium is obtained by sterile filtration and is added to fresh culture medium for up to 1/3 to 1/2 of the final volume (45). The biochemical analysis of the constituents responsible for a particular biological activity is still not completely elucidated to detect secreted growth factors. Despite the fact that components in conditioned medium have not been completely identified, the use of conditioned medium is widely accepted in cell culture.

Chondrogenesis is an orchestrated molecular and cellular process during embryogenesis driven by chondroprogenitors that firstly undergo mescenchymal condensation. Inducing stem cells in media supplemented with only one or two purified growth factors may not be sufficient for chondrogenic lineage commitment compared to culturing stem cells in conditioned media containing mixture of secreted soluble factors. Conditioned medium obtained from bovine chondrocytes was able to induce chondrogenic and osteogenic differentiation of MSCs during in vitro micromass culture (44).

2.6 Stimulation of cells during *in vitro* chondrogenesis

2.6A Mechanical loading

Chondrocytes are connected to their microenvironment by focal adhesion mediated through binding between cell membranes and ECM. This cell-matrix interaction (focal adhesion) plays role in structural integrity of cartilage tissue. In addition, focal adhesions are involved in the process of mechanotransduction, in which cells regulate transcriptional activities based on mechanical signals received at their surface. Although the exact mechanism of mechanotransduction in the chondrocytes has not been completely elucidated, in the molecular viewpoint it has been suggested that elements of the cytoskeleton and integrins allow the coordination of mechanical forces and transcriptional changes. From medical evidences in canine studies, articular cartilage in the knee becomes significantly stiffer following loading in physiological ranges as a result of running on a treadmill (46). It has been proposed that mechanical stimulation serves to maintain and even up-regulate the production of ECM. Therefore, *in vitro* culture has adopted mechanical stimulation applied to engineered cartilage aiming to promote ECM synthesis with the expected outcome of the increase in mechanical properties. Methods to deliver mechanical stimulation to cartilage constructs include hydrostatic pressure, direct compression and shear forces. The parameters that may be varied during application of mechanical stimulation include strain or magnitude, frequency, duration and magnitude of loading as well as the time point at which the cells are subjected to loading.

2.6B Exogeneous ATP

In order to recreate the physiologic loading environment, a majority of cartilage tissue engineering studies has focused on various ways of applying direct compression in combination

with application of growth factors (47-49). This external mechanical stimulation leads to activation of mechanotransduction cascades, which promote chemical signaling inside the cell. However, direct mechanical stimulation is not always a suitable method, and the utilization of mechanisms underlying mechanotransduction might allow for a highly effective and less aggressive alternate means of stimulation. In particular, purinergic, ATP-mediated signaling pathway is strongly implicated in mechanotransduction within articular cartilage. ATP (adenosine 5'- triphosphate) has been indicated as one of the first molecules to be released in response to mechanical stimulation (50-54). To recreate the physiologic loading environment in the absence of externally applied forces, exogenous ATP was supplemented in culture medium aiming to activate purinergic signaling pathway in chondrocytes. Significant increases in equilibrium and dynamic modulus of engineered cartilage were observed after 4 weeks of culture (55).

CHAPTER 3

Silk Hydrogel for Cartilage Tissue engineering

1. Background

Cartilage tissue engineering is a new treatment option for joint repair. Engineered cartilage constructs are expected to have sufficient mechanical and functional outcomes at the time of implantation to survive the physical demands of joint loading. Currently, agarose-based engineered cartilage can yield tissue constructs with biochemical and mechanical properties comparable to native cartilage and thereby serve as gold standard of *in vitro* engineered cartilage. However, agarose have limited studies in animal models because of its non-degradability, which hinders graft integration to the surrounding host tissue. Furthermore, it is still not understood which characteristics of agarose contribute to its superior functionality. The systematic studies of cartilage tissue formation cannot be easily conducted in agarose hydrogel, because the capability to modify and customize agarose structure and composition is rater limited. On the other hand, a novel biomaterial, silk fibroin, can be fabricated in various formats, e.g., film, fiber, porous scaffold, hydrogel, and be conjugated with functional groups to promote cell adhesion (56, 57). The versatility of silk fibroin allows it to be a powerful tool for understanding the mechanism underlying beneficial effects of hydrogel on cartilage tissue formation and optimizing protocols in future material development.

This chapter focuses on the use of silk hydrogel in cartilage tissue engineering. Comparative studies of two silk fibroin formats (hydrogel and porous scaffold), which provide

3D environment to cells will be demonstrated. An endeavor to improve mechanical properties of silk hydrogel by fiber reinforcement will be described at the end of this chapter.

2. Specific aims

Aim 1. To optimize silk fibroin properties for functional cartilage tissue engineering

Silk fibroin materials in various structural forms (fiber, porous, thin film) have been successfully used as tissue engineering scaffolds because of their versatility, biodegradation and biocompatibility. To explore the influence of different 3D silk structures on tissue development, hydrogel, a standard supportive material for cartilage tissue engineering, and porous scaffold are compared. Silk hydrogel is further examined for concentration, and mechanical and diffusional properties. To this end, the silk hydrogel concentration is selected to match the diffusivity of agarose that yielded constructs with mechanical properties approaching those of native cartilage. Silk fibers are also included to modify mechanical properties of silk hydrogel.

Aim 2. To correlate the hydrogel material properties to cartilage tissue development

The mechanically optimized silk hydrogels from specific aim 1 are used as supportive material to investigate tissue development. This study attempts to test the hypothesis that silk hydrogel with mechanical properties matched to agarose can yield cartilage constructs approaching to native tissue in 6 weeks of culture.

3. Methodology

3.1 Silk hydrogel preparation

Silk fibroin solution was extracted from cocoons of *Bombyx mori* as previously described (58). Briefly, the cocoons were boiled for 40 min in 0.02 M sodium carbonate (Na_2CO_3) and then silk protein was dissolved in 9.3M LiBr solution followed by dialysis against distilled water for 4 days using Slide-a-Lyzer dialysis cassette (MWCO 3,500, Pierce). To make a silk hydrogel, the silk solution was adjusted to concentration of 2% or 4% (w/v) and sonicated with a Branson 450 Sonifier (Branson Ultrasonics Co. Danbury, CT) at 12% amplitude for 15 seconds to initiate gelation. Then sonicated silk was poured into sterile mold made of 2 glass plates, which were separated by 2.5 mm thick spacer. Cylindrical disks (4 mm in diameter x 2.5 mm thick) were cored out using a biopsy punch.

3.2 Silk porous scaffold preparation

Silk fibroin solution from above step was diluted to 6 - 8% (w/v). Two ml of the silk fibroin and 4 g NaCl particles were mixed together in Teflon cylinder containers and sit in room temperature for 24 hours. Then, NaCl particles were leached out in distilled water for 2 days, leading to porous silk scaffolds with pore size of 500 - 600 μm.

3.3 Silk fiber preparation

The development of these micron-sized non-immunogenic silk fibers has recently been accomplished by Mandal et al (33). The formation of these fibers involves rapid alkaline hydrolysis of degummed silk fibers in sodium hydroxide solution. Sodium hydroxide pellets (NaOH) weighing 3.5 g (to obtain 17.5 M solution) were added to 5 ml of distilled water. When approximately 70% of the NaOH pellets are dissolved, the dried degummed silk fibers weighing 0.35 g were added and stirred with a spatula. Then the digested reaction was stopped by adding 45 ml of water and centrifuged at 3,500 rpm for 5 minutes. Washing step is repeated from 5 to 8 times to remove excess remaining alkali. The pH of the solution is measured and the pH is adjusted to 7.0 using hydrochloric acid. Finally the fibers are suspended in PBS and lyophilized to generate a silk fiber powder. To obtain large (400 - 500 μm long) and medium (150 - 200 μm long) silk microfibers, the hydrolysis reaction was carried for 30 and 180 seconds, respectively. To obtain very fine/smaller (10 - 20 μm long) silk fibers, the reaction mixture was set up in a boiling water bath for 60 seconds to aid rapid hydrolysis. Once the fibers have been washed and lyophilized they can be stored indefinitely at ambient conditions.

3.4 Preparation of cell-hydrogel constructs (silk and agarose)

Sterilized silk solution were diluted into 2(%w/v), mixed with DMEM powder and sodium bicarbonate ($NaHCO_3$) to get the final concentration of 1.34% and 0.37%, respectively. The mixture was sonicated using a Branson 450 Sonifier (Branson Ultrasonics Co., Danbury, CT) for 15 seconds with the 12% amplitude to initiate gelation. Primary bovine chondrocyte suspension in as less as 50 μl was added into the sonicated silk solution to get final seeding of of 20 x 10^6 cells/ml in hydrogel. After mixing, the cell/hydrogel mixture was poured into sterile

molds and allowed to become gel in the same way as described in acellular constructs preparation. Cylindrical disks (4 mm in diameter x 2.5 mm thick) were cored out using a biopsy punch, resulting in 6.2×10^5 cells per disc.

For the preparation of cell/agarose hydrogel constructs, one volume of cell suspension (at 40×10^6 cells/ml in culture medium) was mixed with an equal volume of 4% low-melt agarose (Type VII, Sigma) in phosphate buffered saline (PBS) at 37 °C to yield a final cell concentration of 20×10^6 cells/ml in 2% agarose hydrogel. The cell/ agarose hydrogel mixture was casted and cored out as described in silk hydrogel construct preparation.

3.5 Preparation of cell-porous silk constructs

The porous scaffolds were then sterilized via autoclaving and hydrated by incubation in culture medium (overnight). Similar to the hydrogel constructs, disks (4 mm in diameter x 2.5 mm thick) were cored out using a biopsy punch from the porous silk scaffold stock. Chondrocytes (6.2×10^5 cells per scaffold) were suspended in 25 μl of culture medium and slowly loaded into the hydrated scaffold. Constructs were incubated at 37 °C for 2 hours for complete attachment. The culture medium was then switched to chondrogenic growth medium for the duration of the culture period.

3.6 Preparation of cell-fiber reinforced hydrogel

Fiber-reinforced agrarose hydrogel was prepared by mixing 4% agrose with equal volume of PBS containing silk fibers with or without cells to obtain final concentration of 2%

agarose, with 20 x 10^6 cells/ml and 2 (%w/v) fibers; (%w/v = %weight of fibers/volume of hydrogel). For fiber-reinforced silk hydrogel was prepared by pre-sonication 8% silk solution for 60 seconds at 12% amplitude and mixing with an equal volume of PBS containing silk fibers with or without cells to obtain final concentration of 4% silk hydrogel with 2 (%w/v) fibers. Cells/gel/fibers mixture was allowed to set and cored out from a gel slab by the method described above.

3.7 Construct cultivation

Constructs from hydrogel, porous scaffold fiber-reinforced hydrogel were maintained in culture for up to 42 days, with the twice weekly change of chondrogenic growth medium (hgDMEM supplemented with 5 mg/mL proline, 1% ITS+, 100 nM dexamethasone, 50 µg/mL ascorbate, and 10 ng/mL TGF-β3 for the first 2 weeks.

3.8 Diffusion measurement by FRAP

Acellular agarose and silk hydrogels (2.5 mm thick x 4 mm diameter) of 2 and 4 (%w/v) were soaked in a saturated (0.5 mg/mL) 70 kDa fluorescein-conjugated solution for over 24 hours. Samples were placed on a Olympus Fluoview FV1000 Confocal Microscope subjected to fluorescent recovery after photobleaching (FRAP) of a thin line using a 405 nm laser for 30 seconds. Images (320 x 320 pixels) were acquired using a 20X objective before, during, and after the photobleaching process, allowing for analysis using a custom MATLAB code according to (Albro+ 2009), which fits the FRAP to the Gaussian equation,

$$I(x,t) = \frac{M}{\sqrt{\pi w^2}} e^{-x^2/w^2}$$

in which I is the fluorescence intensity as a function of position (x) and time (t), M is the total amount of bleached species, and $w^2 = 4Dt$, with D being the diffusion coefficient. A linear regression was applied to a plot of w^2 against t ($R^2 \sim 0.99$) to acquire a value for D. D values outside two standard deviations were removed as outliers, and a 2-way ANOVA (Statistica, Tulsa, OK) with Tukey's Honest Significant Difference Test, $\alpha = 0.05$, was used to determine significance. For each group, $n > 5$ samples.

3.9 Mechanical properties

Compressive properties of constructs were measured in unconfined compression using a custom-made mechanical testing device (59). Constructs were placed in a testing chamber and equilibrated under a creep tare load of 0.5 g for 30 minutes. Stress-relaxation tests were performed at the ramp velocity of 1 μm/s up to 10% strain. The equilibrium Young's modulus (E_Y) was determined from the equilibrium stress-strain data.

3.10 Biochemical assay

Constructs (n = 5 per group and time point) were harvested on days 0, 7, 14, 21 and 28 and digested for 16 hours at 56 °C with 20 μl/ml papain in 1 mg/ml of proteinase K (Fisher Scientific, Pittsburgh, PA) containing 1mM iodoacetamide and 10 mg/ml pepstatin-A (Sigma Aldrich, St. Louis, MO). Total DNA content was quantified using PicoGreen assay (Invitrogen, Carlsbad, CA) following the manufacturer's protocol. For Proteoglycan content, aliquots of digested tissue samples were analyzed using the 1,9-dimethylmethylene blue dye binding (DMMB) assay to determine the glycosaminoglycan (GAG) content (60).

3.11 Scanning electron microscopy

Cell-free hydrogels were freeze-dried and the fractured sections were obtained using razor blade. The fractures surfaces were sputter-coated with gold/palladium in the presence of argon gas at room temperature. Amray 1830 scanning electron microscope was used to visualize surface features at 200x and 500x magnification.

3.12 Histology and immunohistochemistry

Constructs were fixed in 4% paraformaldehyde overnight at 4 ^{o}C, transferred to 70% ethanol, embedded in paraffin and sectioned at 8 mm. The sections were stained with hematoxylin and eosin for general evaluation, Alcian Blue for GAG, and picrosirius red for bulk collagen. Sections for immunohistochemistry staining were hydrated, and antigen retrieval was performed using heated 0.01 M citrate buffer with pH 6.0 for 15 minutes. Quenching of the endogenous peroxidase was done by immersing the sections in 0.3% H_2O_2/methanol for 10 minutes at room temperature. The sections were incubated with blocking serum (Vectastain ABC, Burlingame, CA) for 30 minutes at room temperature, rinsed with PBS, incubated overnight at 4 ^{o}C with 1:1000 of type II collagen monoclonal antibody (Millipore, Temecula, CA) and for 30 minutes with biotinylated secondary antibody (Vectastain ABC, Burlingame, CA). For signal enhancement and detection, Vectastain ABC Kit with peroxidase and DAB Peroxidase Substrate Kit (Vectastain ABC, Burlingame, CA) were added as described in the manufacturer's protocol.

3.13 Statistical analysis

Statistics were performed with STATISTICA software (Statsoft, Tulsa, OK). Data were expressed as the average ± SD of n = 4 - 6 samples per group and time point. The differences in construct properties between the groups were examined by analysis of variance ($\alpha = 0.05$), with DNA, matrix contents, E_Y or relative level of target gene expression as the dependent variable, followed by Tukey's Honest Significant Difference Test.

4. Results

4.1 Cartilage tissue formation in silk hydrogel and silk porous scaffold

Chondrocytes cultured in both silk formats demonstrated an increase of DNA content up to day 28 **(Figure 4A)**. The slightly reduction of DNA content observed on day 42 **(Figure 4A)** associated with an increase in wet weight. Specifically, there was a 29 and 42% increase of wet weight from day 28 to 42 for the hydrogel and porous scaffold groups, respectively. GAG content gradually accumulated in hydrogel, while in the porous scaffold group the GAG content reached a plateau on day 42 **(Figure 4B)**. The compressive modulus of porous scaffold group slowly increased and yield 123 ± 37 kPa on day 42, whereas the hydrogel group showed excellent mechanical properties of 174 ± 23 kPa **(Figure 4C)**.

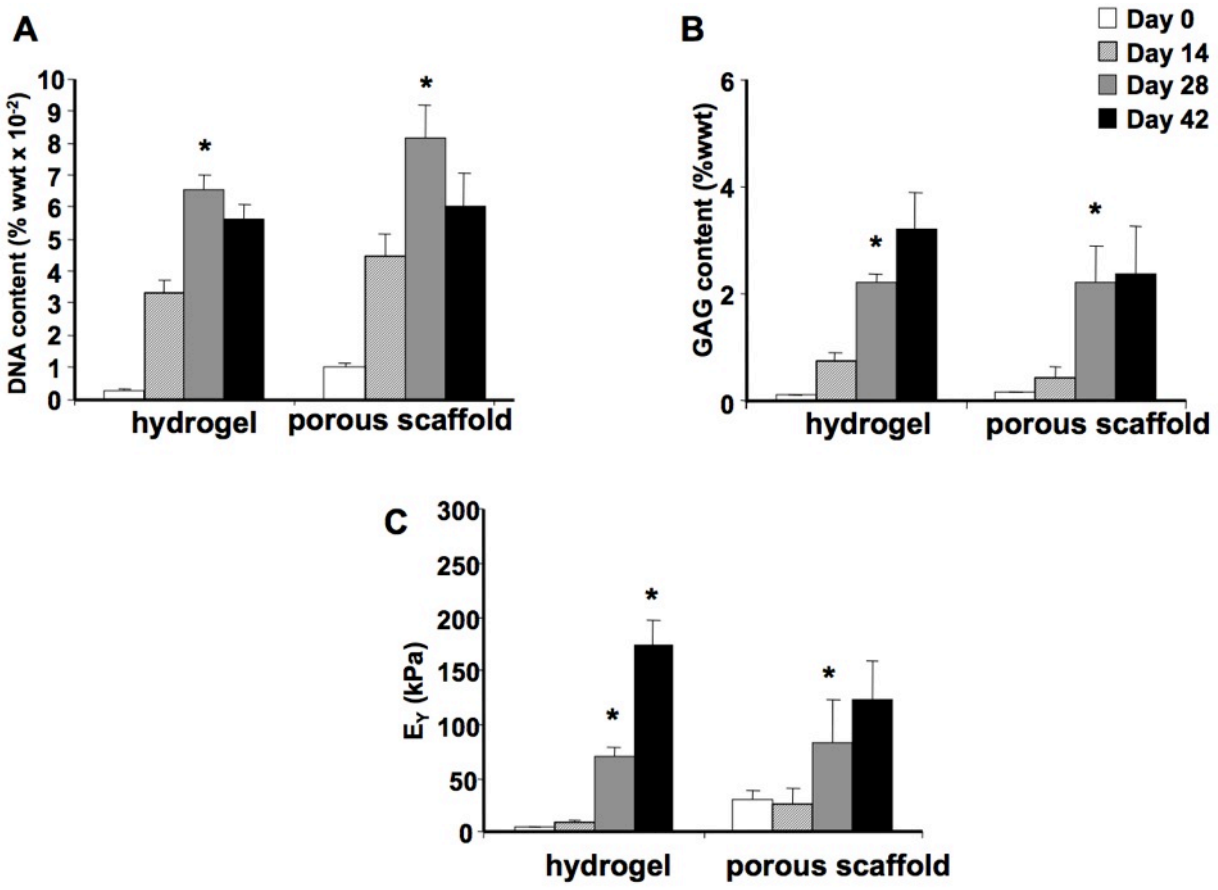

Figure 3. Biochemical content and mechanical properties of hydrogel and porous scaffold

DNA content **(A),** GAG content **(B)** and compressive modulus **(C)** were measured every 2 weeks (*$p < 0.05$ compared to the previous time point, n = 4).

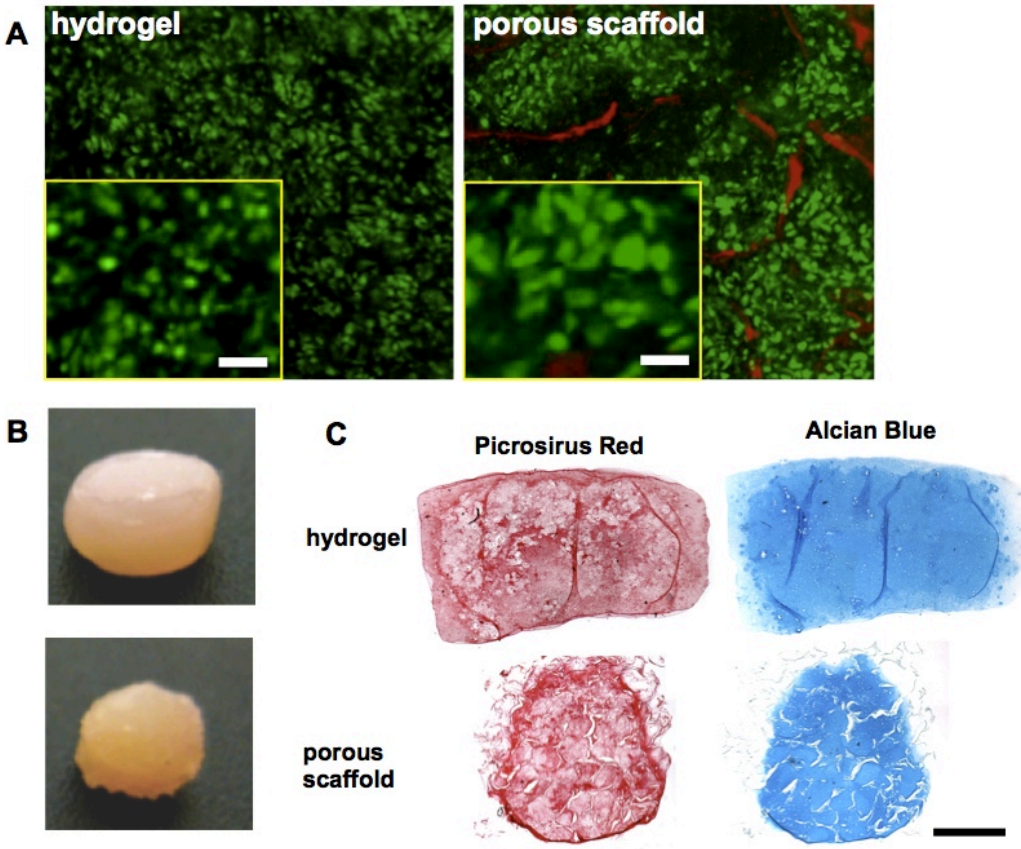

Figure 4. Cartilage tissue development in silk hydrogel and porous scaffold

A: Live/dead staining on Day 42 (insert-magnified for cell morphology, bar = 50 μm). **B**: Construct macroscopic view after 42 days of culture. **C**: Picrosirius red (top) and Alcian blue (bottom) staining for collagen and GAG content, respectively, bar = 1 mm.

Chondrocytes encapsulated in the silk hydrogel exhibited spherical morphology, in contrast to a fibroblastic, spindle-like morphology of cells in porous scaffolds (**Figure 5A**). In addition, cells appeared smaller in size in hydrogel than in the porous scaffolds. **Figure 5B** illustrates the macroscopic view of constructs after 42 days of culture. The silk hydrogel group

maintained the cylindrical disk shape with a smooth surface while the porous scaffolds appeared to be more irregular. Histological staining of collagen and GAG revealed uniform matrix distribution in the hydrogel construct with lacunae formations (**Figure 5C**). Furthermore, immunohistochemical staining revealed stronger and more uniform type II collagen staining throughout the constructs and faint type I collagen signal (**Figure 6**).

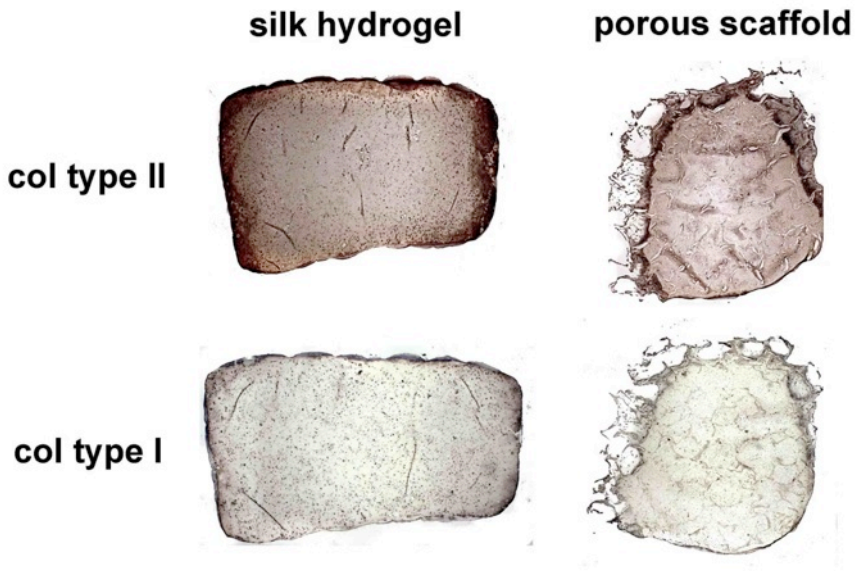

Figure 5. Immunochemistry of collagen type II and type I

Collagen type II was detected in hydrogel and porous scaffold constructs while low collagen type I was observed in both groups, bar = 1 mm

4.2 Intrinsic mechanical properties of materials

Equilibrium and dynamic (at 1 Hz) compressive moduli of the cell-free hydrogels and the porous scaffolds were compared to examine if the intrinsic mechanical properties could be a

factor in cartilage development **(Figure 7)**. Porous silk scaffold with sponge-like texture showed the highest mechanical properties. The 2% silk hydrogel used in cell encapsulation in previous study had the lowest equilibrium and dynamic moduli. Its mechanical properties of 2% silk gel were far behind agarose and porous silk scaffold. When concentration of silk increased from 2% to 4%, equilibrium modulus of silk gel (18 ± 2 kPa) was similar to agarose (14 ± 2 kPa). Interestingly, dynamic modulus of 4% silk gel (189 ± 29 kPa) was higher than that of agarose (64 ± 8 kPa) and approaching to that of silk porous scaffold (215 ± 72 kPa).

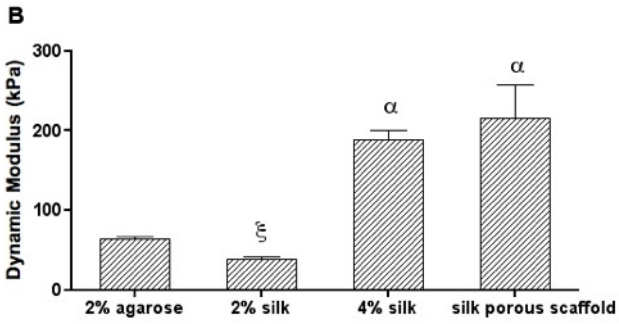

Figure 6. Intrinsic biomechanical properties of the materials

Equilibrium (A) and dynamic (B) modulus (at 1 Hz) (a $p < 0.05$ compared with the agarose hydrogel group, x $p < 0.05$ compared with the silk porous scaffold group, n = 3 - 5)

4.3 Diffusivity of solute molecule in silk hydrogel and agarose hydrogel

Diffusion coefficient (D) is a parameter that measures the rate of diffusive transport, and appears as a coefficient of the diffusion equation. The effects of hydrogel concentration on fluorescent tracers diffusivity in agarose and silk hydrogel was investigated using Fluorescence Recovery After Photobleaching (FRAP) technique. Hydrogels were bleached in a thin line to

generate region of interest (ROI) and fluorescence recovery by FITC-dextran (MV = 70 kDa) diffusion was monitored. Diffusion rate of FITC-dextran depended on the types and concentrations of a hydrogel, as demonstrated in **Figure 8**. The diffusivity of agarose and silk hydrogels significantly decreased when the concentration of the hydrogel was raised to 4%. Interestingly, 2% agarose did not show differences in solute transport as compared to 4% silk hydrogel**.** Because of this diffusive similarity, the samples with 2% agarose and 4 % silk hydrogel will be used for further comparison – first, with respect to the fiber sizes, and then with respect to their tissue development properties.

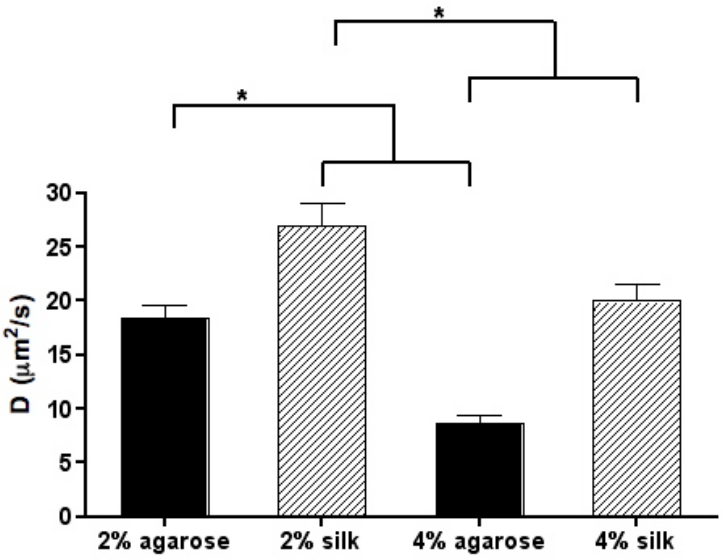

Figure 7. FITC-dextran diffusivity in agarose and silk hydrogels

Agarose and silk hydrogels were soaked with FITC-dextran overnight and measured diffusivity using FRAP technique. * indicates significant difference

4.4 Mechanical properties of fiber-reinforced hydrogels

Hydrogels obtained from previous studies were subjected to modify mechanical properties by silk fibers reinforcement. Acellular hydrogel constructs with various fiber sizes were formed in the dimension of 2.5 mm thick x 4 mm in diameter and measured equilibrium and dynamic moduli in an unconfined compression machine. The silk hydrogel with fibers showed an increase of mechanical properties in regard to different fiber sizes **(Figure 9)**. The highest equilibrium (34 ± 3 kPa) and dynamic (353 ± 56 kPa) moduli were found in silk hydrogel when it was reinforced by fibers 500 μm long. The dynamic modulus of all fiber-reinforced silk hydrogel groups responded to different frequencies. However, there was no mechanical improvement in agarose hydrogel associated with fiber reinforcement. Equilibrium and dynamic moduli did not show significant differences between reinforced agarose and agarose control group (no fibers).

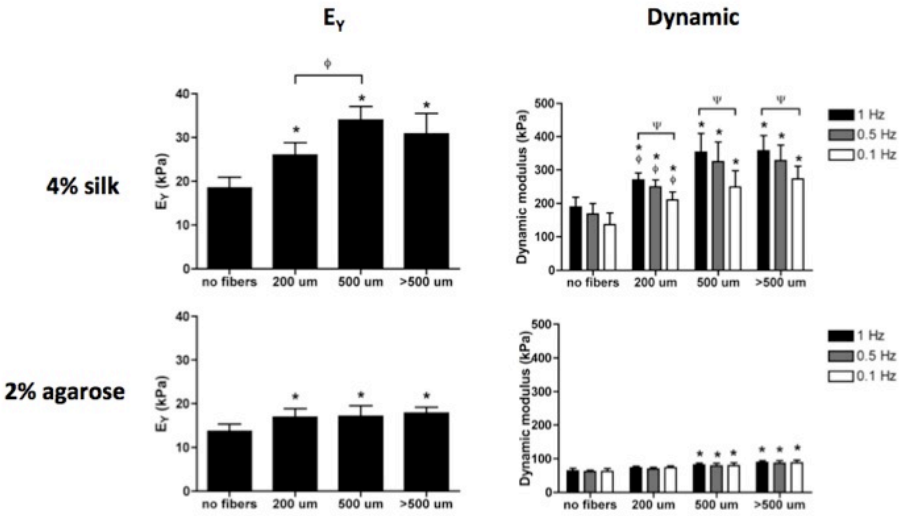

Figure 8. Mechanical properties of fiber-reinforced hydrogels

Cell-free constructs incorporated with different sizes of fibers were measured equilibrium and dynamic moduli. * $p < 0.05$ compare with control group (no fibers). $^{\Psi}$ $p < 0.05$ compare with 1 Hz within the same group, $^{\phi}$ $p < 0.05$ compare with 500 μm, (n = 20)

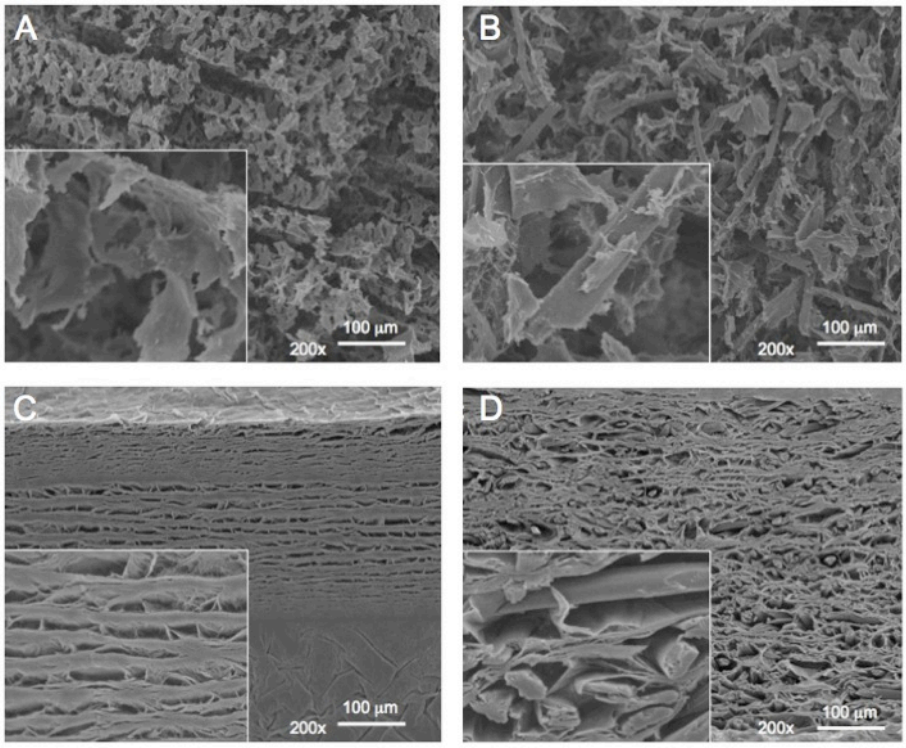

Figure 9. Scanning electron micrograph of fiber-reinforced hydrogels

Cell-free constructs of 4% silk and 2% agarose hydrogel were freeze-dried and visualized microscopic structures. Silk hydrogel **(A)**, fiber-reinforced silk hydrogel **(B)**, agarose hydrogel **(C)** and fiber-reinforced agarose hydrogel **(D)**. Silk fibers are clearly seen in 500x inserts

Microarchitecture of hydrogels and fibers was visualized under SEM. Silk hydrogel showed organized flake-like structures **(Figure 10A).** When fibers were introduced to create reinforced silk hydrogel, the disorientation of hydrogel flakes was observed and they could adhere to fibers **(Figure 10B)**. Agarose hydrogel formed intact layer with pores size between 30 – 50 μm **(Figure 10C)**, while reinforced agarose showed bigger pore size 50 – 100 μm **(Figure 10D)**. The fiber showed smooth surface and clearly separated from agarose hydrogel.

4.5 Cartilage tissue development in fiber-reinforced silk hydrogel

Mechanical integrity of engineered construct is important at the time of implantation to survive the harsh physical demands of joint loading. Acellular silk hydrogel constructs reinforced by fibers size 500 μm showed the highest mechanical integrity and thereby this reinforced fiber-silk hydrogel formula was subject to study tissue development compared to agrose hydrogel. Primary chondrocytes were encapsulated in silk hydrogel or fiber-reinforced silk hydrogel at a density of 20 x 10^6 cells/ml. Viability and distribution of encapsulated cells were observed under fluorescent microscope.

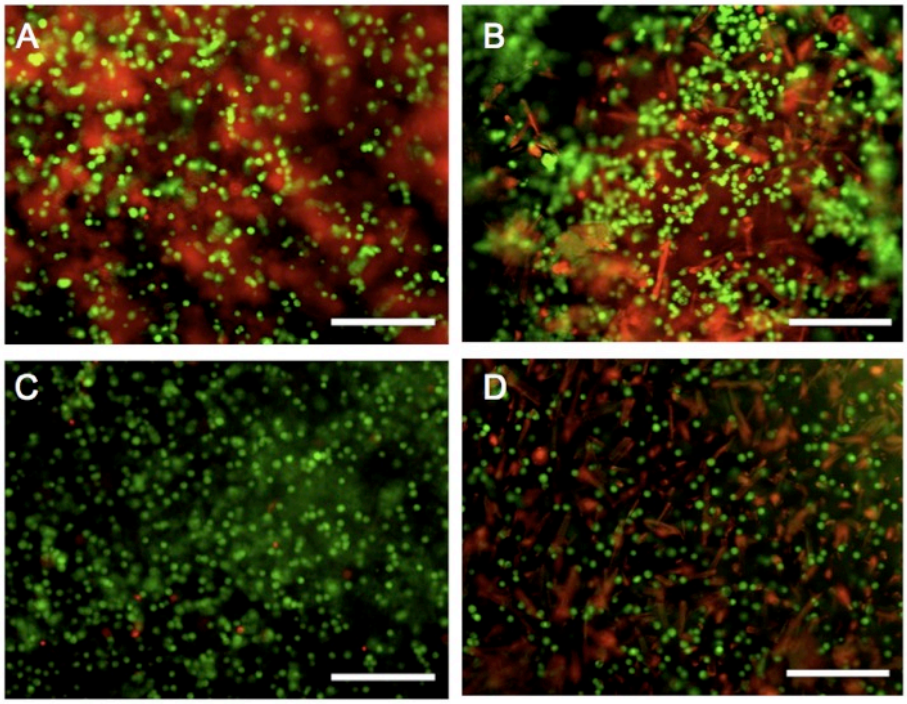

Figure 10. Chondrocytes seeded in hydrogel at day 3

Live/dead assay showed viable chondrocytes in hydrogel. Silk hydrogel (A), fiber-reinforced silk hydrogel (B), agarose hydrogel (C) and fiber-reinforced agarose hydrogel (D). Bar = 200 mm

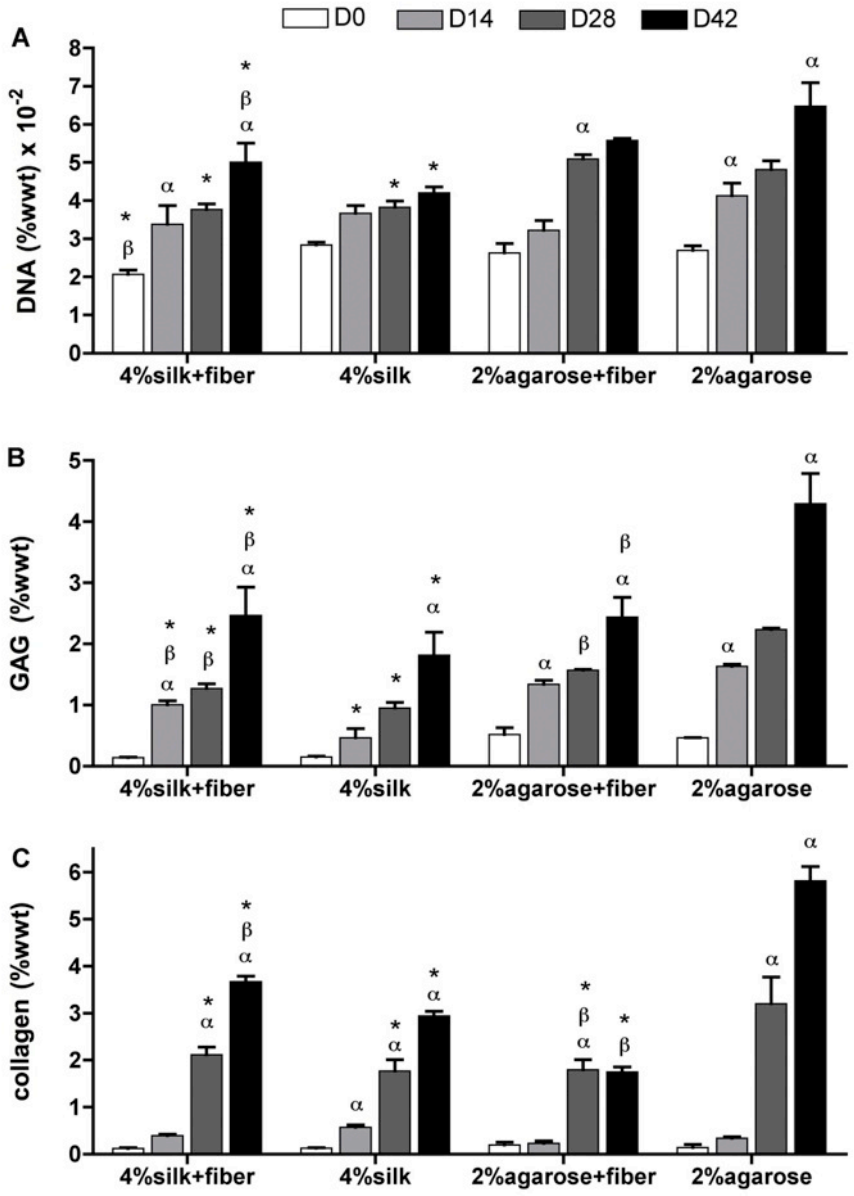

Figure 11. Biochemical assay of engineered cartilage constructs

DNA **(A)**, GAG **(B)** and total collagen **(C)** content. $^{\alpha}$ $p < 0.05$ compared to previous time point within the same group, $^{\beta}$ $p < 0.05$ compared effects of fiber reinforcement of the same hydrogel, * $p < 0.05$ compared to agarose at the same time point, n = 5

Chondrocytes encapsulated in hydrogels showed homogeneous cell distribution. Live cells were observed in constructs cultured at all hydrogel groups **(Figure 11)**. DNA content significantly increased over course of study in reinforced silk and agarose hydrogels **(Figure 12A)**. The beneficial effects of fibers on cell proliferation could be detected in silk hydrogel. On day 42, an increase in DNA content was observed in reinforced silk hydrogel compared to silk hydrogel without fibers. However, DNA content of reinforced agarose and agarose control was comparable at the end of study.

Silk fibers improved proteoglycan production as demonstrated by greater amount of GAG content at Day 42 in fiber-reinforced silk hydrogel (2.5 ± 0.5 (%wwt)) compared to silk hydrogel (1.8 ± 0.4 (%wwt)) **(Figure 12B)**. The control cartilage constructs made from agarose showed an excellent GAG content (4.3 ± 0.5 (%wwt)). Interestingly, in contrast to silk hydrogel, fibers did not improved proteoglycan production in agarose as shown in low GAG content (2.4 ± 0.3 (%wwt)) at the end of study.

Collagen content in native cartilage ranges from 7 to 16 (%wwt) depending on age and species (61). In this study, the highest collagen content was obtained in agarose group (5.8 ± 0.3 (%wwt)), whereas fiber-reinforced agarose had the lowest collagen content (1.8 ± 0.1 (%wwt)) **(Figure 12C)**. For silk hydrogel, combining fibers promoted collagen production as demonstrated by an increase of collagen content from (2.9 ± 0.1 (%wwt)) in silk hydrogel to (3.7 ± 0.1 (%wwt)) in reinforced silk hydrogel.

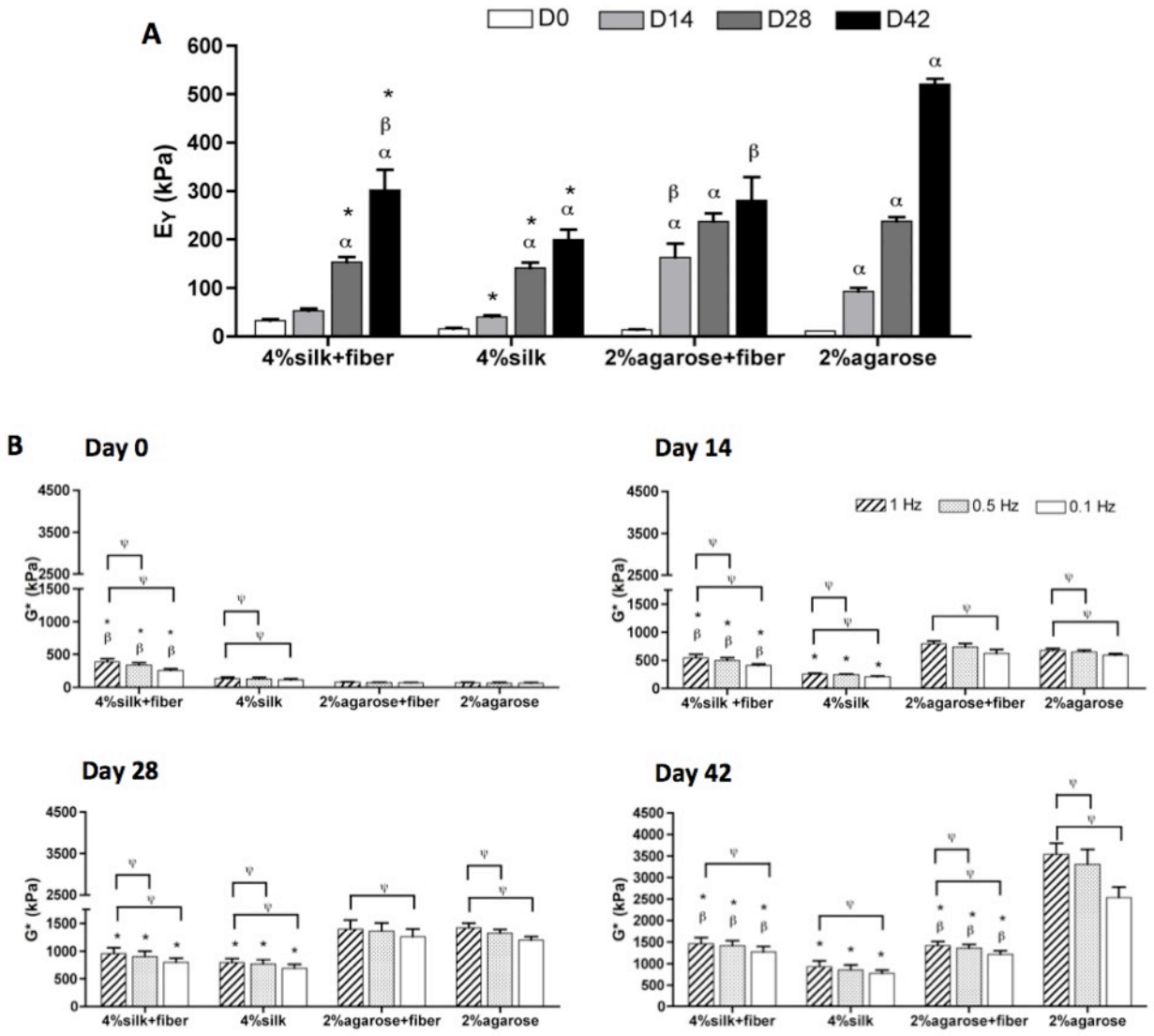

Figure 12. Mechanical properties of engineered cartilage constructs

Young's modulus **(A)** and dynamic modulus **(B)**. $^{\alpha}$ $p < 0.05$ compared to previous time point within the same group, $^{\beta}$ $p < 0.05$ compared effects of fiber reinforcement of the same hydrogel, * $p < 0.05$ compared to agarose at the same time point, $^{\Psi}$ $p < 0.05$ compare with 1 Hz within the same group, n = 5

4.6 Mechanical properties and matrix elaboration of fiber-reinforced hydrogels

Constructs (n = 5) in all groups were measured compressive modulus every week for 6 weeks. At end of culture period, agarose constructs yielded the highest compressive Young's modulus (E_Y) of 521 ± 11 kPa as compared to constructs made from fiber reinforced agrose (281 ± 48 kPa), silk hydrogel (201 ± 20 kPa), and fiber reinforce silk hydrogel (303 ± 42 kPa) **(Figure 13A)**.

In **Figure 13B**, fiber reinforcement effectively improved dynamic modulus of silk hydrogel, while combining fibers into agarose hydrogel adverse dynamic modulus of the constructs. It is interesting to note that dynamic modulus of constructs made from fiber-reinforced agarose was initially comparable to those made from agarose without fibers (day 0 to 28). Then after the day 28, reinforced agarose showed inferior mechanical properties **(Figure 13A – B)** and ECM composition **(Figure 12B - C)**.

By day 42, constructs made from fiber-reinforced silk hydrogel exhibited uniform cartilage-like tissue organization and glycosaminoglycan (GAG) production similar to those made from agarose **(Figure 14)**. Light GAG staining was observed in engineered cartilage constructs made from fiber-reinforced agarose and silk hydrogels **(Figure 14D)**. In **figure 15**, collagen type II was abundantly found in constructs made from agarose control compared to other hydrogels. Within the silk groups, fiber-reinforced constructs showed stronger collagen type II than fiber-free constructs **(Figure 15A and B)**. Immunostaining in **figure 15 E-H** was not able to detect collagen type I in all groups.

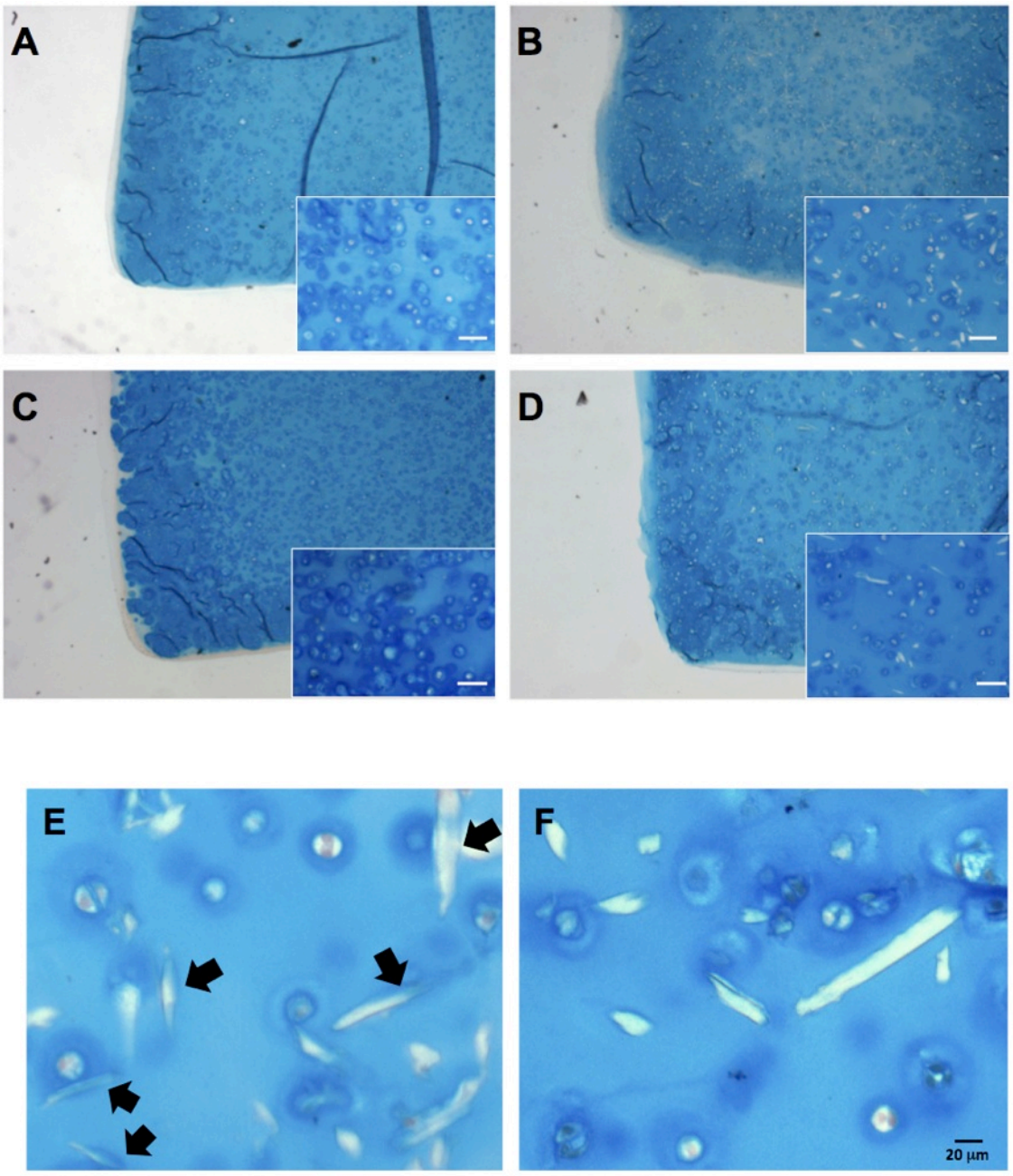

Figure 13. Alcian Blue staining for glycosaminoglycan

Glycosaminoglycan distribution in silk hydrogel **(A)**, reinforced silk hydrogel **(B)**, agarose **(C)** and reinforced agarose **(D)**, bar = 100 mm. Fibers and GAG co-localization is clearly seen in magnified images of reinforced silk hydrogel **(E)** as indicated by arrows, but not in agrose **(F)**.

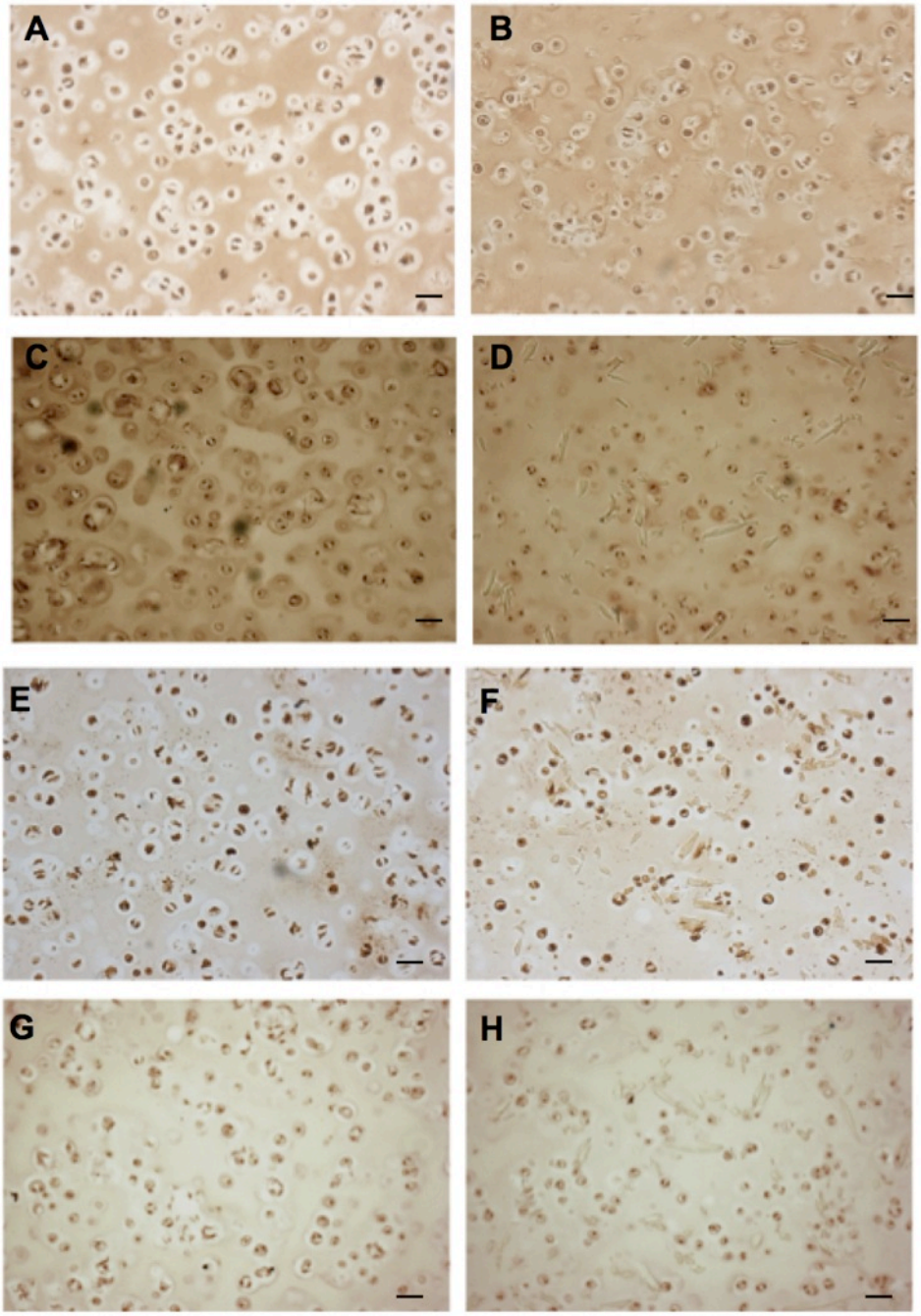

Figure 14. Immunohistochemistry for collagen

A-D: Collagen type II. **E-H:** Collagen type I. Silk gel **(A and E),** reinforced silk gel (B and F), agarose **(C and G)** and reinforced agarose **(D and H)**

5. Discussion

Unique characteristics of silk fibroin, which are repetitive primary sequence that leads to significant homogeneity in secondary structure β-sheet and physical crosslink of inter-peptide chains, generate a stable hydrophilic and neutral pH environment that supports cells. In previous study, it was shown that one particular type of silk hydrogel preparation can support tissue viability and yield cartilaginous constructs (58). A number of other hydrogels – alginate, collagen and chitosan – have been investigated for cartilage tissue engineering, however, none of these materials have resulted in mechanical functionality approaching that of native cartilage. At the beginning, 3D formats of silk fibroin (hydrogel and porous scaffold) were examined for cartilage development potential and the 2% silk hydrogel was used in comparative aspects to 2% agarose hydrogel, the "gold standard" of engineered cartilage. Even though the 2% silk hydrogel had, at the start, 6 times less mechanical properties than those of porous scaffold, the resultant cartilaginous tissues of silk hydrogel constructs showed higher mechanical properties and more matrix content on day 42 than those made of porous scaffold. This finding suggested that the initial mechanical properties of materials are not the only factor to direct cartilage tissue formation. Chondrocytes prefer to reside in 3D hydrogel matrix rather than in porous structures. The hydrogel may provide immediate locations for newly synthesized matrix to deposit as compared to porous scaffold does.

An intensive investigation of silk hydrogel concentration contributing to mechanical integrity revealed that the mechanical and mass transport properties of the 2% silk hydrogel did not match those of the 2% agarose hydrogel. When concentration of silk hydrogel increased to 4%, its equilibrium modulus was comparable to that of 2% agarose. Also, the diffusivity of 70 kDa FITC-conjugated molecules, which are approximately the same size as growth

factors/cytokines, in the 4% silk hydrogel was similar to their diffusivity in the 2% agarose hydrogel. To this end, hydrogel mechanics and diffusivity of soluble molecules in the gel matrix are governed by the concentration of silk fibroin. There is a concern that an increase of the silk concentration that was meant to provide an increase of mechanical support may also cause the impedance of the transport of nutrients and waste products into and out of cells in constructs with high hydrogel concentration. However, we demonstrated that the 4% silk hydrogel was found to support cell viability and ECM production.

Mechanical function is desired of the engineered cartilage to prevent joint loading, as soft constructs may fail upon implantation. Taking advantage of the versatility of silk fibroin, the composite substrate for cell encapsulation was systematically developed. Fiber-reinforced silk hydrogel is meant to create a functional cartilage constructs with immediate mechanical support at the shortest possible culture time. Silk fibers form a mesh-like structure and provide tensile stress as collagen fibers do in native tissue. Acellular constructs of fiber-reinforced hydrogels were tested for the optimal length of fibers, which give gel the highest mechanical properties, and this fiber-gel composite was used as a supporting material to assess tissue development. The 4% silk hydrogel reinforced by 500 μm fibers showed the highest mechanical when fibers were added to the final concentration of 2 (%w/v). Fiber-reinforced silk hydrogel constructs showed promising tissue development in term of higher GAG content, collagen type II elaboration and mechanical properties compared to unreinforced constructs. Surprisingly, fiber-reinforced agarose constructs showed inferior cartilage tissue properties compared to the agarose control.

The discrepancy of biochemical and mechanical properties of fiber-reinforced agarose can be explained by discontinuity at the interphase boundary between fiber and agarose hydrogel. The reinforced agarose had low GAG staining where the silk fibers are located, whereas the

fibers embedded in silk hydrogel were surrounded by GAG **(Figure 14E).** Silk fibers and silk gel are the same protein-based materials, which were homogeneously mixed and the fiber-gel adhering was observed under scanning electron micrographs **(Figure 10B).** In contrast to reinforced-agarose, fibers and gel were clearly separated **(figure 14F).** Further studies will elucidate the underlying fiber-gel interaction that causes positive and negative effects on tissue formation, i.g., we may study the local stain around where fiber-gel is present.

Agarose has been used as a "gold standard" for developing cell-based repair for cartilage injuries, because it yields mechanical and tissue properties approaching to those of native tissues. However, agarose is nondegradable and has minimal capability for customizing its structure and composition, which seriously limits systematic studies of chondrogenesis as a function of hydrogel properties. Silk is biodegradable and has been FDA approved as an implant material for soft tissue repair (62). This dissertation has demonstrated the feasibilities of silk fibroin for generation of engineered constructs that is compatible to agarose, and therefore silk fibroin could be an alternative material for cartilage tissue engineering. Versatility of material formats is needed for elucidating the mechanism that underlies the efficacy of hydrogel for cartilage tissue development. A comparative study of tissue formation in the same material but in different formats may lead to the understanding of required scaffold properties for a particular tissue and provide a systematic modification of biomaterials for every tissue engineering.

6. Summary

Silk fibroin could be fabricated into various formats (hydrogel and fibers) and was demonstrated to be a novel composite material for cartilage tissue engineering. The 4% silk hydrogel showed similar mechanical and diffusional properties to the 2% agarose hydrogel.

Texture and dynamic modulus of this silk hydrogel were modified by silk fibers, which might play a similar role to collagen in native tissues. The resulting fiber-reinforced silk hydrogel supports cell viability and yields constructs with promising mechanical properties. Together with biocompatibility and biodegradability, silk fibroin is an attractive biomaterial for cartilage tissue engineering.

CHAPTER 4

Chondrogenic differentiation of human embryonic stem cells – recreating physiological conditions of articular joints: hypoxia and chondrocyte-secreted factors

1. Background

Cell-based cartilage tissue engineering offers therapeutic options for patients with cartilage injury and osteoarthritis (33). Tissue engineering involves combining cells with matrices in order to support cell growth and *de novo* extracellular matrix accumulation and growing cell/matrix constructs under optimal conditions, supplemented with chondrogenesis-inducing factors. In this respect, the cells serve as basic building blocks, which respond to the chemical and physical stimuli applied in culture system and preserve characteristics of specific tissues. Chondrocytes isolated from articular cartilage and expanded *in vitro* have been widely used in cartilage tissue engineering. However, the complications associated with invasive procedures, donor site morbidity, chondrocyte de-differentiation during expansion and fibrocartilage formation at implanted sites are motivating the search for new cell sources for cartilage tissue engineering (6).

Adult stem cells, e.g., from bone marrow (human mesenchymal stem cells, hMSCs) and fat (human adipose-derived stem cells, hASCs) have been studied over the last two decades and exhibit varying degrees of proliferation and chondrogenic differentiation potential (63, 64). The

low success of hMSCs and hASCs chondrogenic differentiation may be due to limited self-renewal and differentiation with increasing donor or patient age, and/or impaired articular chondrogenic lineage commitment (65). Importantly, differentiation pathway of MSCs *in vivo* is very tightly regulated since the same pathway of endochondral ossification is responsible for both bone and cartilage development (66). In order to effectively recapitulate the chondrogenesis from MSCs, it is necessary to have a very stringent control of MSC differentiation to chondrocytes, to avoid premature hypertrophy, mineralization and ossification (67). However, most common *in vitro* protocols induce in MSCs an unnatural pathway of differentiation to chondrocyte-like cells that fails to produce permanent cartilage formation. Umbilical cord stem cells (USCs) are considered to be earlier stage than adult stem cells and to contain proliferative mesenchymal progenitor cells which can differentiate into osteoblasts, chondrocytes and adipocytes (68, 69). Despite the fact that USCs show promising differentiation potential, engineered chondrogenic tissues derived from USCs produced collagen type I which is abundantly found in fibrocartilage (70). Moreover, an umbilical cord contains mostly hematopoietic stem cells in much higher percentage than mesenchymal stem cells, thereby USCs are not the best source of cells for chondrognesis.

Pluripotent human embryonic stem cells (hESCs) possess the capacity to differentiate into all germ layers and offer an opportunity to obtain an unlimited supply of cells for cartilage tissue engineering. hESCs line H9 were derived from inner cell mass of a blastocyst in 1998 (71) and have been continuously used in tissue engineering research (72, 73). Chondrogenic differentiation of H9 has been achieved *in vitro* by using different combinations of growth factors and supplements to induce the chondrogenic lineage from hESC colonies or embryoid

bodies (EBs), followed by progenitor cell expansion in monolayer culture, and cartilage-like tissue development in monolayer, pellets and hydrogels (74-76).

In addition to soluble supplements in culture media and physical forces provided by the bioreactors, oxygen tension has been shown to regulate chondrogenic differentiation. Beneficial effects of hypoxia have been widely accepted for up-regulating the expression of *Sox9*, a key transcription factor of chondrocyte differentiation (26). However, the effects of low oxygen tension on early chondrogenic induction of hESCs have not been evaluated despite the fact that cartilage tissue formation *in vivo* occurs in hypoxic environment.

In the first part of this study, bovine chondrocytes, the standard cell model in cartilage engineering with well described characteristics, were used for optimizing cell culture conditions under low oxygen tension. In the next step, the established hypoxic condition protocol in conjunction with soluble biochemical cues from bovine chondrocytes was applied to the novel cellular model comprised of cultured human EBs to induce chondrogenic differentiation.

2. Specific aims

Aim 1. To study the effects of hypoxia-normoxia regimes on cartilage tissue properties in a robust cellular model

The regulation of cartilage ECM production under low oxygen tensions is studied to determine if hypoxia is a favorable condition for maintaining cartilage structure and function. The investigation is carried out using bovine chondrocyte-laden agarose hydrogel. Engineered cartilage constructs are cultured in hypoxic condition (5% O_2) with various exposure times and tested for tissue properties compared to those cultured under normal oxygen levels (21% O_2).

<u>Aim 2.</u> To establish protocol for chondrogenic differentiation of hESCs through combined controlled oxygen tension and molecular conditioning

The limited self-renewal and differentiation of human mesenchymal stem cells (hMSCs) with increasing patient age have motivated utilization of human embryonic stem cells (hESCs) for chondrogenic differentiation. Soluble morphogenetic factors secreted from bovine chondrocytes in conjunction with hypoxia are used to induce embryoid bodies (EBs) for 3 weeks. The resulting induced cells were evaluated for chondrogenic differentiation potentials in pellet culture for 6 weeks.

3. Methodology

3.1 Aim 1 materials and methods

3.1A Preparation of cell-agarose constructs

Bovine chondrocytes were encapsulated in agarose hydrogel at a final concentration of 20 x 10^6 chondrocytes/ml in 2% agarose. The cell-agarose mixture was cast between two sterile glass plates separated by a 1 mm spacer to form a rectangular slab (70 mm x 80 mm x 1 mm). Cylindrical discs were cored out using biopsy punch and then transferred into 24 well plates integrated with an oxygen sensor platform (PreSens, Germany). Each construct was cultured in a separate well in 1 ml of chondrogenic medium with medium changed twice a week. For the first 14 days, chondrogenic medium was additionally supplemented with 10 ng/ml TGF-β3 (Invitrogen, Carlsbad, CA).

3.1B Experimental design

All experiments were performed in triplicate, using 4 joints in each of the three individual studies (n = 12 joints total). Data are represented as mean ± SD for n=5 constructs engineered using cells from one animal, to minimize batch-to-batch variability, as reported in several previous studies (77, 78). Cartilage constructs were cultured in static culture under three different oxygen supply regimes as shown in **Figure 16**. ***Normoxic group*** (21% oxygen for 28 days) was cultured in a chamber (Billups-Rothenberg, Inc., Del Mar, CA) that was maintained in humidified air containing 21% O_2, 5% CO_2 (normal incubator conditions). ***Hypoxic group*** (5% oxygen for 28 days) was cultured in an airtight chamber flushed daily with a humidified gas mixture (5%O_2, 5%CO_2 and 90%N_2) to equilibrate culture medium at 5% oxygen. ***Reoxygenated group*** was maintained at 5% O_2, 5% CO_2, and 90% N_2 for 7 days and then transferred to 21% O_2, 5% CO_2 and 90% N_2 for additional 21 days. Humidity was maintained by adding 20 ml water into a Petri dish placed in the chamber. To validate the consistency of oxygen levels during cultivation, oxygen levels in culture medium were monitored continuously by oxygen Sensor Dish Reader (PreSens, Germany) for 20 hours after each medium change (**Figure 16**).

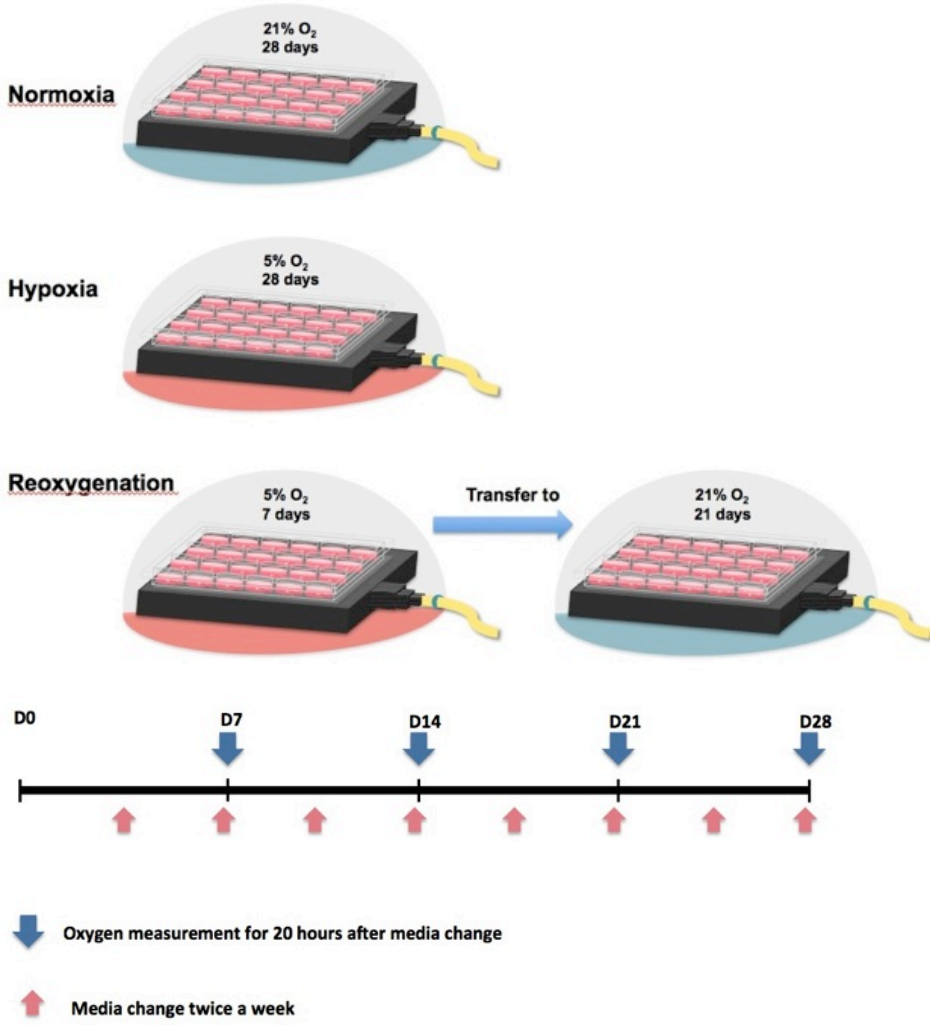

Figure 16. Experimental design of transient hypoxia on cartilage tissue formation

Tissue constructs were cultured in 24 well plates. Each well contained one tissue construct and was fitted with an oxygen sensor that measured oxygen concentration in real time by using a SDR SensorDish® Reader. Normoxic and hypoxic groups were maintained at 21% O_2 and 5% O_2, respectively, for 28 days. Reoxygenation group was maintained at 5% O_2 for 7 days followed by 21% O_2 for 21 days. Medium was changed twice a week (red arrows). Oxygen levels were measured and recorded for 20 hours after media replacement (blue arrows).

3.1C Measurement of cartilage tissue properties

Constructs (n = 5 per group and time point) were harvested on days 0, 7, 14, 21 and 28 and analyzed for DNA content, GAG content, and cartilaginous gene expression. Equilibrium modulus (E_Y) of constructs was accessed every 2 weeks. At the end of culture period (day 28), constructs were harvested and specifically detected for collagen type II using ELISA. Histology analysis was performed to visualize extracellular matrix distribution. All methods were described in **Appendix A.**

3.2 Aim 2 materials and methods

3.2A Cell culture

hESCs (H9) were maintained in 6-well plates on mouse embryonic fibroblast (MEF) feeders (Globalstem) in hESC medium composed of DMEM-F12, 10% Knockout Serum Replacer, 1 mM L-Glutamine, 0.1 mM MEM Non-essential Amino Acids, 0.1 mM 2-Mercaptoethanol and 4 ng/ml bFGF. hESCs were passaged every 3-4 days with daily medium changes. Human mesenchymal stem cells (hMSCs) were obtained from Lonza, seeded at a density of 5 x 10^3 cells/cm^2 and cultured in expansion medium (highGlucose DMEM 10%, FBS, 100 U/ml penicillin, 100 μg/ml streptomycin and supplement with 0.1 ng/ml bFGF) with medium changes twice a week.

3.2B Embryoid body (EB) formation and induction

hESCs cultures were incubated in 1 mg/ml collagenase IV (Life Technologies) in Knockout DMEM at 37 °C for 5 min. Collagenase IV solution was aspirated and replaced with 2

ml of hESC medium (KnockOut™ DMEM, 25% KnockOut™ Serum Replacement, 1 mM $_L$-Glutamine, 100 nM 2-Mercaptoethanol, 1x non-essential amino acid, 4 ng/ml b-FGF). Peeled hESC colonies were removed from wells by cell scrapers, transferred into 50 ml conical tube and centrifuged at 200 x g for 5 minutes. Supernatant was discarded and replaced with chondrocyte-conditioned medium (CCM). Cell suspension was mixed, distributed into Ultra-Low Attachment 6 well plates (Corning, Tewksbury, MA) and cultured as noted in specific studies, with medium changes twice a week.

3.2C Chondrocyte-conditioned medium (CCM)

Bovine chondrocytes were isolated from carpometacarpal joints of 4 to 6 month-old bovine calves as described previously (4). Chondrocytes were seeded at a high density of 2.5 x 10^5 cells/ cm^2 and cultured in growth medium (highGlucose DMEM 10%, FBS, 100 U/ml penicillin, and 100 μg/ml streptomycin) for 24 hours. Attached cells were rinsed twice with PBS. Conditioned medium was obtained by incubating the chondrocyte cultures in growth medium without FBS for 48 hours. The medium was collected, passed through 0.2 μm filtered, and kept in 20 ml aliquots at -80 ºC until use. Chondrocyte conditioned medium (CCM) was prepared by diluting the filtered medium (1:1) with fresh growth medium to get a final concentration of 5% FBS for EB induction.

3.2D Experimental designs of EB induction and chondrogenic differentiation

Study 1. Effects of conditioned medium and hypoxia on EBs gene expression

EBs were prepared and cultured in CCM or growth medium with 5% FBS. Three groups were compared (**Figure 17**): EBs in CCM cultured at 5% O_2, EBs in CCM cultured at 21% O_2, and

EBs in growth medium cultured at 21% O_2 (control group). EBs were cultured for 3 weeks, and collected weekly to assay gene expression.

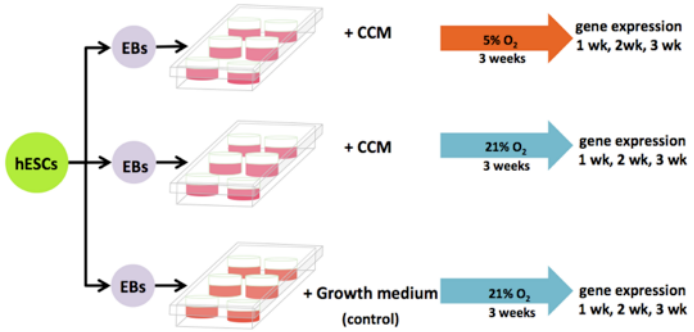

Figure 15. Study 1 experimental setup: effects of conditioned media and hypoxia on EBs induction

EBs were prepared from hESCs and cultured in CCM or growth medium for three weeks under 5% O_2 or 21% O_2 to determine the effects of media and oxygen levels on gene expression.

Study 2. Effects of hypoxic culture duration on EBs induction

EBs were prepared and cultured in CCM for total of 3 weeks. Four groups were compared: 3 weeks of 5% O_2 ***(hypoxia group)***, 2 weeks of 5% O_2 followed by 1 week of 21% O_2 ***(transient 2 hypoxia group)***, 1 week of 5% O_2 followed by 2 weeks of 21% O_2 ***(transient 1 hypoxia group)*** and 3 weeks of 21% O_2 with no hypoxic exposure ***(normoxia group)***. At the end of experiment, EBs were collected to assay gene expression (**Figure 18**).

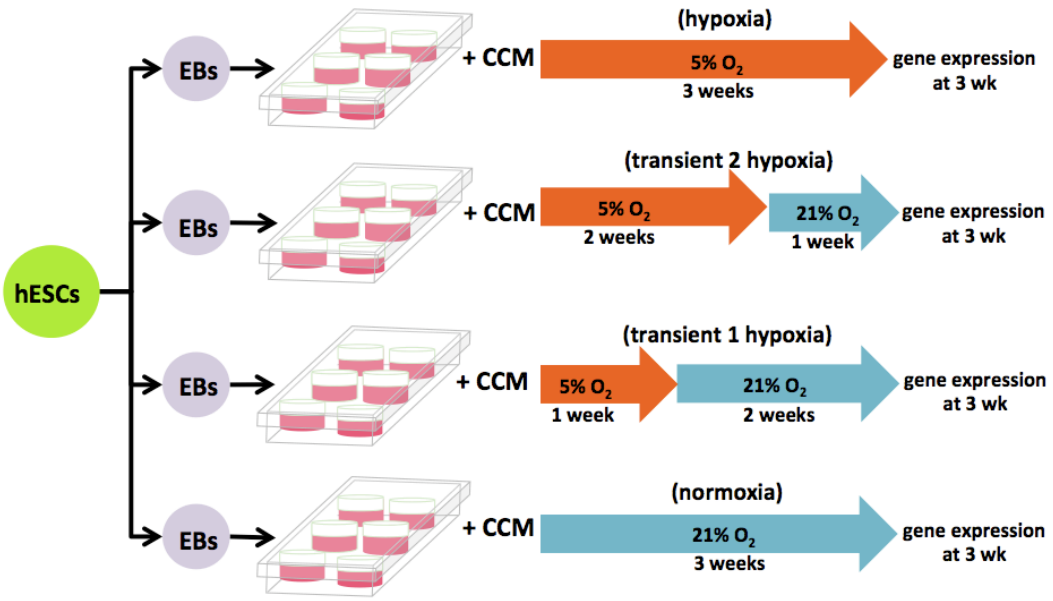

Figure 16. Study 2 experimental setup: effects of hypoxic culture period on EBs induction

EBs were induced in CCM with different hypoxic (5% O_2) exposure periods: 3 weeks (hypoxia group), 2 weeks (transient 2 hypoxia), 1 week (transient 1 hypoxia) and no exposure (normoxia).

Study 3. Chondrogenic differentiation of cells induced in EBs

Chondrogenic differentiation potential of EBs derived from i) ***transient 2 hypoxia group***, the best induction condition from **Study 2**, and ii) ***normoxia group*** were compared. After 3 weeks of induction, the EBs were dissociated into single cells (79), counted and 2 x 10^5 cells were used to prepare chondrogenic pellets. The pellets were cultured for 6 weeks under 21% O_2 in chondrogenic medium (ChondM), composed of high glucose DMEM supplemented with 10 ng/ml TGF-β3 (Peprotech, NJ), 5 mg/ml proline, 1% ITS+ (BD Biosciences), 100 nM dexamethasone (Sigma), 50 µg/ml ascorbate-2-phosphate (Sigma), 10 mM HEPES, 100 U/ml penicillin, and 100 µg/ml streptomycin, with medium changes twice a week. Chodrogenic differentiation control pellets were prepared from 2 x 10^5cells hMSCs and cultured in parallel

(Figure 19). Pellets were collected weekly to assay gene expression, and at the end of experiment for biochemical analyses and histology.

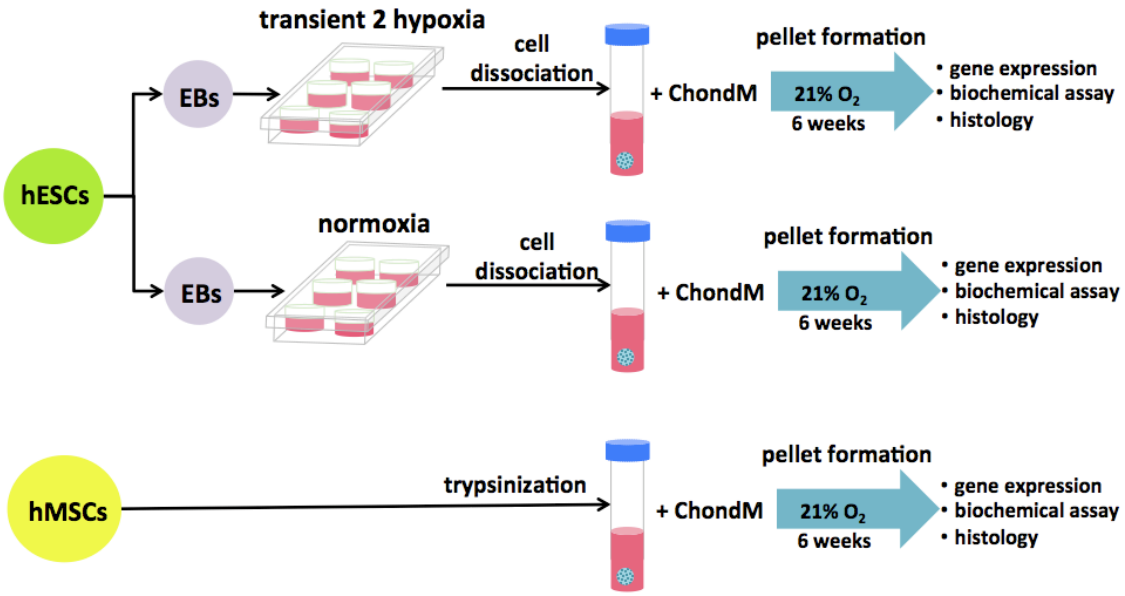

Figure 19. Study 3 experimental setup: chondrogenic differentiation of EB-induced cells

Pellet culture was used to assess the potential for cartilage tissue formation. *Transient 2 hypoxia* EBs and *normoxia* EBs were dissociated into single cells, pelleted and cultured in ChondM for 6 weeks. hMSC pellets were used as chondrogenic differentiation control.

3.2E Embryoid body and pellet dissociation

The EBs and chondrogenic pellets (1 week) were dissociated into single cells as previously described (79). Briefly, EBs or pellets were collected, washed in PBS and incubated in 0.2% collagenase type II (Gibco) for 1 hour at 37 ºC. The cell suspension was centrifuged at 200 x g for 5 minutes, discarded supernatant, and incubated in 0.25% trypsin for 5 minutes at 37 ºC. Then, an equal volume of DMEM containing 10% FBS was added to quench the enzymatic

digestion. Clumped cells were dissociated by drawing the cell suspension through a 20G needle for 6 -10 times. Dissociated EBs were washed with DMEM and resuspended in ChonM for chondrogenic differentiation in **Study 3**. An aliquot of dissociated pellets was washed with PBS and subjected to stain with antibodies for flow cytometric analysis.

3.2F Flow cytometry

Dissociated pellets (1 week) and washed out cells from those pellets were rinsed with PBS, counted and 2 x 10^5 cells were resuspended in staining buffer (1% BSA in PBS). Cells were stained with N-cadherin monoclonal antibody conjugated with DyLight®488 (clone EPR1792Y, Abcam) at 4 ºC for 30 minutes and fixed in 4% paraformaldehyde and incubated at 4 ºC for 15 minutes. Analysis was performed on the BD FACSCalibur™ (BD). For control, cells were stained with rabbit IgG isotype antibody (clone ab153686, Abcam).

3.2G Soluble receptors array of embryoid bodies

To determine differential expression of soluble receptors of EBs which were induced in *transient 2 hypoxia* condition, total protein from *transient 2 hypoxia* EBs was extracted and prepared using Proteome Profiler™ Array according to the manufacturer's instructions (R&D Systems). The array contains 119 antibodies specific for soluble receptors printed duplicate on membrane. Chemiluminescent signals generated from Streptavidin-HRP were detected by Image Station 4000MM Pro (KODAK) and analyzed using ImageJ software (National Institutes of Health). The intensity signals of induced EBs were normalized with those of non-induced EBs which were cultured in DMEM containing 5% FBS under 21% O_2 for 3 weeks. Predicted protein functional interaction was generated from Search Tool for the Retrieval

of Interacting Genes/Proteins (STRING 9.0) based on occurrence, co-expression, experiments and text mining database (80).

3.2H Real-time PCR

Total RNA was extracted from embryoid bodies and chondrogenic pellets using RNeasy® Mini Kit, and the DNA was removed by RNase-Free DNase Set according to the manufacturer's instructions (QIAGEN). Total RNA was quantified using NanoDrop™ Spectrophotometer (Thermo Scientific, Wilmington, DE), and 10 ng was used for reverse transcription with High Capacity cDNA Reverse Transcription Kit (Applied Biosystems®). Gene expression was evaluated using the StepOnePlus™ Real-Time PCR system (Applied Biosystems®). The following TaqMan® Gene Expression Assays were used for detection of transcription factors: *SOX9* (Hs01001343_g1), *RUNX2* (Hs00231692_m1), *FOXA2* (Hs00232764_m1), *PAX6* (Hs00240871_m1), *OCT4 or POU5F1* (Hs01654807_s1) and *NANOG* (Hs02387400_g1), extracellular matrix components: *COL1A1* (Hs01076780_g1), *COL2A1* (Hs00264051_m1), *COL10A1* (Hs00166657_m1) and *ACAN* (Hs00153936_m1), and cell adhesion molecule: *CDH2* encoding N-cadherin (Hs00983056_m1). Gene expression values were normalized to *GAPDH* (Hs02758991_g1) by the $2^{-\Delta Ct}$ method (81). All reactions were performed in triplicates. Representative graphs are shown with error bars indicating standard deviation of 4 samples for each time point.

3.2I Mesenchymal stem cell PCR array

RNA samples of hESCs-derived pellets from *transient 2 hypoxia* EBs at week 4 and hMSCs (reference cells) were isolated, treated to remove genomic DNA and used for cDNA synthesis by using RT^2 First Strand Kit (QIAGEN). Microarray was performed in 96 well format of RT^2 Profiler PCR Array of Human Mesenchymal Stem Cells (QIAGEN) using RT^2 SYBR Green Fluor qPCR Mastermix (QIAGEN). The array has collection of genes involved in hMSC-specific markers, hMSC differentiation markers (chondrogenesis, ostogenesis, adipogenesis), stem cell markers and other genes associated with hMSCs. House keeping genes, validation of genomic DNA contamination, reverse transcription and PCR transcription control were included in the array. The C_T values were analyzed using web-based data analysis software (QIAGEN) to determine fold changes at p-value < 0.05.

3.2J Histology, immunohistochemistry and immune fluorescence

Chondrogenic pellets were fixed in 4% paraformaldehyde overnight at 4 ºC, transferred to 70% ethanol, encapsulated in HistoGel™ (Thermo Scientific), embedded in paraffin and sectioned at 5 μm. The sections were stained with Alcian Blue to detect glycosaminoglycanes (GAG) using standard procedures. Collagen type I and type II were evaluated by immunohistochemistry. Pellet sections were rehydrated, and antigen retrieval was performed using heated 0.01 M citrate buffer (pH 6.0) for 15 minutes. Blocking endogenous peroxidase activity was performed by immerging the sections in 0.3% H_2O_2/methanol for 30 minutes at room temperature. The sections were incubated with blocking serum (Vectastain ABC, Burlingame, CA) for 30 minutes at room temperature, rinsed 3 times in PBS for 5 minutes each, incubated overnight at 4 ºC with 1:100 mouse anti-human IgG collagen type I or type II

monoclonal antibodies (Millipore, Temecula, CA), washed and incubated for 30 minutes with biotinylated secondary antibody. For signal detection, Vectastain ABC Kit with peroxidase and DAB Peroxidase Substrate Kit were added as described in the manufacturer's protocol (Vectastain ABC, Burlingame, CA). For human nuclei immunofluorescence staining, the sections were permeabilized with 0.2% Triton X-100 in PBS for 45 minutes, blocked with normal goat serum for 1 hour at room temperature, incubated overnight at 4 ºC with 1:100 anti-human nuclei antibody (clone 235-1, Millipore, Temecula, CA). The sections were incubated with goat anti-mouse IgG secondary antibodies conjugated with FITC and counterstained with DAPI.

3.2K Biochemical analysis

Chondrogenic pellets (n = 4) were harvested every week and digested for 16 hours at 56 ºC with 20 µl/ml papain in 0.5 mg/ml of proteinase K (Fisher Scientific, Pittsburgh, PA) containing 1 mM iodoacetamide and 10 mg/ml pepstatin-A (Sigma Aldrich, St. Louis, MO). Aliquots of digested pellets were analyzed for the glycosaminoglycan (GAG) content using the 1,9-dimethylmethylene blue dye binding (DMMB) assay (60). GAG content was normalized to DNA content which was quantified using PicoGreen assay (Invitrogen, Carlsbad, CA) following the manufacturer's protocol.

3.2L Western blot analysis

Chondrogenic pellets were washed in PBS and homogenized in buffer containing 50 mM Tris-HCl, pH 7.4, 150 mM NaCl, 1% Triton X-100, 0.1% SDS and protease inhibitor cocktail (Sigma). Tissue lysate was centrifuged at 4 ºC for 10 minutes at 12,000 x g. The supernatant was

transferred to a new tube and the total protein concentration was quantified. Equal amount of protein of 15 μg was fractionated for all groups by 10% SDS-PAGE and transferred to PVDF membrane using standard protocol. Purified human collagen type II (Millipore) was loaded into the gel as positive control. The membrane was blocked overnight with 5% skim milk in TBST (2 mM Tris, 50 mM NaCl and 0.1% Tween 20), incubated overnight at 4 ºC with 1 μg mouse anti-human IgG collagen type II or 1:500 mouse anti-human IgG actin monoclonal antibody (Millipore). The membrane was incubated with 1:1000 of goat anti-mouse IgG conjugated with alkaline phosphatase antibody for 1 hour and washed with TBST for 5 minutes 3 times. For signal detection, 1-Step™ NBT/BCIP solution was added to the membrane and incubated for 5-15 minutes until desired color developed. Collagen type II and actin protein band intensities were quantified using ImageJ software (National Institutes of Health).

3.2M In vivo Studies

Chondrogenic pellets were subcutaneous transplanted into immunocompromised (SCID-Beige) mice. Animal protocols were approved by the Institutional Animal Care And Use Committee (IACUC). Mice were obtained at 6 weeks of age and anesthetized using an intraperitoneal injection of ketamine (80 mg/kg) and xylazine (5 mg/kg). hESCs- and hMSCs-derived chondrogenic pellets were implanted into separate sides of the dorsal region of the same animal. The pellets (n = 3) were harvested 4 weeks after implantation, fixed in 4% paraformaldehyde for 24 hours at 4 ºC and further processed for histology.

3.2N Statistical Analysis

Statistical analysis was performed with STATISTICA software (Statsoft, Tulsa, OK). Data were expressed as the average ± SD of n = 4 samples per group at each time point. The differences in gene expression and GAG content between the groups were evaluated using two-way ANOVA, followed by Tukey's Honest Significant Difference Test. $p < 0.05$ were considered statistically significant.

4. Results

4.1 Results of specific aim 1

4.1A Oxygen levels in culture medium

The level of O_2 in culture medium was measured to validate each of the oxygen regimes (normoxia, hypoxia, reoxygenation). Partial pressures of O_2 were measured in wells containing constructs and reference wells without constructs (**Appendix B, Supplemental figure 1**). Oxygen uptake rate (OUR) was estimated from a steady-state balance of O_2 in medium (82):

$$\frac{d[O_2]}{dt} = k_L a \left([O_2]_{reference} - [O_2]_{construct}\right) - OUR$$

where $[O_2]_{reference}$ and $[O_2]_{construct}$ are dissolved O_2 concentration in wells without constructs and wells containing a cartilage construct, respectively, and $k_L a = 0.9\ h^{-1}$ is the volumetric liquid phase mass transfer coefficient (83). Assuming steady state without change in total O_2 level over a period of 20 hours, OUR could be calculated as follows:

$$k_L a \left([O_2]_{reference} - [O_2]_{construct}\right) = OUR$$

The cells consumed less oxygen in hypoxic conditions than in normoxic and reoxygenated conditions as indicated by measured values of the oxygen uptake rate (OUR) (**Appendix B, Supplemental figure 2**). The calculated values of OUR were in the range of those previously reported (**Appendix B, Supplemental table 1**).

4.1B Effects of hypoxia on cell proliferation, proteoglycan synthesis and mechanical properties of engineered cartilage

Chondrocytes encapsulated in agarose hydrogel survived at all oxygen levels, from 21% O_2 (normoxia) to 5% O_2 (hypoxia) either continuously or followed by reoxygenation. Live cells were observed in constructs cultured at all oxygen tensions. Cell proliferation under hypoxic conditions was similar to normoxic conditions by day 7 (**Figure 20)**. Effects of hypoxia on cell proliferation were seen by day 14 (9 ± 0.3 μg DNA in hypoxia v.s. 8 ± 0.5 μg in normoxia, p = 0.016) and day 21 (12 ± 0.3 μg at hypoxia v.s. 10 ± 0.7 μg at normoxia, p = 0.00017). Reoxygenated cultures showed similar cell proliferation patterns to hypoxic cultures up to day 21. The hypoxia and hypoxia-reoxygenation groups initially demonstrated significant growth in comparison with the normoxia group. However, a decrease in DNA content in the hypoxic group (9 ± 1.6 μg) was observed by day 28 while normoxic (11 ± 1.4 μg) and reoxygenated groups (12 ± 1.5 μg) maintained cell proliferation throughout the duration of study.

Proteoglycan production was initially comparable in normoxic and reoxygenated cultures. However, the GAG content of normoxic group reached a plateau at day 21 (501 ± 15 μg on day 21 and 481 ± 17 μg on day 28), whereas that of the reoxygenated group continued to increase (486 ± 6 μg on day 21 and 598 ± 10 μg on day 28). The GAG content of the

reoxygenated group was significantly higher than that in either normoxic or hypoxic groups at day 28 (**Figure 20)**.

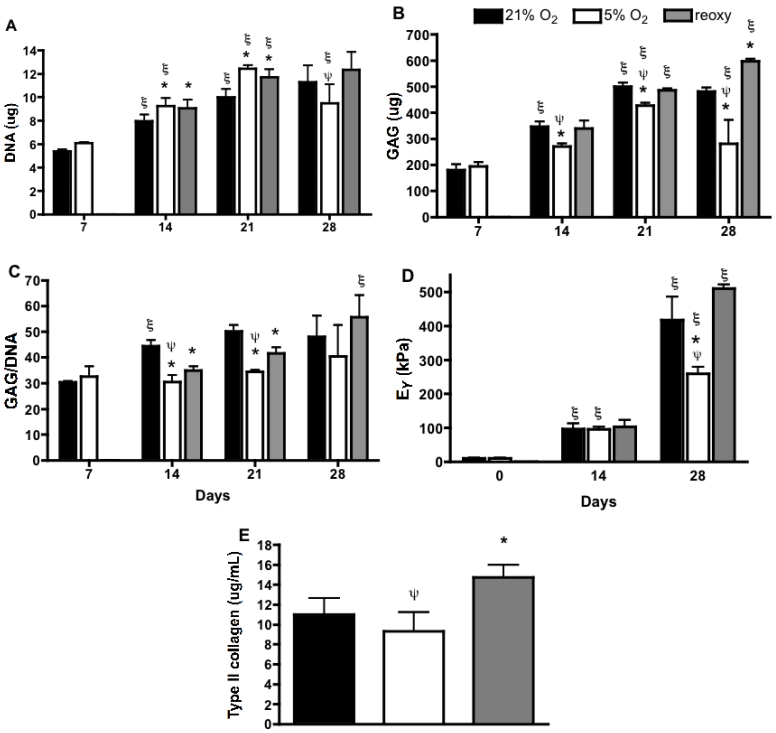

Figure 20. Effect of oxygen exposure on cartilage tissue development

Constructs from the three experimental groups described in **Figure 16** were analyzed for DNA content (**A**), GAG production (**B**), GAG/DNA (**C**), equilibrium modulus, E_Y (**D**) and type II collagen content (**E**). Hypoxia-reoxygenation culture best maintained DNA content and promoted GAG synthesis. Constructs cultured for 28 days at different oxygen levels were specifically quantified for type II collagen content. There were no differences in type II collagen production between constructs cultured at 21% O_2 and 5% O_2, whereas hypoxia-reoxygenation significantly promoted type II collagen synthesis. Error bars denote standard deviation, * $P<0.05$ compared to 21% O_2, $^{\Psi}$ $P<0.05$ versus reoxy, $^{\xi}$ $P<0.05$ versus previous time point within the same group, n = 5

GAG accumulation in the hypoxic group on day 28 was significantly lower in comparison to both the normoxic and reoxygenated groups, consistent with the low cell proliferation. Hypoxic group had low values of GAG/DNA on day 14, corresponding to the time-point when DNA content was higher and GAG content lower than in the other groups **(Figure 20A and B)**. Continuous normoxia maintained the DNA and GAG production over time in culture as indicated by the constant GAG/DNA values in this group. The reoxygenated group gradually increased GAG/DNA production as the tissue constructs were maturing **(Figure 20C)**, in accordance with the increase in mechanical properties (**Figure 20D)**. At the end of the culture period, reoxygenated constructs yielded the highest equilibrium modulus (E_Y) of 510 ± 28 kPa as compared to constructs cultured in normoxic (418 ± 68 kPa) and hypoxic (280 ± 21 kPa) conditions.

4.1C Reoxygenation promotes cartilaginous gene expression

Real-time PCR was performed to evaluate cartilage tissue development at the transcriptional level. Total RNA of constructs was used to detect the expression of cartilaginous markers (*COL2A1* and *ACAN*), a key transcription factor of chondrocytes (*SOX9*), and a key dedifferentiation marker (*COL1A1*) (**Figure 21)**. During early phases of culture, chondrocytes in all groups showed low expression of *COL2A1*, the gene encoding for type II collagen. By day 21, normoxic cultures gradually increased the *COL2A1* gene expression and suppressed expression of *COL1A1*, the gene encoding for type I collagen. The *COL2A1* gene expression in the reoxygenated group was upregulated to an even higher degree than in normoxic group, whereas hypoxia downregulated *COL2A1* gene expression by half. Reoxygenation temporarily

promoted *COL1A1* gene expression (on day 14), followed by suppression of this de-differentation marker in mature constructs (day 21 and 28).

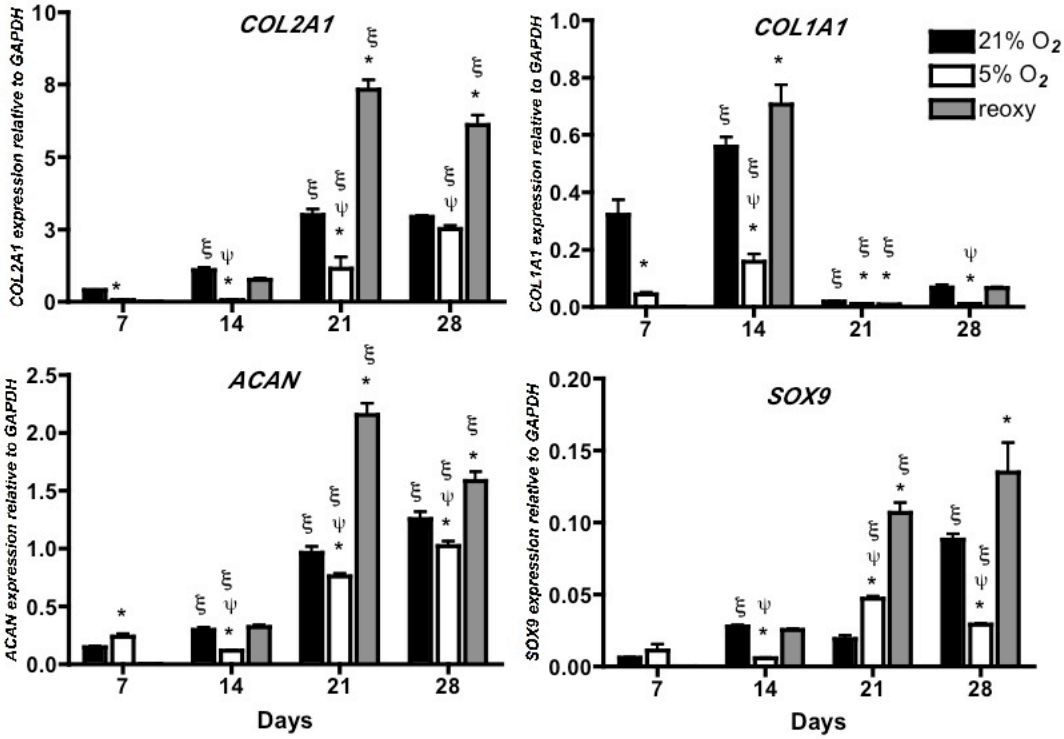

Figure 17. Gene expression of cartilaginous markers in normoxic, hypoxic and reoxygenated cultures

Cartilaginous gene expression in constructs grown in normoxic, hypoxic or hypoxia-reoxygenation conditions were determined by real-time PCR and normalized to GAPDH levels. The chondrogenic dedifferentiation marker, *COL1A1,* decreased with time in all groups. The expression levels of *COL2A1*, *ACAN* and *SOX9* genes significantly increased in the hypoxia-reoxygenation group as compared to either normoxic or hypoxic groups. Data are shown as average ± SD (n = 5). * $P<0.05$ versus 21% O_2, $^{\Psi}$ $P<0.05$ versus reoxygenated group, $^{\xi}$ $P<0.05$ versus the previous time point within the same group.

The expression of *ACAN*, the gene encoding for core protein aggrecan, increased over time in all groups and the expression profiles were consistent with type II collagen expression. *SOX9* was upregulated in the reoxygenated group by day 21, and increased further by day 28. Enhanced expression of *SOX9* paralleled with enhanced expressions of *COL2A1* and *ACAN*.

4.1D Type II collagen synthesis in engineered cartilage

The ability to synthesize type II collagen, a trimeric fibrous protein abundant in articular cartilage, is a specific marker of cartilage tissue development. Constructs were collected on day 28 and enzymatically digested to obtain monomeric collagen before performing ELISA. Reoxygenated culture resulted in significantly more type II collagen (15 ± 1 μg/ml) than either normoxic (10 ± 2 μg/ml) or hypoxic (9 ± 2 μg/ml) conditions (**Figure 20E**).

4.1E Histology of engineered cartilage

Constructs cultured at normoxic, hypoxic and transiently hypoxic conditions exhibited similar gross histomorphology. Chondrocyte-seeded hydrogels progressively transformed to stiff and opaque constructs over 28 days of culture. Chondrocytes at the construct centers were uniformly distributed in small cell clusters, while chondrocytes at the periphery formed larger clusters **(Figure 22A).** Safranin O staining showed homogeneous distribution of GAG in the constructs **(Figure 22B).** Partial GAG loss was observed by faint GAG staining on the edges, especially in hypoxic conditions. Type II collagen was located at intercellular spaces and was more abundant around cells, as shown by immunohistochemistry **(Figure 22C).** Notably, reoxygenated constructs showed stronger type II collagen staining than the other two groups.

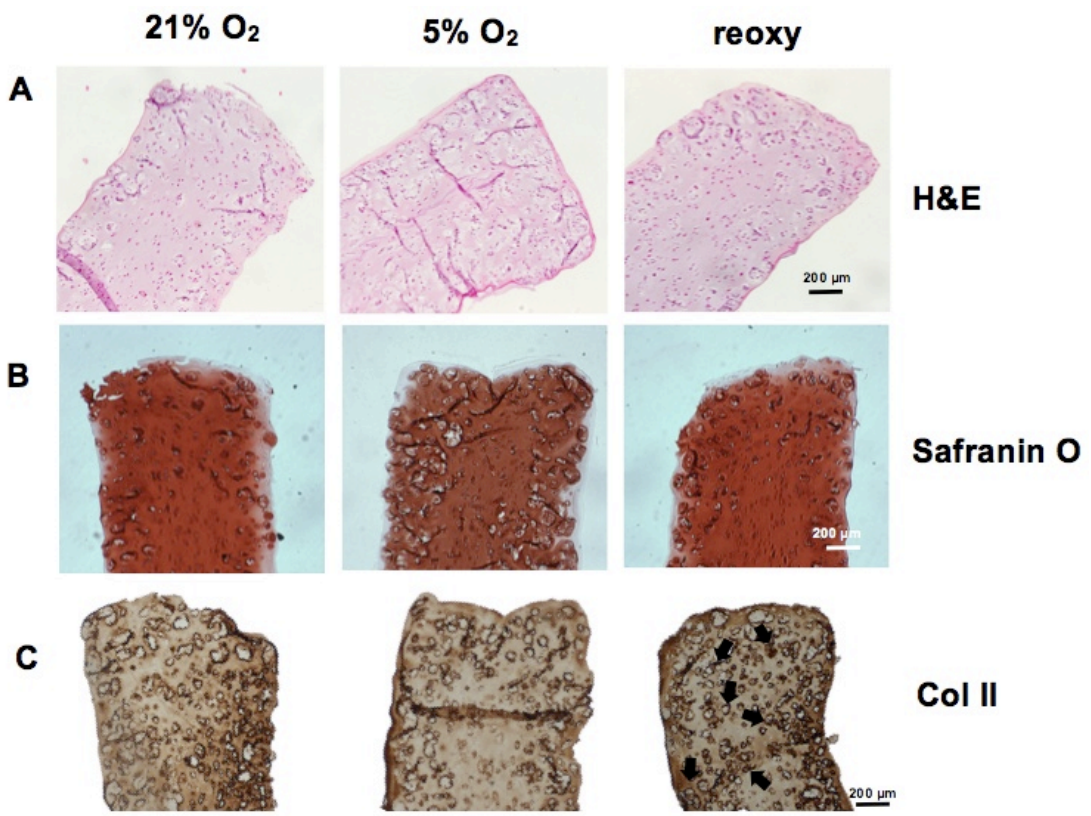

Figure 22. Histology and immunohistochemistry of 28-day constructs from the normoxic, hypoxic and hypoxia-reoxygenation groups

A: H&E staining showed that chondrocytes are distributed throughout constructs, with larger cell clusters located on the periphery. **B:** Safranin O stain for glycosaminoglycan (GAG). **C:** Immunostaining for type II collagen. Arrows indicate strong type II collagen staining areas in the reoxygenated group.

4.2 Results of specific aim 2

4.2A Synergistic effects of CCM morphogenetic factors and hypoxic culture on EB gene expression

We performed chondrogenic lineage induction by culturing EBs in CCM for 3 weeks (**Figure 17**). Real-time PCR revealed that EB formation in CCM under 21% O_2 up-regulated *SOX9* expression on week 2 compared to EBs cultured in growth medium under 21% O_2. To investigate effects of hypoxia on chondrogenic linage induction, EB culture was conducted in 5% O_2. We found that CCM medium and hypoxia were able to up-regulate *SOX9* compared to CCM with 21% O_2 **(Figure 23A)**. The kinetics of *SOX9* expression in CCM EBs under hypoxia and normoxia was similar, with temporary up-regulation of *SOX9* at 2 weeks, followed by a decrease at 3 weeks **(Figure 23A)**. On week 2, EBs in hypoxia increased *SOX9* by 3 fold ($p < 0.05$) over EBs in normoxia.

We found that CCM also significantly induced osteogenic transcription factor *RUNX2* **(Figure 23B)**. Unlike *SOX9* expression, *RUNX2* was higher under 21% O_2 than 5% O_2 tension, and peaked at week 3 of culture. A significant decrease of pluripotent transcription factor gene expression, *OCT4*, was detected over time in all groups **(Figure 23C)**.

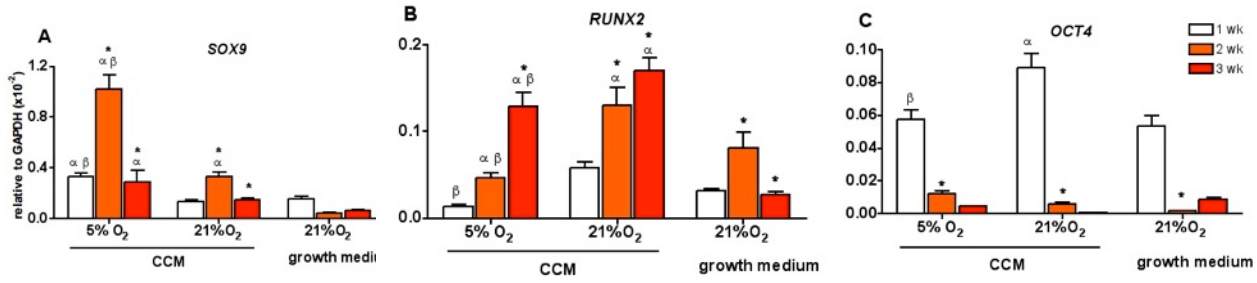

Figure 18. Transcription factor gene expression of EBs cultured in conditioned media under hypoxic condition

Real-time PCR showed expression profiles of *SOX9* **(A)**, *RUNX2* **(B)** and *OCT4* **(C)** over the time course of EB induction. * $p < 0.05$ compared within the same medium group, $^{\alpha}$ $p < 0.05$ compared with growth medium group at the same time point, and $^{\beta}$ $p < 0.05$ compared with 21% O_2 conditioned medium (CCM) at the same time point

4.2B The effects of hypoxic culture period on EB gene expression

The results of **Study 1** suggested that both CCM and hypoxia influenced *SOX9* expression, and that *SOX9* peaked at 2 weeks of hypoxic induction in CCM. Therefore, we conducted **Study 2** to determine the optimal periods of low oxygen tension for chondrogenic EB induction **(Figure 18)**. **Figure 24A** shows that 2 weeks of culture under 5% O_2 followed by 1 week of culture under 21% O_2 *(transient 2 hypoxia)* significantly up-regulated *SOX9* ($p < 0.05$) compared to all other conditions. *SOX9* exhibited the lowest expression in 3 weeks under 21% O_2 *(normoxia)*. Interestingly, varying the hypoxic exposure period affects *RUNX2* expression to a lesser extent, as indicated in **(Figure 24B)**. However, we observed significantly lower *RUNX2* expression in EBs cultured under 5% O_2 for 3 weeks without reoxygenation.

At 3 weeks of EBs induction, *OCT4* expression was low in every chondrogenic induction condition **(Figure 24C)**; especially both transient hypoxic groups showed significant decreases of *OCT4* compared to 3 weeks of 5% O_2 group ***(hypoxia)***.

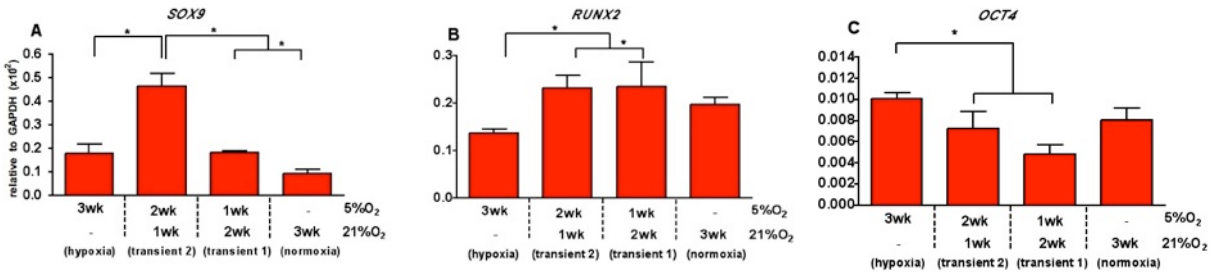

Figure 24. Transient hypoxia promoted *SOX9* expression

EBs were cultured in conditioned media (CCM) with different exposure periods of 5% O_2 for 3 weeks and determined expression of *SOX9* **(A)**, *RUNX2* **(B)** and *OCT4* **(C)**. * $p < 0.05$ significantly different compared to other groups

4.2C Differential soluble receptors of induced EBs

In order to understand the response of cells to the induction regime, 119 receptors of *transient 2 hypoxia* EBs (induced EBs) were compared to those of EBs cultured in 5% FBS in growth medium under 21% O_2 (non-induced EBs) **(Figure 25A)**. Forty two receptors with the expression ratio of induced EBs : non-induced EBs more than 1.5 were showed in **(Figure 25B)**. Based on biological relevance using STRING database, the up-regulated proteins were categorized into 3 groups: involved in cell migration and motility ($p = 0.0073$), cell adhesion ($p = 0.0067$), and cellular component morphogenesis ($p = 0.042$) **(Figure 25B)**. The receptors that were up-regulated were TIMP-1, LGALS3, LGALS3BP, EpCAM and ITGB1.

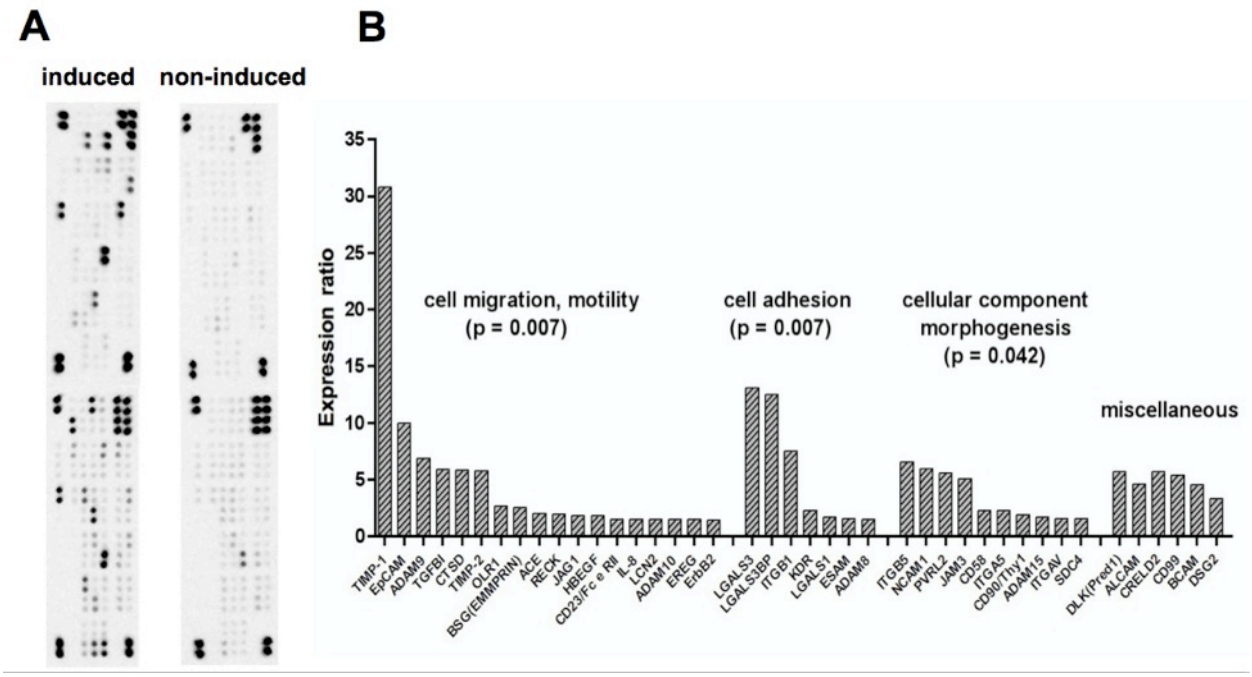

Figure 19. Differential expression of receptors of induced EBs

A: The 119 receptor arrays were printed in duplicate. *Transient 2 hypoxia* induction (left) and non-induction (right). **B:** Up-regulated receptors with the ratio of induced : non-induced more than 1.5 were categorized into 4 sub-groups, cell migration and motility, cell adhesion and cellular component morphogenesis

4.2D Gene expression of lineage markers during chondrogenic differentiation in pellet cultures

Pellet culture was used to evaluate the potential for cartilage tissue formation *in vitro*, by allowing single cells to initiate the first step of chondrogenic differentiation, the cell condensation. EBs induced by *transient 2 hypoxia* and *normoxia* conditions were dissociated into single cells and cultured in ChondM for 6 weeks under 21% O_2. We found that *SOX9* expression in pellets made from *transient 2 hypoxia* EBs increased over time until week 4, followed by a gradual decrease **(Figure 26A)**. The *SOX9* expression of the pellets made from *normoxia* EBs gradually increased at a slower rate and reached a comparable level at 6 weeks as the *transient 2 hypoxia* EBs at 4 weeks. In comparison, hMSC pellets remarkably expressed high *SOX9* level after one week and the peak of expression between 2 and 3 weeks, followed by a significant down-regulation at weeks 4 and 5 **(Figure 26A)**.

RUNX2 expression profiles were similar for pellets derived from *transient 2 hypoxia* EBs and *normoxia* EBs, showing a slow increase over 6 weeks of culture. However, the expression levels during the first 3 weeks were relatively low compared to the pellets derived from hMSCs, which constantly expressed *RUNX2* levels **(Figure 26B)**.

Expression of transcription factors involved in endodermal (*FOXA2*) and ectodermal (*PAX6*) lineage differentiation was monitored to determine the nonspecific lineage induction. *FOXA2* expression in pellets prepared from EBs was detected only at the initiation of cultures (week 0), and was not detected in the following weeks **(Figure 26C)**. The expression of *FOXA2* in hMSCs pellets was not detected before 2 weeks, was slowly up-regulated until week 5, and was not detected on week 6. Pellets derived from *transient 2 hypoxia EBs* exhibited increasing levels of *PAX6* expression until week 4, while pellets derived from *normoxia EBs* showed low

PAX6 expression levels **(Figure 26D)**. We could not detect *PAX6* in hMSCs pellets **(Figure. 26D).**

To test for loss of pluripotency, *OCT4* and *NANOG* were also monitored over the time course of chondrogenic pellet differentiation. After week 1, we did not detect *OCT4* in chondrogenic pellets derived from *transient 2 hypoxia* and *normoxia EBs*, and in hMSC pellets **(Figure 26E)**. *NANOG* expression was detected transiently on weeks 3 and 4 of pellet culture, with higher expression levels in pellets derived from *normoxia EBs* compared to *transient 2 hypoxia EB* **(Figure 26F).** We could not detect *NANOG* expression in hMSC pellets **(Figure 26F).**

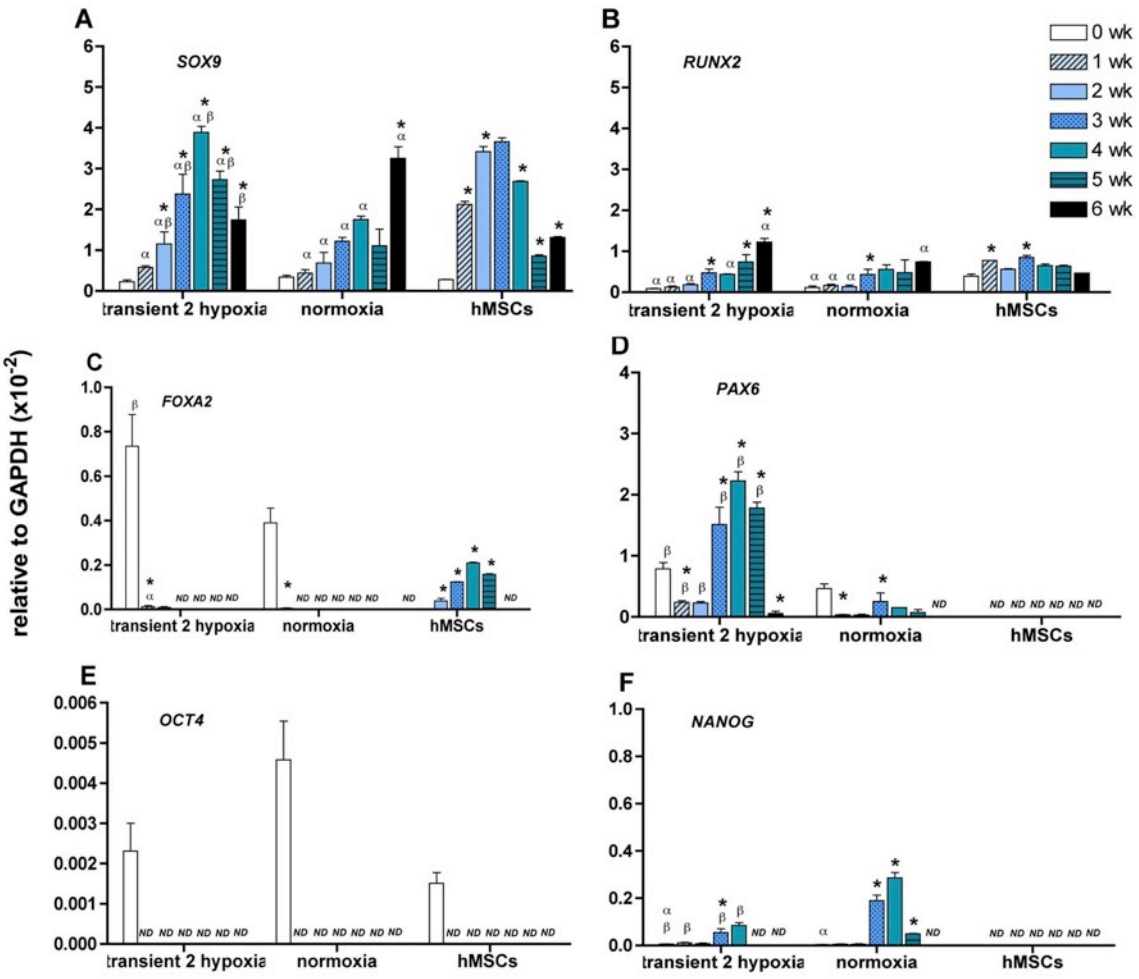

Figure 26. Transcription factor expression of chondrogenic pellets

hESCs-derived chondrogenic pellets in *transient 2 hypoxia* and *normoxia* groups were collected weekly and analyzed the expression of chondrogenic; *SOX9* **(A)**, osteogenic; *RUNX2* **(B)**, endodermal lineage; *FOX2* **(C)**, ectodermal lineage; *PAX6* **(D)**, and pluripotent transcription factors; *OCT4* **(E)** and *NANOG* **(F)**. * $p < 0.05$ compared within the same group, $^{\alpha}$ $p < 0.05$ compared to hMSCs, $^{\beta}$ $p < 0.05$ compared to normoxia, ND = not detectable

4.2E Chondrogenic pellets at week 4 showed distinct gene expression profiles compared to mesenchymal stem cells

We determined chondrogenic differentiation of the week 4 hESC-chodrogenic pellets (the highest *SOX9* expression) derived *from transient 2 hypoxia EBs* using the PCR array containing the collection of mesenchymal lineage genes. In this analysis we used hMSCs as reference cells. The differentially expressed genes considering *p*-value cutoff = 0.05 between the hESC-condrogenic pellets and hMSCs are presented in **Supplemental table 1 of Appendix C**. Among 90 genes in PCR array, 39 genes were significantly altered with fold change larger than 2 (14 up-regulated genes and 25 down-regulated genes) as shown in scatter plot **Figure 27**. The genes that were up-regulated were *BMP6, BMP4, ABCB1, ERBB2* and *SOX9*. Whereas the most down-regulated genes were *MCAM, EGF, NOTCH1*, *KITLG* and *RHOA*. The hESC-chondrogenic pellets showed 29 additional genes with ±2 fold change ($p < 0.05$) compared to hMSCs as summarized in **Supplemental table 1 of Appendix C**. The clustering plot demonstrated two main clusters, the reference hMSCs and the week 4 hESCs-derived chondrogneic pellets. Moderate levels of stem cell markers were expressed in the hESCs-derived chondrogenic pellets expressed stem cells marker (**Figure 28, region 1**) whereas the expression of mesenchymal markers was suppressed (**Figure 28, region 2**). The up-regulation of chondrogenic genes was highly expressed in the hESCs-derived chondrogenic pellets **(Figure 28, region 3).**

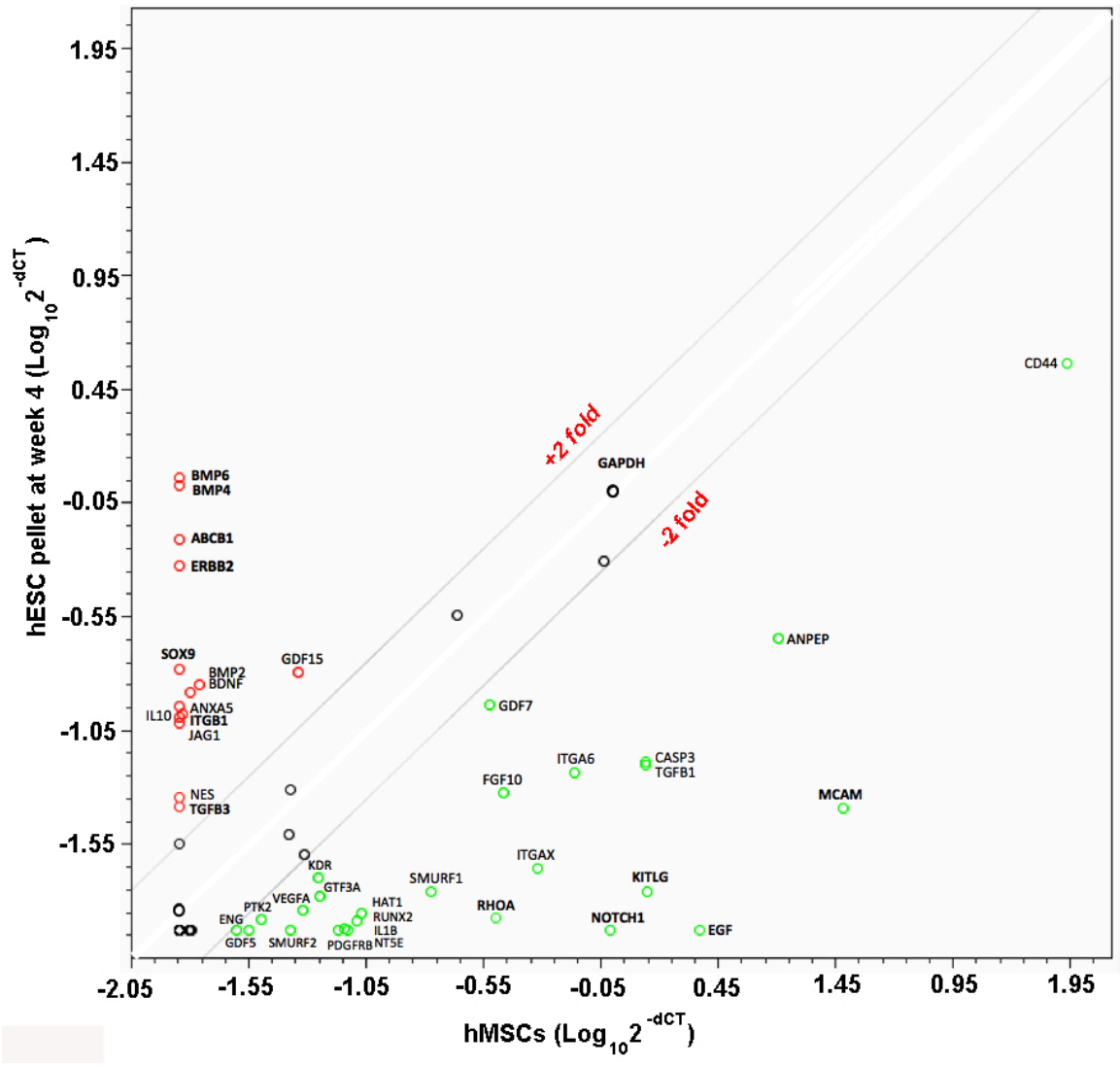

Figure 20. Scatter plot of 90 genes of Human Mesenchymal Stem Cell PCR array

Relative gene expression ($2^{-\Delta C_T}$) of week 4 hESCs-derived chondrogenic pellets was plotted against that of hMSCs. Genes with significant fold change (±2 fold with $p < 0.05$) were showed in the scatter plot.

4.2F Cartilaginous matrix production is increased in chondrogenic pellets derived from *transient 2 hypoxia EBs*

We analyzed gene expression of collagen type I and type II to evaluate the progression of chondrogenic differentiation. Chondrogenic pellets derived from *transient 2 hypoxia EBs* progressively increased *COL2A1* encoding collagen type II which is the marker of chondrocyte maturation **(Figure 29A)**, while those derived from *normoxia EBs* increased the *COL2A1* expression at a slower rate. Chondrogenic pellets from hMSCs expressed *COL2A1* from week 2 onward, exhibiting constant levels over the time course of study. Interestingly, we found a transient increase followed by the decrease in *COL1A1* expression, indicating a switch in profiles from collagen type I to type II in all pellet groups. In the first 2 weeks of culture, pellets exhibited high levels of *COL1A1*, followed by a marked reduction by 70% in both *transient 2 hypoxia* and *normoxia* pellets and by 50% in *hMSC* pellets **(Figure 29B)**. Further more, between weeks 4 and 6, hMSCs-derived chondrogenic pellets maintained the levels of *COL1A1* expression, whereas that of the hESCs-derived chondrogenic pellets was reduced to modest levels. In addition, *COL10A1* encoding collagen type X, the hypertrophic marker, showed minimal expression in both hESCs-derived pellets, whereas *COL10A1* expression in hMSC pellets gradually increased **(Figure 29C)**.

At the end of chodrogenic differentiation, pellets were evaluated for the presence of collagen type II and type I. Pellets derived from *transient 2 hypoxia EBs* stained homogeneously for collagen type II in the extracellular matrix space **(Figure 30A)**, whereas pellets derived from *normoxia EBs* exhibited positive staining in the territorial matrix space only **(Figure 30B)**. hMSC pellets exhibited a weaker and less homogenous staining compared to pellets derived

from *transient 2 hypoxia EBs* in cells and pericellular space **(Figure 30C)**. We were not able to detect collagen type I in all three chondrogenic pellets **(Figure 30D-F).**

An abundance of collagen type II together with the loss of collagen type I corresponded with high *COL2A1* and low *COL1A1* gene expression levels in late chondrogenic differentiation stages (5-6 weeks) **(Figure 29A-B)**. We further confirmed the immunohistochemical data by evaluating the collagen type II using western blot analysis. Collagen type II bands with molecular weight of 140 kDa were detected in pellets made from *transient 2 hypoxia* EBs, *normoxia* EBs and hMSCs **(Figure 30I)**. Semi-quantitative evaluation of the protein band intensity showed a significantly higher amount of collagen type II relative to actin in pellets derived from *transient 2 hypoxia* EBs compared to *normoxia* EBs and hMSCs **(Figure 30J)**.

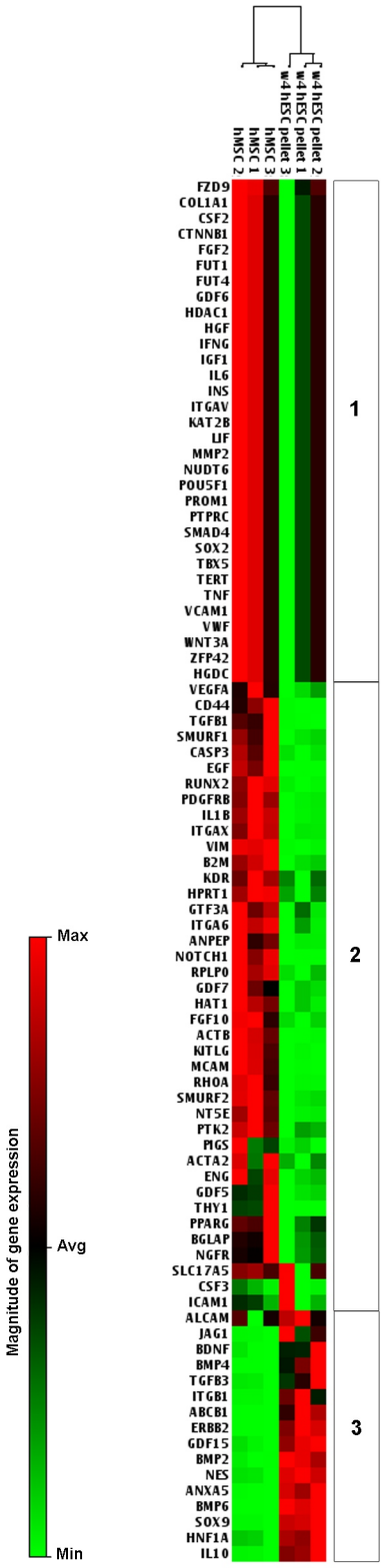

Figure 21. Clustering analysis of differential expressed human mesenchymal genes

Cluster plot displays distinct gene expression profiles of undifferentiated hMSCs (reference cells) and week 4 hESCs-derived chondrogenic pellets. Stem cell markers and other mesenchymal associated genes in hESCs-derived pellets were displayed in moderate levels (region 1). hESCs-derived chondrogenic pellets lost mesenchyme and osteogenic markers (region 2) and highly expressed chondrogenic related genes (region 3). Color gradient of the heat map from green to red represents an increase in expression levels.

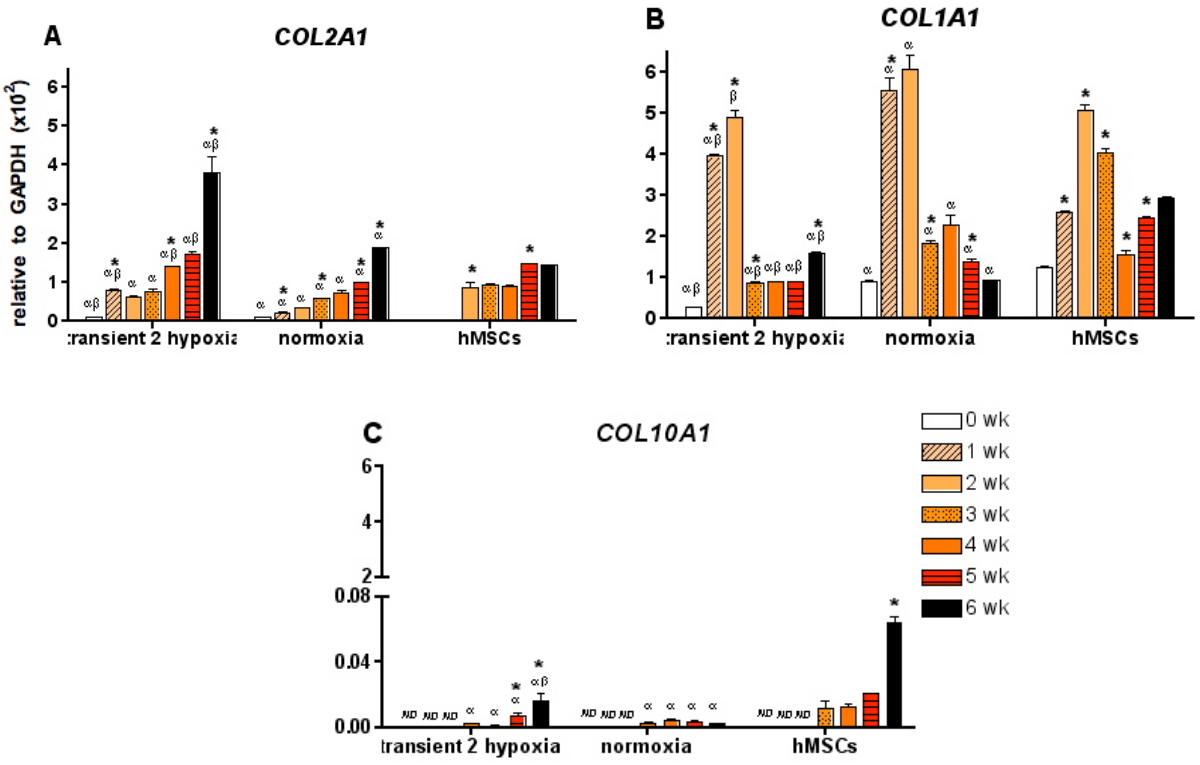

Figure 22. Collagen gene expression of chondrogenic pellets

Pellets derived from *transient 2 hypoxia* EBs, *normoxia* EBs and *hMSCs* were analyzed for gene expression. **A:** *COL2A1* (collagen type II) **B:** *COL1A1* (collagen type I) and **C:** COL10A1 (collagen type X) * $p < 0.05$ compared within the same group, $^{\alpha}$ $p < 0.05$ compared to hMSCs, $^{\beta}$ $p < 0.05$ compared to normoxia, ND = not detectable

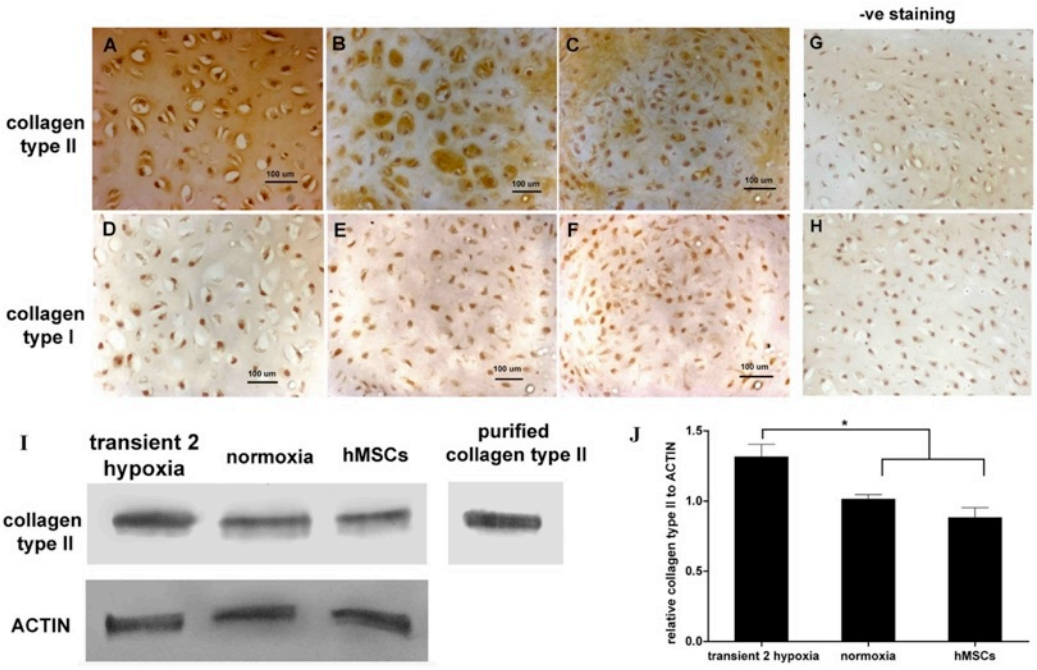

Figure 30. Type II and type I collagen of chondrogenic pellets

Immunohistochemistry showed localization of type II and type I collagen of 6 week pellets derived from *transient 2 hypoxia* EBs **(A and D)**, *normoxia* EBs **(B and E)** and hMSCs **(C and F)**. Negative staining of type II **(G)** and type I **(H)** collagen immunohistochemistry of pellets derived from *transient 2 hypoxia EBs*. **I:** Representative Western blot of collagen type II in chondrogenic pellets. Purified human type II collagen was used as positive signal detection. **J:** Relative intensities of collagen type II levels (n=3) were normalized to Actin levels using ImageJ software. Values are expressed as mean ± SD. * $p < 0.05$ significantly different compared to other groups

4.2G Cell condensation and proteoglycan production in chondrogenic pellets

The initial stage of chondrogenesis is cellular condensation which depends on cell-cell interaction mediated by cell adhesion molecule, N-cadherin (84). hMSCs consistently formed pellets in 24 hours, in contrast to EB-derived progenitors where some of the cells did not pellet and were washed out during the subsequent medium changes. A defined shape of condensed cell aggregates appeared within 4 days in dissociated cells from *transient 2 hypoxia* EBs, whereas the aggregates obtained from dissociated *normoxia* EBs took 12 days to form.

Gene expression studies demonstrated temporally-dependent gene expression of *CDH2* encoding cell adhesion molecule N-cadherin, and *ACAN* encoding chondroitin sulfate proteoglycan core-protein during chondrogenic pellet maturation. The pellets made from EBs in both induction conditions exhibited high *CDH2* expression in the first week of pellet formation **(Figure 31A).** Similarly to hMSC pellets, high expression of *CDH2* was maintained until week 2 in *transient 2 hypoxia* group, followed by a continuous decrease. In contrast, *CDH2* expression started decreasing after the first week in pellets from *normoxia EBs*.

ACAN expression was low in both hESCs-derived pellets during the first three weeks compared to hMSCs-derived pellets, which showed a progressive increase in expression at weeks 2, 4 and 6 **(Figure 31B)**. *ACAN* expression in pellets made from *transient 2 hypoxia* EBs showed an earlier an higher up-regulation compared to pellets derived from *normoxia* EBs, reaching the final expression levels higher than those in hMSC pellets **(Figure 31B)**.

Gene expression data were confirmed by Alcian blue staining, which showed a low glycosaminoglycan (GAG) accumulation for all three groups of pellets after 3 weeks **(Figure 32A, C, E)**. We found homogeneous but light blue staining in hMSCs-derived pellets **(Figure 32E)** and cluster staining in pellets derived from *transient 2 hypoxia* EBs **(Figure 32A)**. After 6

weeks of culture, an abundant, homogenous GAG staining was observed in pellets from *transient 2 hypoxia* EBs and hMSCs **(Figure 32B, and F)**, in contrast to pellets from *normoxia* EBs which stained less, predominantly in the central region **(Figure 32D)**. Biochemical analysis showed a significant increase in the GAG **(Figure 32G)** from week 3 to week 6, which corresponded to the increased GAG accumulation detected by Alcian blue staining **(Figure 32B, D, F)**. The appearance of chondrocyte in lacunar spaces surrounded by dense ECM was clearly seen in pellets made from *transient 2 hypoxia EBs* in magnified view as indicated by arrows **(Figure 32B)**.

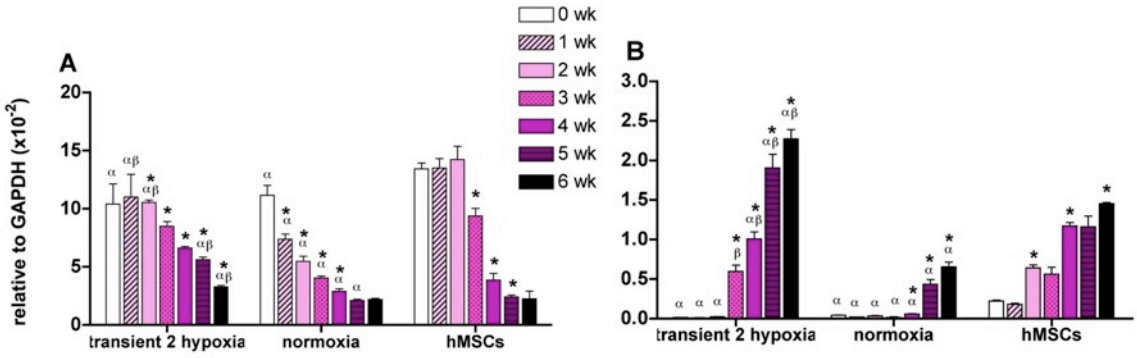

Figure 23. N-cadherin and aggrecan gene expression of chondrogenic pellets

Chondrogenic pellets were assayed gene expression of cell adhesion molecule (*CHD2*) **(A)** and extracellular matrix glycoprotein (*ACAN*) **(B)**. * $p < 0.05$ compared within the same group, $^{\alpha}$ $p < 0.05$ compared to hMSCs, $^{\beta}$ $p < 0.05$ compared to normoxia, ND = not detectable

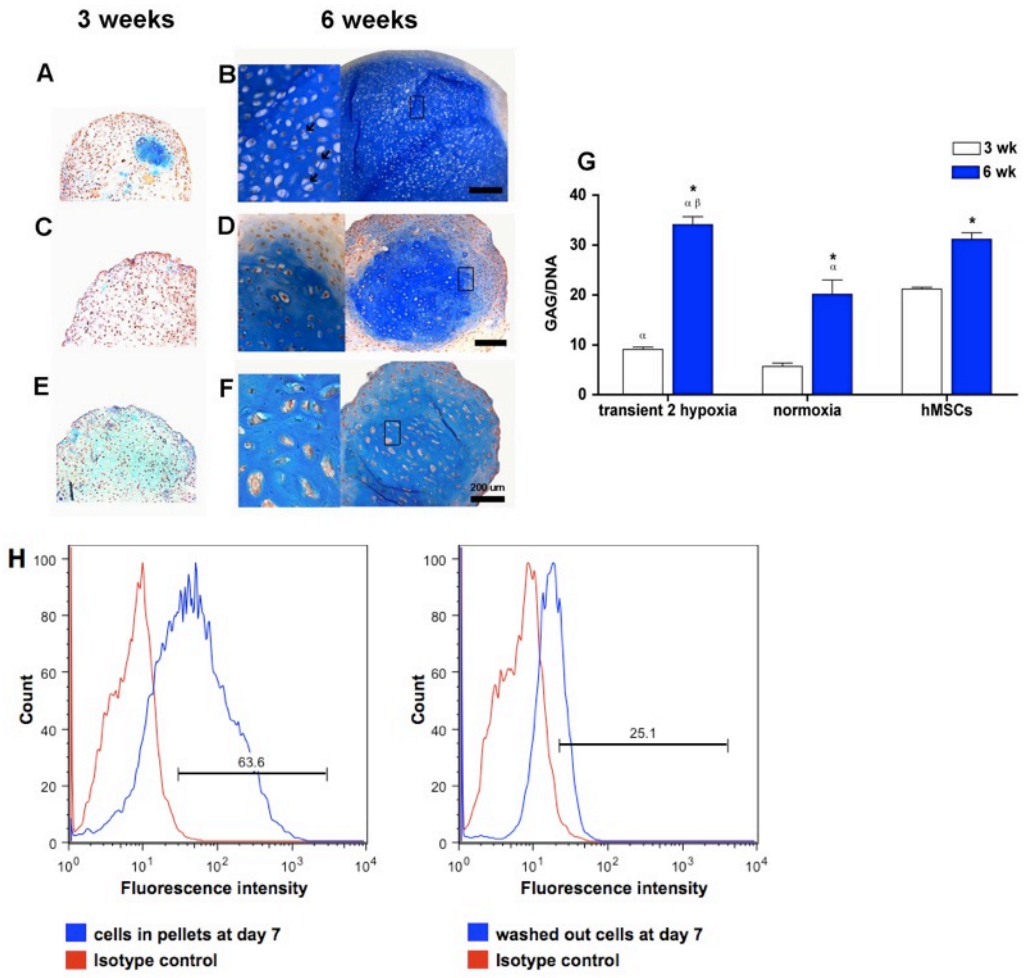

Figure 32. Alcian blue staining and flow cytometric analysis of N-cadherin presenting cells

Transient 2 hypoxia EBs **(3A-B)**, *normoxia* EBs **(3C-D)** and hMSCs **(3E-F)**. Arrows indicate lacunae inside 40x inserts. Bar = 200 μm. **G:** GAG content was presented in GAG/DNA. * $p <$ 0.05 compared within the same group, $^{\alpha}$ $p < 0.05$ compared to hMSCs, $^{\beta}$ $p < 0.05$ compared to normoxia. **H:** Flow cytometric analysis. Cells of 1 week chondrogenic pellets and washed out cells were stained with N-cadherin DyLight®488 antibody. Percentages of N-cadherin positive cells are indicated in each figure.

4.2H Model of chondrogenic differentiation of hESCs

According to **temporal changes** in gene expression of ECM and cell-cell interaction molecules and **spatial organization** of ECM deposition in chondrogenic pellets, we propose the following model for *in vitro* chondrogenic differentiation of hESCs in pellet culture **(Figure 33)**. Cell condensation mediated through N-cadherin expressing cells was confirmed by flow cytometric analysis. Cells from 1 week aggregates and washed out cells of those aggregates were stained with N-cadherin antibody conjugated with DyLight®488. Only a small fraction of washed out cells was positive for N-cadherin, while more than 60% of cells in the pellets were able to detect N-cadherin **(Figure 32H).**

In the model, the 3 week-induced EBs were dissociated into single cells and formed pellets. Some cells were washed out during medium changes. After 1 week, cells were tightly packed (cell condensation occurred), small number of washed out cells was observed and pellet size gradually increased over time. ECM separated neighboring cells away from each other starting from the center of pellets to the periphery. Lacuna-like formation was observed, where dense territorial/capsular matrix being formed around two cells was observed at sites where two cells were getting encapsulated the dense ECM.

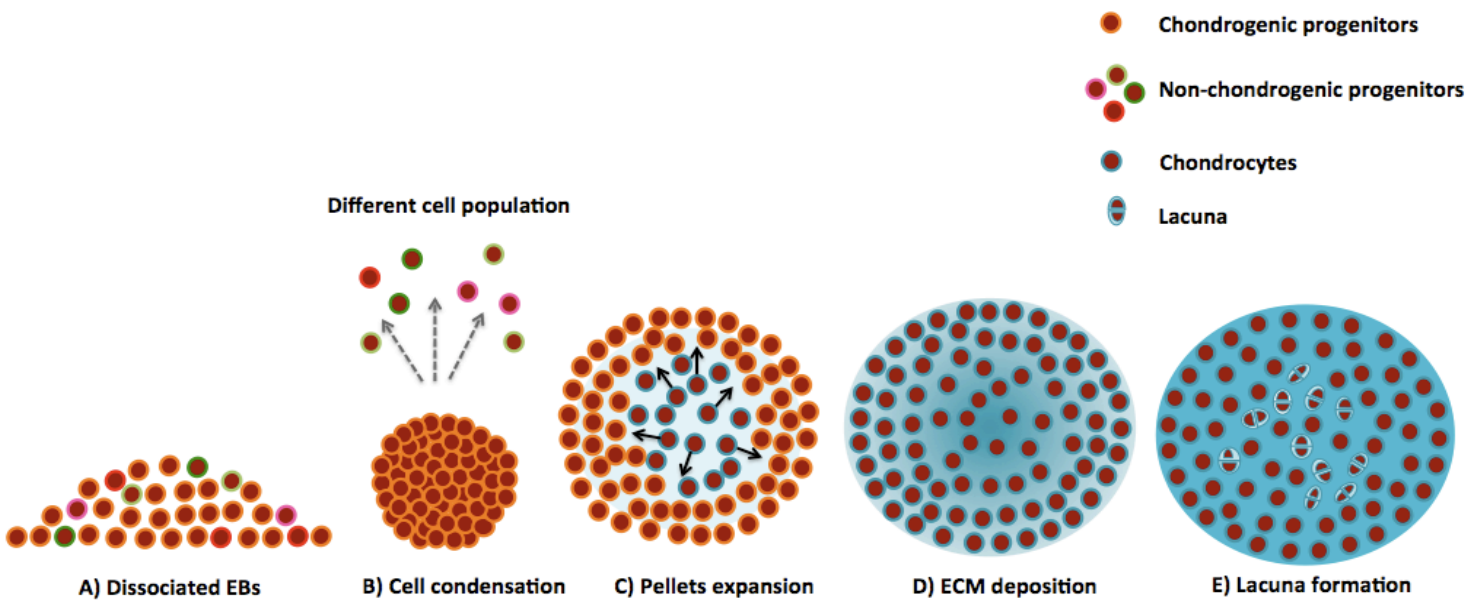

Figure 24. Model of chondrogenesis in vitro

A: Chondrogenic progenitors with partial non-chondrogenic progenitors are obtained after induction for 3 weeks. B: Cell adhesion molecules mediated cell condensation. Non-chondrogenic progenitors are washed away. C: The spherical pellets increase size as ECM production continues resulting in an increase of intercellular spaces starting at the middle of pellet toward the out side. The progression of ECM synthesis occurs with a concomitant decrease in cell adhesion molecules. D: ECM in the form of interterritorial matrix occupies entire intercellular spaces of chondrogenic pellets. The progenitor cells differentiate to chondrodcytes. E: After cell division daughter cells located at the same area as parent cells, secrete matrix to separate each other and form an enclosed structure called lacuna.

4.2I Phenotypic stability and in vivo maturation of hESCs-derived chondrogenic pellets

To determine the risk of teratoma formation and ectopic stability of cartilage tissues after transplantation, the 6 weeks hESCs- and hMSCs-derived chondrogenic pellets were subcutaneously implanted into SCID mice, and the developing tissues were examined 4 weeks after implantation. The incidence of teratomas was not found after implantation as indicated by uniform tissue formation. The three germ layers, ectoderm (Nestin), mesoderm (Vimentin) and endoderm (Alpha-fetal protein) were not detected in the pellets (**Figure 34A**). Capillaries could be detected outside of pellets and stained with CD31 antibody specific for mouse vascular endothelial cells (**Figure 34A).** Anti-human nuclei staining confirmed chondrogenic pellets derived from human origin **(Figure 34A).**

hESCs-derived chondrogenic pellets were more intensely stained for collagen type II and GAG than pellets generated by hMSCs (**Figure 34B**). Collagen type I staining did not show in both pellets. Interestingly, we were able to detect the onset of collagen type X in hMSCs-derived chondrogenic pellets (**Figure 34B**). Representative bone markers, ALP and ostepontin, were not observed in implanted pellets (**Figure 34C**).

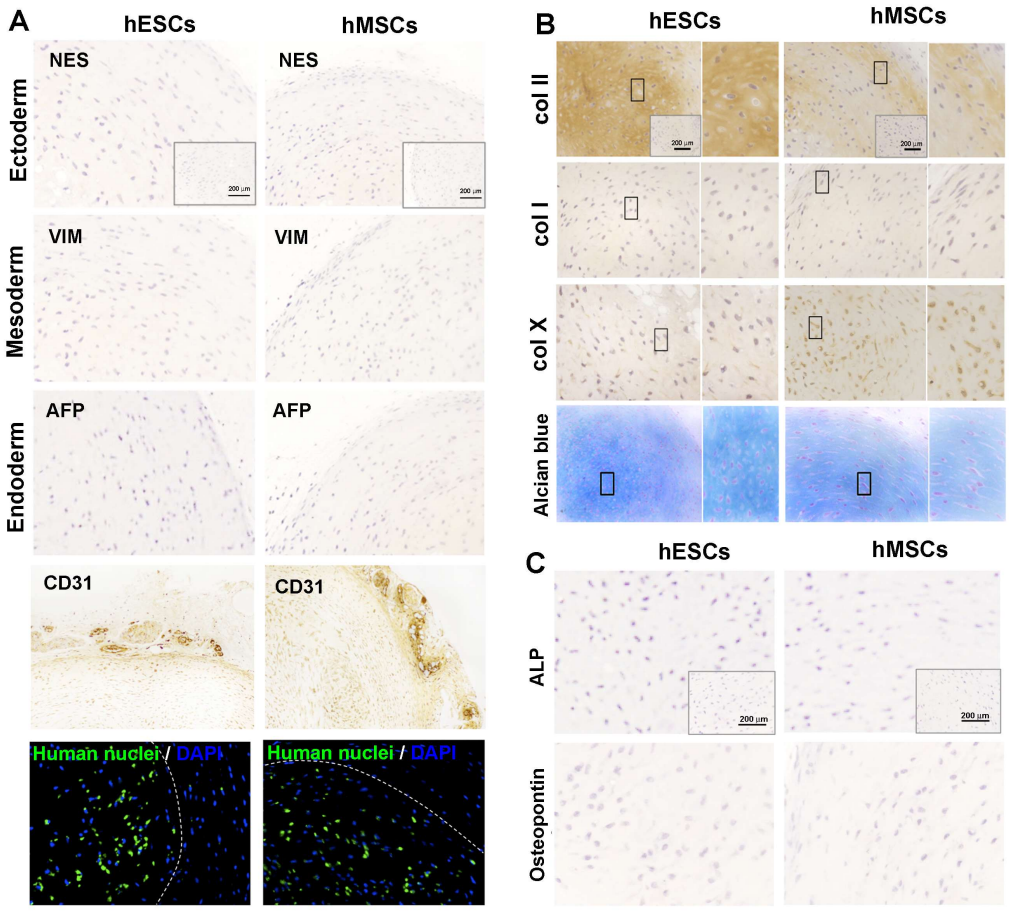

Figure 34. Histological analysis of chondrogenic pellets in vivo

A: Identification of three germ layers by immunohistochemistry. Nestin (NES) indicates ectoderm, Vimentin (VIM) indicates mesoderm and Alpha-fetoprotein (AFP) indicates endoderm. Vascular endothelia cells were stained with CD31 antibody. Immunofluorescence staining confirmed the human origin of chondrogenic pellets (green). The dashed line shows the outline of the pellets. Insert boxes with bar = 200 μm show negative staining of immunohistochemistry. **B:** Immunohistochemistry of collagen and Alcian blue staining for GAG. Rectangular boxes indicate 60x magnified regions. **C:** Immunohistochemistry of bone protein, ALP and Osteopontin.

5. Discussion

Our studies aim to identify alternative cell sources to be used in cartilage tissue engineering instead of the adult stem cells which undergo age-dependent decrease in proliferation and chondrogenic differentiation. Human embryonic stem cells (hESCs) provide unlimited cell supplies and are able to differentiate into cell types in 3 germ layers. Despite the challenges for the use of ESCs, associated with how to control their differentiation potentials into particular lineages as well as with the complications after ESC-derived tissue implantation, ESCs offer a great therapeutic potential and renewable cell source for regenerative medicine.

The directed chondrogenic differentiation protocol was based on the sequence of pathways active in development to create differentiation regime using only 7 exogenous growth factors and supplements (74). Here, we propose a novel approach in chondrogenic differentiation which takes advantage of the physiological conditions found in native joints- low oxygen tension and conditioned medium which has been reported to contain secreted morphogenetic factors necessary for maintenance of the healthy cartilage tissue (85). EB induction was conducted for 3 weeks, the critical period when mesodermal precursors may develop (86) in various induction regimes. We detected that cells derived from *transient 2 hypoxia* EBs showed an excellent chondrogenic differentiation in pellet culture. *Transient 2 hypoxia* EBs were cultured in chondrocyte-conditioned medium (CCM) under 5% O_2 for 2 weeks followed by 21% O_2 for 1 week. At the end of the 3 week induction period, the expression of *SOX9* was significantly increased compared to that of EBs which were continuously cultured in CCM under 21% O_2 for 3 weeks (normoxia group) without switching oxygen levels. Our finding indicated that CCM and low oxygen tension play a role in chondrogenic commitment of hESCs through EB formation **(Figure 23A and 24A).** We were able to detect the up-regulation of *RUNX2* when EBs were

cultured in CCM, albeit the up-regulation was evident only when the culture was maintained in 21% O_2 compared to EBs which were cultured in 5% O_2. These results suggested lineage specific differentiation depends not only on chemical cues from CCM, but also on the oxygen levels.

The *transient 2 hypoxia* was chosen as the best induction regime for chondrogenic differentiation of EBs in pellet culture due to the increase in *SOX9* and decrease in *OCT4*. The up-regulation of *SOX9* together with down-regulation of *OCT4* suggested that hESCs had a tendency to accumulate the population of chondrogenic lineages and lost their pluripotency during EB induction. It indicated that *transient 2 hypoxia condition* may help to suppress stem cell characteristics which could transform cells to other lineages besides chondrocytes. In addition, pluripotent markers *OCT4* and *NANOG*, eventually disappeared when chondrogenic differentiation was conducted in pellet culture. We compared chondrogenic differentiation potential of hMSCs, widely used in chondrogenesis, to hESCs and found early expression of *SOX9* and accumulation of GAG in hMSC pellets. It indicated that hMSCs were promptly differentiated to chondrogenic lineages before hESCs. However, the overall expression levels of *SOX9* together with extracellular matrix genes (*ACAN* and *COL2A1*) in hMSC pellets demonstrated that chondrogenic differentiation potentials of hMSCs were limited compared to hESCs induced by *transient 2 hypoxia* condition. Instead, the mature hMSC pellets expressed collagen X gene, the hypertrophic marker, higher than hESC pellets. Mesenchymal PCR array confirmed not only high expression of *SOX9* in week 4 chondrogenic pellets but also the up-regulation of growth factors in TGF-β family (*BMP6*, *BMP4, GDF15, TGF-β3,* which regulates cartilage growth and development. The PCR array results suggested that hESCs committed to chondrogenic lineages.

The expression of *FOXA2* a key transcription factor of gut formation (the representative of endodermal linages) was suppressed within 1 week in both hESC pellets derived from *transient 2 hypoxia* and *normoxia* EBs. However, the expression of *PAX6*, a transcription factor of eye formation and sensory organs (the representative of ectodermal linages) was up-regulated in pellets derived from *transient 2 hypoxia EBs* and was minimally detected in pellets derived from *normoxia EBs*. It could be possible that hESCs tend to differentiate to neurons by default unless the cells receive specific factors to alter differentiation program to desired lineages (87). Notwithstanding that secreted factors from chondrocytes during EB induction aid cells to preferably become chondrogenic linage, low oxygen tension may also play role in neurogenic inductions (88) - as we can see from low *PAX6* in pellets made from *normoxia EBs* compared that of in pellets made from *transient 2 hypoxia EBs*. Therefore, balance between chemical cues and hypoxia (oxygen levels and exposure periods) is still a great challenge in chondrogenic differentiation of hESCs.

At the end of the induction period levels of EB receptors, which responded to the induction regime (hypoxia and secreted factors from bovine chondrocytes) were determined by antibody array. Receptors which were up-regulated are involved in cell migration, cell adhesion, and cellular component morphogenesis. This result indicated a high degree of dynamic changes occurring during EB induction. Increased receptors expression in hESCs may contribute to understand the mechanism behind lineage choices and lineage decisions. In addition this study may also help to identify soluble factors released from chondrocytes necessary for chondrogenesis. SDS-PAGE analysis and silver staining of condition medium show two molecular weight groups (**Appendix C, Supplemental figure 1**). These two groups are in the approximate molecular weight ranges for secreted extracellular matrix and growth factors.

Identification and efficient isolation of progenitors from EBs for chondrogenesis remains a major challenge. Scarce information about surface markers hinders the use of Fluorescence-Activated Cell Sorting (FACS) method for specific selection of chondrogenic progenitors for tissue engineering. Rather than to adopt cell sorting to select the progenitors, EB dissociation separating blastocyst-like structure to single cells allowed individual cells to undergo self-selection and to form aggregates. An excellent homogeneity in 6-week old chondrogenic pellets was probably obtained through the loss of discordant cells by medium changes during chondrogenic pellet formation. The discordant cells might separate from progenitors, enter apoptotic pathway and leave the aggregate (89). The dissociated cells that express N-cadherin are not necessarily the only chondrogenic progenitors. bFGF receptor and NCAM on cell surface also mediate mesenchymal condensation (84, 90). Although dissociated EBs express N-cadherin, it remains to confirm whether the dissociated EBs also express the bFGF receptors and NCAM. Further studies of the expression of adhesion protein in induced EBs will help to identify markers of chondrogenic progenitors.

Immunocollagen staining and western blot analysis confirmed that transient 2 hypoxia induction expedited the process of chondrogenic differentiation in hESCs in comparison to normal induction or standard hMSC culture. Collagen type II was detected in pellets derived from *normoxia* EBs and hMSCs, but collagen type II was not completely secreted into periclellular spaces. Relative intensity of western blot band of pellets derived from *transient 2 hypoxia* EBs increased in comparison to that derived from other groups.

We propose the model of chondrogenic differentiation of hESCs in pellet culture system based partly on N-cadherin-mediated cell condensation. All together, we demonstrated chondrogenic differentiation of hESCs via EB induction under low oxygen tension in

conjunction with soluble factors from chondrocytes. The dissociated EBs differentiated into a homogeneous chondorgenic pellets without the use of laborious cell sorting.

6. Summary

Roles of physiological oxygen levels in cartilage tissue development were demonstrated in the standard cartilage model, bovine chondrocytes encapsulated in agarose hydrogel. Constructs exposed to 5% O_2 for 1 week + 21% O_2 for 3 weeks increased cartilaginous gene expression and cartilage specific ECM accumulation compared to constructs cultured under 5% O_2 for 4 weeks. This finding suggested that temporal gradients of oxygen tension might play a crucial role during the formation of functional cartilage tissue. The biomimetic physiological conditions, hypoxia, and soluble factors from chondrocytes, were applied to synergistically induce chondrogenic differentiation of hESCs.

The embryoid bodies cultured in chondrocyted-conditioned medium under *transient 2 hypoxia* regime (5% O_2 for 2 weeks + 21% O_2 for 1 week) showed up-regulation of *SOX9* and subsequently **formed** chondrogenic pellets with homogeneous ECM. Human embryonic stem cells can differentiate and serve as unlimited supply for tissue regeneration. However, the central challenge facing embryonic stem cell research is how to direct them into specific cell types. Here, we reported a method for inducing chondrogenic differentiation of hESCs through the combined controll oxygen tension and molecular conditioning. The current findings will contribute to the further development a new cell source for cartilage regeneration.

References

1. Lawrence RC, DT Felson, CG Helmick, et al. (2008). Estimates of the prevalence of arthritis and other rheumatic conditions in the United States. Part II. Arthritis Rheum 58:26-35.

2. Srikulmontree T. Osteoarthritis Available at http://wwwrheumatologyorg/practice/clinical/patients/diseases_and_conditions/osteOArthritisasp (Acceded: 1 May 2013).

3. Van Manen MD, J Nace and MA Mont. (2012). Management of primary knee osteoarthritis and indications for total knee arthroplasty for general practitioners. J Am Osteopath Assoc 112:709-715.

4. Lima EG, PH Grace Chao, GA Ateshian, et al. (2008). The effect of devitalized trabecular bone on the formation of osteochondral tissue-engineered constructs. Biomaterials 29:4292-4299.

5. Iwata H and Y Ikada. " Agarose." Cell Encapsulation Technilogy and Therapeutics. Ed Kuhtreiber, WM, Lanza, RP, Chick, WL Boston: Birkhauser, 1999 97 - 98 Print.

6. Oldershaw RA. (2012). Cell sources for the regeneration of articular cartilage: the past, the horizon and the future. Int J Exp Pathol 93:389-400.

7. Langer R and JP Vacanti. (1993). Tissue engineering. Science 260:920-926.

8. Cabral JD and SC Moratti. (2012). Advances in Biomedical hydrogels. Chemistry in New Zealand:44 - 48.

9. Langer R and DA Tirrell. (2004). Designing materials for biology and medicine. Nature 428:487-492.

10. Clayton HA, RF James and NJ London. (1993). Islet microencapsulation: a review. Acta Diabetol 30:181-189.

11. Spiller KL, SA Maher and AM Lowman. (2011). Hydrogels for the repair of articular cartilage defects. Tissue Eng Part B Rev 17:281-299.

12. Sigma-Aldrich. Agarose. Available at http://wwwsigmaaldrichcom/content/dam/sigma-aldrich/docs/Sigma/Product_Information_Sheet/a0701pispdf (Acceded: 1 May 2013) 2012.

13. Cao Z, RJ Gilbert and W He. (2009). Simple agarose-chitosan gel composite system for enhanced neuronal growth in three dimensions. Biomacromolecules 10:2954-2959.

14. Kato N. Cross-sectional image of a silk thread. Available at http://wwwhiroshima-uacjp/en/top/kenkyu/now/no18/ (Acceded: 13 April 2013).

15. Park SY, CS Ki, YH Park, et al. (2010). Electrospun silk fibroin scaffolds with macropores for bone regeneration: an in vitro and in vivo study. Tissue Eng Part A 16:1271-1279.

16. Bessa PC, ER Balmayor, J Hartinger, et al. (2010). Silk fibroin microparticles as carriers for delivery of human recombinant bone morphogenetic protein-2: in vitro and in vivo bioactivity. Tissue Eng Part C Methods 16:937-945.

17. Wang X, JA Kluge, GG Leisk, et al. (2008). Sonication-induced gelation of silk fibroin for cell encapsulation. Biomaterials 29:1054-1064.

18. Kim UJ, J Park, C Li, et al. (2004). Structure and properties of silk hydrogels. Biomacromolecules 5:786-792.

19. Murphy AR and DL Kaplan. (2009). Biomedical applications of chemically-modified silk fibroin. J Mater Chem 19:6443-6450.

20. Wang Y, DD Rudym, A Walsh, et al. (2008). In vivo degradation of three-dimensional silk fibroin scaffolds. Biomaterials 29:3415-3428.

21. Toh WS, EH Lee and T Cao. (2011). Potential of human embryonic stem cells in cartilage tissue engineering and regenerative medicine. Stem Cell Rev 7:544-559.

22. Benya PD and JD Shaffer. (1982). Dedifferentiated chondrocytes reexpress the differentiated collagen phenotype when cultured in agarose gels. Cell 30:215-224.

23. Grimshaw MJ and RM Mason. (2000). Bovine articular chondrocyte function in vitro depends upon oxygen tension. Osteoarthritis Cartilage 8:386-392.

24. Mobasheri A, S Richardson, R Mobasheri, et al. (2005). Hypoxia inducible factor-1 and facilitative glucose transporters GLUT1 and GLUT3: putative molecular components of the oxygen and glucose sensing apparatus in articular chondrocytes. Histol Histopathol 20:1327-1338.

25. Lee RB and JP Urban. (2002). Functional replacement of oxygen by other oxidants in articular cartilage. Arthritis Rheum 46:3190-3200.

26. Amarilio R, SV Viukov, A Sharir, et al. (2007). HIF1alpha regulation of Sox9 is necessary to maintain differentiation of hypoxic prechondrogenic cells during early skeletogenesis. Development 134:3917-3928.

27. Bell DM, KK Leung, SC Wheatley, et al. (1997). SOX9 directly regulates the type-II collagen gene. Nat Genet 16:174-178.

28. Bryant SJ and KS Anseth. (2002). Hydrogel properties influence ECM production by chondrocytes photoencapsulated in poly(ethylene glycol) hydrogels. J Biomed Mater Res 59:63-72.

29. Domm C, M Schunke, K Christesen, et al. (2002). Redifferentiation of dedifferentiated bovine articular chondrocytes in alginate culture under low oxygen tension. Osteoarthritis Cartilage 10:13-22.

30. Coyle CH, NJ Izzo and CR Chu. (2009). Sustained hypoxia enhances chondrocyte matrix synthesis. J Orthop Res 27:793-799.

31. Murphy CL and A Sambanis. (2001). Effect of oxygen tension on chondrocyte extracellular matrix accumulation. Connect Tissue Res 42:87-96.

32. Malladi P, Y Xu, M Chiou, et al. (2006). Effect of reduced oxygen tension on chondrogenesis and osteogenesis in adipose-derived mesenchymal cells. Am J Physiol Cell Physiol 290:C1139-1146.

33. Tuan RS, G Boland and R Tuli. (2003). Adult mesenchymal stem cells and cell-based tissue engineering. Arthritis Res Ther 5:32-45.

34. Knippenberg M, MN Helder, B Zandieh Doulabi, et al. (2006). Osteogenesis versus chondrogenesis by BMP-2 and BMP-7 in adipose stem cells. Biochem Biophys Res Commun 342:902-908.

35. Davidson D, A Blanc, D Filion, et al. (2005). Fibroblast growth factor (FGF) 18 signals through FGF receptor 3 to promote chondrogenesis. J Biol Chem 280:20509-20515.

36. Goodrich LR, C Hidaka, PD Robbins, et al. (2007). Genetic modification of chondrocytes with insulin-like growth factor-1 enhances cartilage healing in an equine model. J Bone Joint Surg Br 89:672-685.

37. Kieswetter K, Z Schwartz, M Alderete, et al. (1997). Platelet derived growth factor stimulates chondrocyte proliferation but prevents endochondral maturation. Endocrine 6:257-264.

38. Hanada K, LA Solchaga, AI Caplan, et al. (2001). BMP-2 induction and TGF-beta 1 modulation of rat periosteal cell chondrogenesis. J Cell Biochem 81:284-294.

39. Indrawattana N, G Chen, M Tadokoro, et al. (2004). Growth factor combination for chondrogenic induction from human mesenchymal stem cell. Biochem Biophys Res Commun 320:914-919.

40. Kaplan BA, CR Gorman, AK Gupta, et al. (2003). Effects of transforming growth factor Beta and insulinlike growth factor 1 on the biomechanical and histologic properties of tissue-engineered cartilage. Arch Facial Plast Surg 5:96-101.

41. Bonassar LJ, AJ Grodzinsky, EH Frank, et al. (2001). The effect of dynamic compression on the response of articular cartilage to insulin-like growth factor-I. J Orthop Res 19:11-17.

42. Hung CT, RL Mauck, CC Wang, et al. (2004). A paradigm for functional tissue engineering of articular cartilage via applied physiologic deformational loading. Ann Biomed Eng 32:35-49.

43. Bian L, DY Zhai, RL Mauck, et al. (2011). Coculture of human mesenchymal stem cells and articular chondrocytes reduces hypertrophy and enhances functional properties of engineered cartilage. Tissue Eng Part A 17:1137-1145.

44. Hwang NS, S Varghese and J Elisseeff. (2008). Derivation of chondrogenically-committed cells from human embryonic cells for cartilage tissue regeneration. PLoS One 3:e2498.

45. Ibelgaufts H. Conditioned Medium. http://wwwcopewithcytokinesde/copecgi?key=conditioned medium (Accedded: 1 April 2013).

46. Jurvelin J, I Kiviranta, M Tammi, et al. (1986). Effect of physical exercise on indentation stiffness of articular cartilage in the canine knee. Int J Sports Med 7:106-110.

47. Erickson IE, AH Huang, C Chung, et al. (2009). Differential maturation and structure-function relationships in mesenchymal stem cell- and chondrocyte-seeded hydrogels. Tissue Eng Part A 15:1041-1052.

48. Lima EG, L Bian, KW Ng, et al. (2007). The beneficial effect of delayed compressive loading on tissue-engineered cartilage constructs cultured with TGF-beta3. Osteoarthritis Cartilage 15:1025-1033.

49. Mauck RL, MA Soltz, CC Wang, et al. (2000). Functional tissue engineering of articular cartilage through dynamic loading of chondrocyte-seeded agarose gels. J Biomech Eng 122:252-260.

50. Graff RD, ER Lazarowski, AJ Banes, et al. (2000). ATP release by mechanically loaded porcine chondrons in pellet culture. Arthritis Rheum 43:1571-1579.

51. Graff RD, M Picher and GM Lee. (2003). Extracellular nucleotides, cartilage stress, and calcium crystal formation. Curr Opin Rheumatol 15:315-320.

52. Picher M, RD Graff and GM Lee. (2003). Extracellular nucleotide metabolism and signaling in the pathophysiology of articular cartilage. Arthritis Rheum 48:2722-2736.

53. Pingguan-Murphy B, M El-Azzeh, DL Bader, et al. (2006). Cyclic compression of chondrocytes modulates a purinergic calcium signalling pathway in a strain rate- and frequency-dependent manner. J Cell Physiol 209:389-397.

54. Garcia M and MM Knight. (2010). Cyclic loading opens hemichannels to release ATP as part of a chondrocyte mechanotransduction pathway. J Orthop Res 28:510-515.

55. Gadjanski I, S Yodmuang, K Spiller, et al. (2013). Supplementation of Exogenous Adenosine 5'-Triphosphate Enhances Mechanical Properties of 3D Cell-Agarose Constructs for Cartilage Tissue Engineering. Tissue Eng Part A 19:2188-2200.

56. Hofmann S, S Knecht, R Langer, et al. (2006). Cartilage-like tissue engineering using silk scaffolds and mesenchymal stem cells. Tissue Eng 12:2729-2738.

57. Meinel L, O Betz, R Fajardo, et al. (2006). Silk based biomaterials to heal critical sized femur defects. Bone 39:922-931.

58. Chao PH, S Yodmuang, X Wang, et al. (2010). Silk hydrogel for cartilage tissue engineering. J Biomed Mater Res B Appl Biomater 95:84-90.

59. Soltz MA and GA Ateshian. (1998). Experimental verification and theoretical prediction of cartilage interstitial fluid pressurization at an impermeable contact interface in confined compression. J Biomech 31:927-934.

60. Farndale RW, DJ Buttle and AJ Barrett. (1986). Improved quantitation and discrimination of sulphated glycosaminoglycans by use of dimethylmethylene blue. Biochim Biophys Acta 883:173-177.

61. Ceuninck FD, M Sabatini and P Pastoureau. *Cartilage and Osteoarthritis (Methods In Molecular Medicine)*. (2004). Humana Press, United States.

62. FDA clears Serica's silk tissue repair tech. Available at http://wwwbizjournalscom/boston/blog/mass-high-tech/2009/02/fda-clears-sericas-silk-tissue-repair-techhtml (Acceded: 1 March 2013).

63. Meinel L, S Hofmann, V Karageorgiou, et al. (2004). Engineering cartilage-like tissue using human mesenchymal stem cells and silk protein scaffolds. Biotechnol Bioeng 88:379-391.

64. Steck E, J Fischer, H Lorenz, et al. (2009). Mesenchymal stem cell differentiation in an experimental cartilage defect: restriction of hypertrophy to bone-close neocartilage. Stem Cells Dev 18:969-978.

65. Stolzing A, E Jones, D McGonagle, et al. (2008). Age-related changes in human bone marrow-derived mesenchymal stem cells: consequences for cell therapies. Mech Ageing Dev 129:163-173.

66. Long F and DM Ornitz. (2013). Development of the endochondral skeleton. Cold Spring Harb Perspect Biol 5:a008334.

67. Pelttari K, A Winter, E Steck, et al. (2006). Premature induction of hypertrophy during in vitro chondrogenesis of human mesenchymal stem cells correlates with calcification and vascular invasion after ectopic transplantation in SCID mice. Arthritis Rheum 54:3254-3266.

68. Majore I, P Moretti, R Hass, et al. (2009). Identification of subpopulations in mesenchymal stem cell-like cultures from human umbilical cord. Cell Commun Signal 7:6.

69. Arufe MC, A De la Fuente, J Mateos, et al. (2011). Analysis of the chondrogenic potential and secretome of mesenchymal stem cells derived from human umbilical cord stroma. Stem Cells Dev 20:1199-1212.

70. Wang L, I Tran, K Seshareddy, et al. (2009). A comparison of human bone marrow-derived mesenchymal stem cells and human umbilical cord-derived mesenchymal stromal cells for cartilage tissue engineering. Tissue Eng Part A 15:2259-2266.

71. Thomson JA, J Itskovitz-Eldor, SS Shapiro, et al. (1998). Embryonic stem cell lines derived from human blastocysts. Science 282:1145-1147.

72. Sa S and KE McCloskey. (2012). Stage-specific cardiomyocyte differentiation method for h7 and h9 human embryonic stem cells. Stem Cell Rev 8:1120-1128.

73. Zhang J, GF Wilson, AG Soerens, et al. (2009). Functional cardiomyocytes derived from human induced pluripotent stem cells. Circ Res 104:e30-41.

74. Oldershaw RA, MA Baxter, ET Lowe, et al. (2010). Directed differentiation of human embryonic stem cells toward chondrocytes. Nat Biotechnol 28:1187-1194.

75. Nakagawa T, SY Lee and AH Reddi. (2009). Induction of chondrogenesis from human embryonic stem cells without embryoid body formation by bone morphogenetic protein 7 and transforming growth factor beta1. Arthritis Rheum 60:3686-3692.

76. Toh WS, EH Lee, XM Guo, et al. (2010). Cartilage repair using hyaluronan hydrogel-encapsulated human embryonic stem cell-derived chondrogenic cells. Biomaterials 31:6968-6980.

77. Lima EG, L Bian, KW Ng, et al. (2007). The beneficial effect of delayed compressive loading on tissue-engineered cartilage constructs cultured with TGF-beta3. Osteoarthritis Cartilage 15:1025-1033.

78. Kelly TA, CC Wang, RL Mauck, et al. (2004). Role of cell-associated matrix in the development of free-swelling and dynamically loaded chondrocyte-seeded agarose gels. Biorheology 41:223-237.

79. Yang L, MH Soonpaa, ED Adler, et al. (2008). Human cardiovascular progenitor cells develop from a KDR+ embryonic-stem-cell-derived population. Nature 453:524-528.

80. von Mering C, MA Huynen, D Jaeggi, et al. (2003). STRING: a database of predicted functional associations between proteins. Nucleic Acids Res 31:258-261.

81. Schmittgen TD and KJ Livak. (2008). Analyzing real-time PCR data by the comparative C(T) method. Nat Protoc 3:1101-1108.

82. Deshpande RR and E Heinzle. (2004). On-line oxygen uptake rate and culture viability measurement of animal cell culture using microplates with integrated oxygen sensors. Biotechnol Lett 26:763-767.

83. John GT, I Klimant, C Wittmann, et al. (2003). Integrated optical sensing of dissolved oxygen in microtiter plates: a novel tool for microbial cultivation. Biotechnol Bioeng 81:829-836.

84. Tavella S, P Raffo, C Tacchetti, et al. (1994). N-CAM and N-cadherin expression during in vitro chondrogenesis. Exp Cell Res 215:354-362.

85. Meier S, M Solursh and S Vaerewyck. (1973). Modulation of extracellular matrix production by conditioned medium. Am Zool 13:1051-1060.

86. Keller GM. (1995). In vitro differentiation of embryonic stem cells. Curr Opin Cell Biol 7:862-869.

87. Hemmati-Brivanlou A and D Melton. (1997). Vertebrate embryonic cells will become nerve cells unless told otherwise. Cell 88:13-17.

88. Zhu LL, LY Wu, DT Yew, et al. (2005). Effects of hypoxia on the proliferation and differentiation of NSCs. Mol Neurobiol 31:231-242.

89. Yamashita A, R Krawetz and DE Rancourt. (2009). Loss of discordant cells during micro-mass differentiation of embryonic stem cells into the chondrocyte lineage. Cell Death Differ 16:278-286.

90. Ornitz DM and PJ Marie. (2002). FGF signaling pathways in endochondral and intramembranous bone development and human genetic disease. Genes Dev 16:1446-1465.

91. Shintani N, T Kurth and EB Hunziker. (2007). Expression of cartilage-related genes in bovine synovial tissue. J Orthop Res 25:813-819.

92. Haselgrove JC, IM Shapiro and SF Silverton. (1993). Computer modeling of the oxygen supply and demand of cells of the avian growth cartilage. Am J Physiol 265:C497-506.

93. Heywood HK, DL Bader and DA Lee. (2006). Rate of oxygen consumption by isolated articular chondrocytes is sensitive to medium glucose concentration. J Cell Physiol 206:402-410.

94. Johnson K, A Jung, A Murphy, et al. (2000). Mitochondrial oxidative phosphorylation is a downstream regulator of nitric oxide effects on chondrocyte matrix synthesis and mineralization. Arthritis Rheum 43:1560-1570.

Appendix A

Histology and immunohistochemistry

Constructs were fixed in 4% paraformaldehyde overnight at 4^{o}C, transferred to 70% ethanol, embedded in paraffin and sectioned at 8 mm. The sections were stained with hematoxylin and eosin for general evaluation, and safranin-O for GAG. Sections for immunohistochemistry staining were hydrated, and antigen retrieval was performed using heated 0.01 M citrate buffer with pH 6.0 for 15 minutes. Quenching of the endogenous peroxidase was done by immersing the sections in 0.3 % H_2O_2/methanol for 10 minutes at room temperature. The sections were incubated with blocking serum (Vectastain ABC, Burlingame, CA) for 30 minutes at room temperature, rinsed with PBS, incubated overnight at 4^{o}C with 1:1000 of type II collagen monoclonal antibody (Millipore, Temecula, CA) and for 30 minutes with biotinylated secondary antibody (Vectastain ABC, Burlingame, CA). For signal enhancement and detection, Vectastain ABC Kit with peroxidase and DAB Peroxidase Substrate Kit (Vectastain ABC, Burlingame, CA) were added as described in the manufacturer's protocol.

Collagen Type II ELISA

Constructs harvested after 28 days of culture were homogenized in an ice-cold mortar, resuspended in 0.8 ml of 0.05 M acetic acid containing 0.5 M NaCl, pH 3.0, mixed with 0.1 ml of 10 mg/ml pepsin solution in 0.05 M acetic acid, and stored at 4 °C for 48 hours. The pH of samples was adjusted to 8.0 using 1 N NaOH. The samples were digested using 0.1 ml of 1 mg/ml pancreatic elastase in 1X TBS (0.1M Tris, 0.2 M NaCl, 5mM $CaCl_2$, pH 8) at 4 °C overnight on a rotating rocker and centrifuged at 10,000 rpm for 5 minutes. This double

enzymatic digestion was performed to obtain monomeric collagen, by first digesting collagen fibrils into polymeric collagen by protease (pepsin) and then converting polymeric collagen into monomeric form by elastase digestion. Supernatant was collected and diluted in assay buffer according to the manufacturer's protocol (M.D. Bioproducts, St Paul, MN). The absorbance at 450 nm was plotted against concentration to obtain a standard curve by a 4-parameter logistic (4-PL) curve fit that was used to determine the amounts of collagen type II.

Mechanical properties

Compressive properties of constructs were measured in unconfined compression using a custom-made mechanical testing device (59). Constructs were placed in a testing chamber and equilibrated under a creep tare load of 0.5 g for 30 minutes. Stress-relaxation tests were performed at the ramp velocity of 1 μm/s up to 10% strain. The equilibrium Young's modulus (E_Y) was determined from the equilibrium stress-strain data.

Real-time PCR

Constructs were extracted to isolate the total RNA using TRIzol® Reagent (Invitrogen, Carlsbad, CA), treated with DNAse I (Ambion, Austin, TX) and quantified using NanoDrop™ Spectrophotometer (Thermo Scientific, Wilmington, DE). Reverse transcription was performed using High Capacity cDNA Reverse Transcription Kit (Applied Biosystems, Foster City, CA). Quantitative PCR was carried out using the 7500 Fast Real-Time PCR System. The following TaqMan® Gene Expression Assays were used for detection of cartilaginous gene expression: *COL2A1* (Bt03251861_m1), *COL1A1* (Bt03225322_m1), *ACAN* (Bt03212186_m1), and *SOX9* (custom designed forward primer: ACGCCGAGCTCAGCAAGA; reverse primer:

CACGAACGGCCGCTTCT; probe: CGTTCAGAAGTCTCCAGAGCTTGCCCA) (91). Gene expression values were reported in relative levels to *GAPDH* (Bt03210913_g1) by the $2^{-\Delta Ct}$ method(81). All reactions were performed in triplicates. Representative graphs are shown with error bars indicating standard deviation of 4 samples for each oxygen condition.

Statistical Analysis

Statistics were performed with STATISTICA software (Statsoft, Tulsa, OK). Data were expressed as the average ± SD of n = 4-6 samples per group and time point. The differences in construct properties between the groups were examined by analysis of variance ($\alpha = 0.05$), with DNA, matrix contents, E_Y or relative level of target gene expression as the dependent variable, followed by Tukey's Honest Significant Difference Test.

Appendix B

Supplemental figure 1. Oxygen level in culture medium at day 7, 14, 21, and 28

Oxygen levels were measured for 20 hours after each medium change. Traces show the measured partial pressure of oxygen. Black lines refer to the wells without tissue constructs, colored lines refer to wells with tissue constructs. The Oxygen Uptake Rate for each data set was calculated from the average difference between the two corresponding oxygen levels as explained in the Methods section.

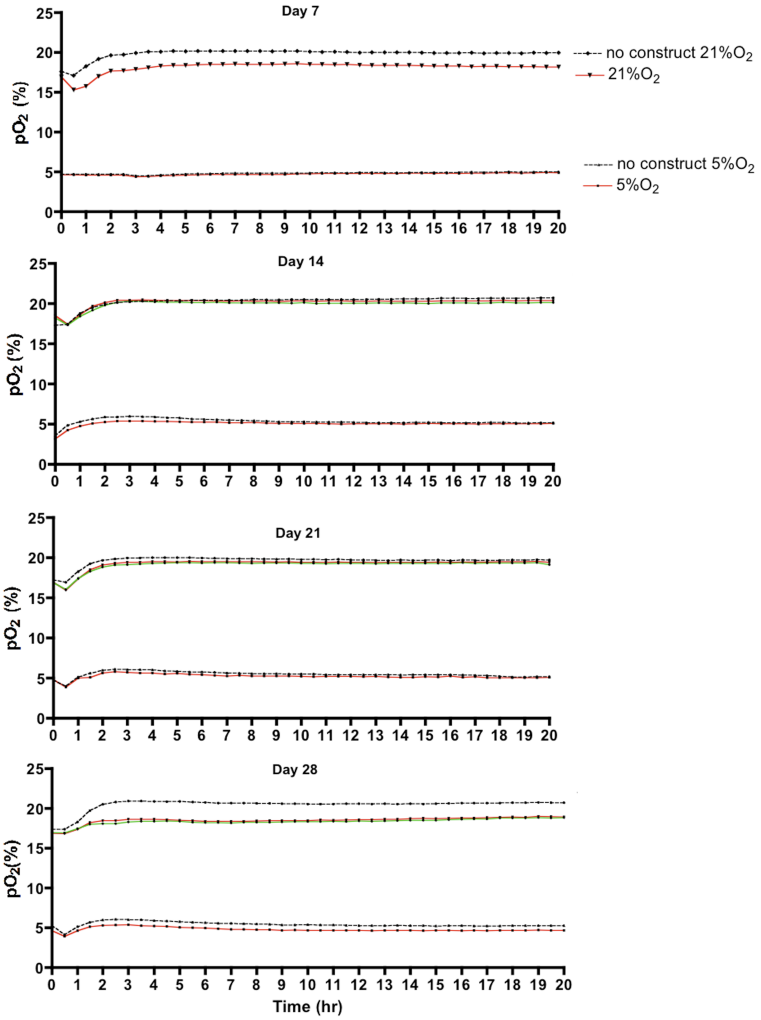

Supplement figure 2. Oxygen Uptake Rates (OUR) of engineered cartilage constructs

Cells in hypoxic conditions consumed less O_2 than other groups. Data are shown as average ± SD (n = 5) of values calculated from experimental data (one example of such data is shown in S-Figure 1). * $P<0.05$ versus 21% O_2 , $^{\xi}$ $P<0.05$ versus the previous time point within the same group.

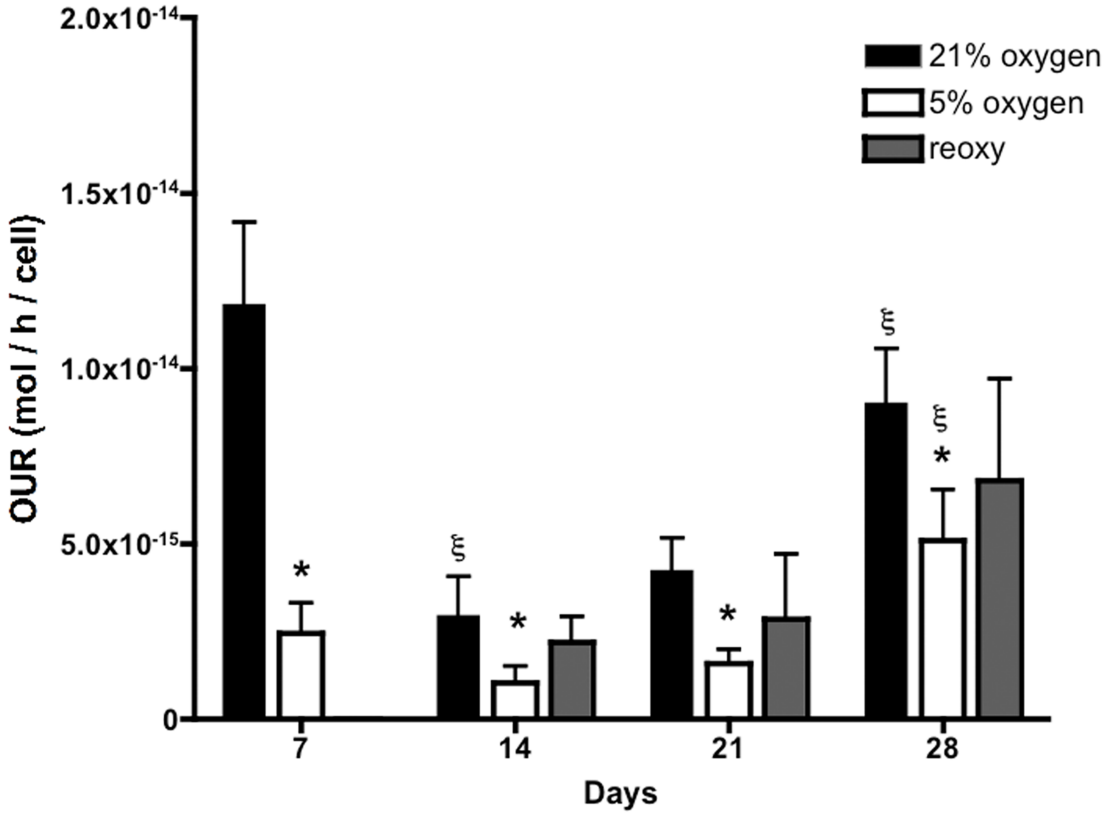

Supplemental table 1. Oxygen uptake rates for chondrocytes from different species

Chondrocytes	Oxygen consumption rate ($\times 10^{-15}$ mol/cell/hr)	Reference
Bovine articular cartilage	**1.84**	**(92)**
Bovine chondrocytes in suspension culture	**0.96**	**(92)**
Human chondrocytes in monolayer	**36**	**(93)**
Avian growth plate at hypertrophic zone	**93.2**	**(94)**

Appendix C

Supplemental table 1. Up- and down-regulated genes of week 4 hESCs-derived chondrogenic pellets compared to hMSCs

(± 2 fold change, n = 3, $p < 0.05$)

Reference seq.	Gene Symbol	Description	Fold regulation	*p-value*
NM_001718	*BMP6*	Bone morphogenetic protein 6	81.237	0.000001
NM_130851	*BMP4*	Bone morphogenetic protein 4	75.5103	0.009437
NM_000927	*ABCB1*	ATP-binding cassette, sub-family B (MDR/TAP), member 1	43.2346	0.002377
NM_004448	*ERBB2*	V-erb-b2 erythroblastic leukemia viral oncogene homolog 2, neuro/glioblastoma derived oncogene homolog (avian)	33.4393	0.0003
NM_000346	*SOX9*	SRY (sex determining region Y)-box 9	11.6406	0.000008
NM_001200	*BMP2*	Bone morphogenetic protein 2	8.2226	0.000049
NM_001709	*BDNF*	Brain-derived neurotrophic factor	8.1751	0.03162
NM_000572	*IL10*	Interleukin 10	7.955	0.000358
NM_001154	*ANXA5*	Annexin A5	7.2051	0.000076
NM_000214	*JAG1*	Jagged 1	7.1511	0.027269
NM_002211	*ITGB1*	Integrin, beta 1 (fibronectin receptor, beta polypeptide, antigen CD29 includes MDF2, MSK12)	6.7638	0.011628
NM_004864	*GDF15*	Growth differentiation factor 15	3.492	0.000193
NM_006617	*NES*	Nestin	3.1779	0.000009

NM_003239	*TGFB3*	Transforming growth factor, beta 3	2.9194	0.0238
NM_006500	*MCAM*	Melanoma cell adhesion molecule	-236.4152	0.001649
NM_001963	*EGF*	Epidermal growth factor	-197.7788	0.000338
NM_017617	*NOTCH1*	Notch 1	-82.2336	0.000245
NM_003994	*KITLG*	KIT ligand	-80.0848	0.001354
NM_001664	*RHOA*	Ras homolog gene family, member A	-23.9324	0.002331
NM_000610	*CD44*	CD44 molecule (Indian blood group)	-23.6385	0.003398
NM_001150	*ANPEP*	Alanyl (membrane) aminopeptidase	-22.3961	0.003434
NM_000660	*TGFB1*	Transforming growth factor, beta 1	-22.0013	0.003567
NM_000887	*ITGAX*	Integrin, alpha X (complement component 3 receptor 4 subunit)	-21.7384	0.000336
NM_004346	*CASP3*	Caspase 3, apoptosis-related cysteine peptidase	-21.0014	0.001091
NM_000210	*ITGA6*	Integrin, alpha 6	-11.9345	0.000224
NM_020429	*SMURF1*	SMAD specific E3 ubiquitin protein ligase 1	-9.6176	0.002113
NM_004465	*FGF10*	Fibroblast growth factor 10	-7.2574	0.004142
NM_004348	*RUNX2*	Runt-related transcription factor 2	-6.2551	0.000208
NM_002526	*NT5E*	5'-nucleotidase, ecto (CD73)	-6.2323	0.001009
NM_003642	*HAT1*	Histone acetyltransferase 1	-6.0939	0.000644
NM_000576	*IL1B*	Interleukin 1, beta	-5.9739	0.000093
NM_002609	*PDGFRB*	Platelet-derived growth factor receptor, beta polypeptide	-5.7338	0.000368
NM_022739	*SMURF2*	SMAD specific E3 ubiquitin protein ligase 2	-3.5897	0.001052
NM_002097	*GTF3A*	General transcription factor IIIA	-3.3619	0.003657

NM_003376	*VEGFA*	Vascular endothelial growth factor A	-3.2631	0.015938
NM_002253	*KDR*	Kinase insert domain receptor (a type III receptor tyrosine kinase)	-2.7741	0.005661
NM_182828	*GDF7*	Growth differentiation factor 7	-2.5779	0.010635
NM_005607	*PTK2*	PTK2 protein tyrosine kinase 2	-2.4408	0.001707
NM_00011	*ENG*	Endoglin	-2.1149	0.027684

Supplemental figure 1. Chondrocyte conditioned medium silver-stained SDS-PAGE gel

Bovine chondrocytes were cultured in serum albumin-free DMEM for 48 hours and collected to analyzed in in 8% and 15% polyacrylamide gel. Bovine serum albumin from the chondrocytes is the major component of conditioned medium located around 60 kDa. Protein bands size below the serum are expected to be secreted growth factors and subjected to further characterized.